WORKSHOP ON THE ANALYSIS OF INTERPLANETARY DUST PARTICLES

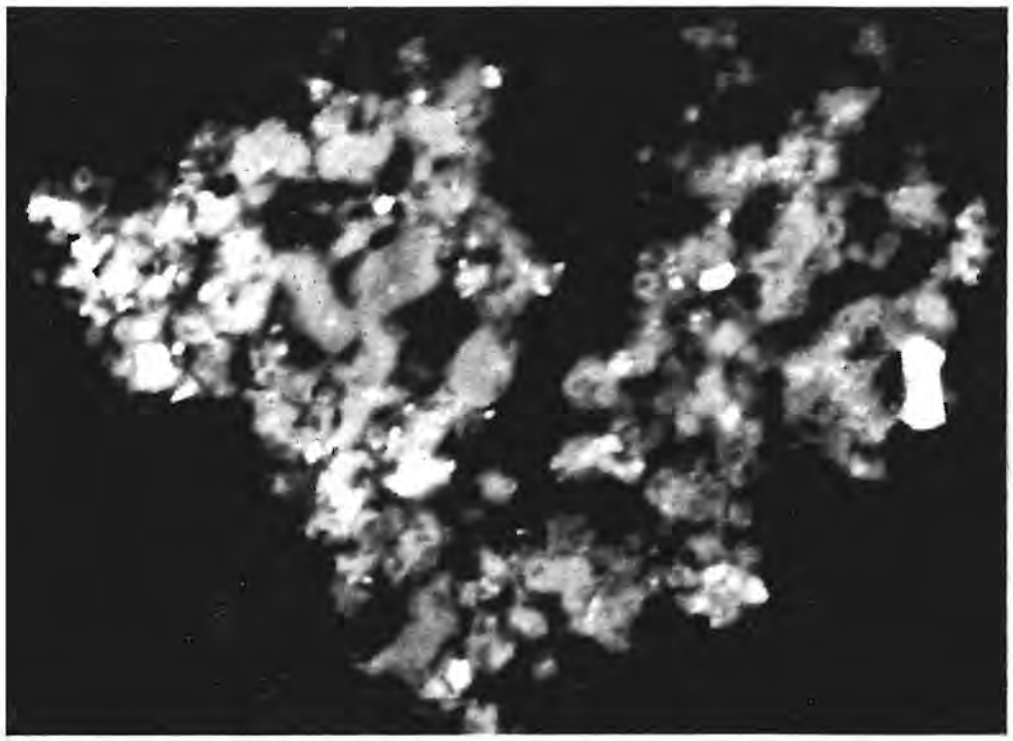

LPI Technical Report Number 94-02

Lunar and Planetary Institute 3600 Bay Area Boulevard Houston TX 77058-1113

LPI/TR--94-02

WORKSHOP ON
THE ANALYSIS OF INTERPLANETARY DUST PARTICLES

Edited by

M. Zolensky

Held at
Lunar and Planetary Institute

May 15–17, 1993

Sponsored by
Lunar and Planetary Institute

Lunar and Planetary Institute 3600 Bay Area Boulevard Houston TX 77058-1113

LPI Technical Report Number 94-02
LPI/TR--94-02

Compiled in 1994 by
LUNAR AND PLANETARY INSTITUTE

The Institute is operated by the University Space Research Association under Contract No. NASW-4574 with the National Aeronautics and Space Administration.

This report may be cited as

M. Zolensky, ed. (1994) *Workshop on the Analysis of Interplanetary Dust Particles*. LPI Tech. Rpt. 94-02, Lunar and Planetary Institute, Houston. 62 pp.

This report is distributed by

ORDER DEPARTMENT
Lunar and Planetary Institute
3600 Bay Area Boulevard
Houston TX 77058-1113

Mail order requestors will be invoiced for the cost of shipping and handling.

Cover: Backscattered electron image of a hydrated, chondritic interplanetary dust particle, measuring 17 μm across.

Program

Saturday, May 15, 1993

7:30–8:30 a.m. *Registration and Continental Breakfast*

8:30 a.m.–5:00 p.m.

INVITED PRESENTATIONS AND DISCUSSION TOPICS

An Overview of the Origin and Role of Dust in the Early Solar System
D. Brownlee

Modern Sources of Dust in the Solar System
S. Dermott

Remote Sensing of Cometary Dust and Comparisons to IDPs
M. S. Hanner

What Does the Fine-Scale Petrography of IDPs Reveal About Grain Formation and Evolution in the Early Solar System?
J. Bradley

Solar System Exposure Histories of Interplanetary Dust Particles
A. O. Nier

Changes in IDP Mineralogy and Composition by Terrestrial Factors
G. J. Flynn

5:00–7:00 p.m.

POSTER SESSION AND RECEPTION

Further Analysis of Remnants Found in LDEF and MIR Impact Craters
L. Berthoud and J. C. Mandeville

Solar Energetic Particle Track Densities as an Indicator of the Origin of Interplanetary Dust
G. E. Blanford

Sunday, May 16, 1993

8:30 a.m.–6:00 p.m.

INVITED PRESENTATIONS AND DISCUSSION TOPICS

Mineralogical and Chemical Relationships of Interplanetary Dust Particles, Micrometeorites, and Meteorites
W. Klöck and F. J. Stadermann

Chemical Compositions of Primitive Solar System Particles
S. R. Sutton and S. Bajt

Carbon in Primitive Interplanetary Dust Particles
L. P. Keller, K. L. Thomas, and D. S. McKay

History of Elements in the Early Solar System, Based on Isotope Studies of Dust
R. Walker

A Proposition for the Classification of Carbonaceous Chondritic Micrometeorites
F. J. M. Rietmeijer

Data from Collection of IDPs in Low-Earth Orbit
D. S. McKay and W. Tanner

Collection and Curation of IDPs in the Stratosphere and Below
M. Maurette and M. Zolensky

Monday, May 17, 1993

8:30 a.m.–12:00 noon

Future Opportunities to Return Primitive Materials Directly from Space
W. Kinard

Discussion

12:00 noon *Workshop adjourns*

Contents

Summary of Technical Sessions

Great progress has been made in the analysis of interplanetary dust particles (IDPs) over the past few years, demonstrated by short presentations made at meetings of the Meteoritical Society, Lunar and Planetary Science Conferences, and electron microscopy conclaves. However, dust workers wanted a more focused showcase for recent IDP results, and opportunity for consolidation of past work and the forging of new research collaborations. The recent availability of larger IDPs from the Large Area Collectors, and consequent particle analysis consortia, had made the necessity of a dedicated workshop even more acute. To satisfy this need, this first workshop dedicated to the analysis of IDPs was organized by D. Brownlee (University of Washington), J. Bradley (MVA Associates), G. Flynn (SUNY Plattsburgh), A. Nier (University of Minnesota), F. Rietmeijer (University of New Mexico), and M. Zolensky (NASA Johnson Space Center). From the start the principle goal of the workshop was to provide a forum for free and relatively uninterrupted discussion. To provide for the maximum degree of participant interplay and productive discussion, the workshop was designed around a few review talks, each of which was intended to review past results in a specific branch of IDP research and suggest future potentially fruitful directions. Following each of these presentations, workshop participants were free to discuss any aspects of the specific subject, and introduce and discuss their own results and ideas. Contributed presentations were made in the form of posters, although these results were folded into the discussions at appropriate times.

For each discussion, one workshop participant served as a summarizer. These summaries, and recordings of the talks and discussions, are now being used to facilitate production of a workshop proceedings volume, which will be published by the American Institute of Physics. Not all of the ideas presented at the workshop are adequately covered by the abstracts in the present volume. Accordingly, here we present a brief summary of the major points raised at the workshop.

INTRODUCTION

This is well covered by Brownlee's abstract, and most of the points he raised were addressed at greater length by subsequent presentations and discussions. In particular, Brownlee made the points that IDPs are probably the only samples now available of outer-belt asteroids and comets, including Kuiper belt objects. IDPs could have turned out to be merely additional fragments of H6 chondrites, but (fortunately for us) detailed work over the past two decades has shown them to be compositionally and mineralogically distinct from meteorites. These important distinctions include greater porosity, aggregate structure, higher volatile content, and unique mineralogy. Great progress has been made in the development of new analytical techniques, permitting measurements to be made of bulk compositions (including trace elements by four different and complementary techniques, noble gases, and some organic compounds), infrared spectra (both transmittance and reflectance), isotopes, and physical properties. Important problems remain, including the establishment of a useful classification scheme, resolving differences in terminology (e.g., tar balls vs. granular units, etc.), elucidation of the relationships between different types of IDPs (chondritic vs. refractory vs. basaltic; hydrous vs. anhydrous). Finally, future collection technologies were discussed, including replacement of silicone oil in stratospheric collection, and the role of dust collection in space.

OBSERVATION AND MODELING OF DUST IN THE SOLAR SYSTEM

S. Dermott presented the results of analysis of IRAS and COBE data, which indicate that main-belt asteroids are the source of approximately 40% of the dust providing zodiacal light. The remainder must be provided by near-Earth asteroids, comets, and interstellar sources. In particular, it seems to be useful to make detailed dynamical calculations of the evolution of grains from near-Earth asteroids. Apparently, dust grains derived from some asteroid families are distinguishable from one another, in inclination space. Differences in orbital elements for asteroidal grains from different families also cause different encounter velocities at Earth, and hence differential atmospheric entry heating levels that vary temporally. A. Jackson and H. Zook also presented results of calculations of which indicate that cometary and asteroidal particles can be distinguished, if their velocities and trajectories are measured in space. This is a critical requirement for proposed dust collection efforts in low Earth orbit. Zook presented data from the Ulysses spacecraft cosmic dust experiment indicating the presence of streams of interstellar dust focused by interaction with Jupiter.

M. Hanner reviewed the available spectroscopic information on comets, of which there is all too little. The main point of this presentation was that the comets observed to date appear to differ significantly from one another in mineralogy. While it is possible that these differences are due to differential aging of comets, it is also likely that there is considerable inherent intercomet heterogeneity. Recent measurements of the reflectance spectra of chondritic IDPs by Bradley reveal some features found in some comets, including features possibly due to noncrystalline phases. Definite ties between specific comets and IDPs have yet to be demonstrated by spectroscopic work, although this is clearly a promising line

of research. Still unknown is the relationship between cometary dust and interstellar grains, and whether hydrated materials are found on comets. This latter point is currently very contentious.

MINERALOGY AND PETROGRAPHY OF IDPS

Bradley summarized what has been learned concerning the mineralogy of chondritic IDPs. A fascinating aspect of IDP petrography is the frequent occurrence of fine-grained aggregates, which can have bulk chondritic composition at the femtogram scale. These objects are still the subject of nomenclaturial disagreement: Bradley has called them "tar balls," while Rietmeijer has used the term "granular units." Bradley has now identified three flavors of aggregates, which he calls unequilibrated, equilibrated, and reduced aggregates (UAs, EAs, and RAs), depending upon the mineral assemblage. (Rietmeijer presented an alternate classification scheme in much the same vein; see **Classification**, below.) Are these aggregates the products of nebular accretion, with subsequent processing in the cases of the EAs? Keller has suggested that some of these aggregates could be agglutinates from parent body regoliths. These objects clearly will receive much more attention in the future, although it is unfortunate that they are so small, being right at the analytical limit for present instruments. Bradley also reviewed the evidence for hydration on the IDP parent bodies, concluding that the frequent occurrence of hydrated and anhydrous phases within the same grain is probably due to the incipient nature of the alteration event. Zolensky described work on the compositions of olivines and pyroxenes n chondritic IDPs. The common occurrence of diopside in hydrous IDPs probably indicates parent body metamorphism. Considerable attention is also centering on the noncrystalline component of IDPs.

PROCESSING OF IDPs IN THE SOLAR SYSTEM AND TERRESTRIAL ATMOSPHERE

Nier has been measuring noble gas contents of individual IDPs by step heating. He has realized that examination of the temperature-gas release profile for a particle will reveal the peak temperature of atmospheric entry heating. This latter value can be used to infer cometary vs. asteroidal origin for the particle, as the cometary grains enter the atmosphere at considerably higher velocities (on the average). This technique appears to be the only current course for distinguishing cometary from asteroidal particles.

Flynn reviewed the evidence indicating the degree of atmospheric entry heating experienced by IDPs. Despite the obfuscatory effect this has on nebular and parent body processes, recognition of the degree of heating can provide unique source information (see above). Documented entry-heating effects include formation of magnetite rims, depletion of volatile elements like Zn, dehydration of phyllosilicates, and the changes in the release temperatures of noble gases mentioned above. At one time it was hoped that inspection of solar flare track densities and their density variation across a grain would provide useful information on space-exposure duration and entry heating level; however, track densities appear to be too low to permit useful estimates to be made of these values. The explanation of these heating effects is still somewhat controversial. Some researchers believe that magnetite rims could form by sublimation onto the particles from the atmospheric E-layer gases. However, most workshop participants felt that this sublimation process would be unlikely, due to the low Fe concentration of the E layer, and the short atmospheric residence time of the particles. Some researchers are unsure of the proposed nebular origin of the Br and Zn enrichments reported for many chondritic IDPs, making heating/depletion estimations potentially uncertain. All participants concluded that we need to better understand the concentration and sources of Zn, Br, and Fe in the upper atmosphere.

Discussion also centered on the potential for particulate contamination during collection in silicone oil on the inertial inpaction collectors currently used by NASA. Although workers have not found indications of contamination from this material (except for Si, which can apparently be removed), lingering uncertainties on this subject indicate that care must be taken during the interpretation of compositional analyses.

COMPARISONS OF IDPs TO METEORITES AND MICROMETEORITES

This topic is well covered by W. Klöck's abstract. Basically, most IDPs appear to have significant differences from meteorites, although certain IDPs appear to be identical to some carbonaceous chondrite matrix materials. These differences do not preclude derivation from the same parent bodies as meteorites, however, but require that different materials from them are being sampled. In general, low-strength, poorly consolidated materials like IDPs would not be expected to survive as meteorite-sized bodies, only as dust. Klöck also compared IDPs to the larger ($\geq$100 mm) micrometeorites collected in the oceans (deep sea spheres), and polar ice caps. These latter materials are generally highly contaminated and severely heated by atmospheric entry, which often precludes useful comparison. However, the most pristine of these larger materials bear considerable resemblance to CI, CR, and CM chondrites. There are sufficient differences between these micrometeorites and IDPs to warrant continued study of the former, particularly since they are considerably easier to

handle and are available in abundance (thanks largely to the efforts of M. Maurette).

COMPOSITION OF IDPs

S. Sutton's abstract is a good introduction to this subject. Numerous complementary techniques are now routinely utilized for the measurement of the bulk compositions of IDPs. Problems linger concerning potential contamination during atmospheric residence and collection, but progress is being made in understanding the actual dimensions of these hazards. Keller and K. Thomas'abstracts provide a good guide to recent achievements in the measurement of C in IDPs; they find that they contain up to approximately 50 wt% C, far higher than for bulk chondrites. The highest C concentrations appear to always come in IDPs containing pyroxenes.

R. Walker summarized ion probe analyses of chondritic IDPs, with a major goal being the location of preserved interstellar material. Isotopic measurements have been made of H, C, Mg, N, and Si on fewer than 100 IDPs. No large isotopic anomalies have been found in C, Mg, or Si. Approximately half of the analyzed particles exhibited deuterium enrichments (up to 2000‰). Some IDPs have shown ^{15}N enrichments (up to 411‰), usually correlated with a deuterium enrichment. Hydrous and pyroxene-dominated IDPs appear to be isotopically similar; however, no anomalies have been located in olivine-dominated IDPs. Basically, no IDPs have yet been located that are entirely interstellar in origin (as we understand them). While this is a disappointing result, the fact is that only a very small total mass of IDPs has yet been examined; if interstellar materials are present among IDPs in the same concentration as in the Murchison CM chondrite, then (statistically) we should not expect to have seen even one entirely interstellar grain yet. However, isotopic anomalies are found in IDPs, and these remain to be explained satisfactorily.

CLASSIFICATION

Major problems remain with IDP classification. The most widely used scheme discriminates between four types, based upon the dominant crystalline silicate phase: olivine, pyroxene, saponite, and serpentine. Not included in this framework are the refractory IDPs. Rietmeijer reviewed these schemes, proposing a new classification based on the composition and petrography of the micrometer-sized aggregates present in most chondritic IDPs (see above). Rietmeijer proposes that these objects be called "granular units" and "polyphase units," in contrast to Bradley's suggestion. Actually, both classifications have common features. No common classification scheme for IDPs was found acceptable to everyone, although participants agreed that a radically new classification scheme along the lines of those proposed was desirable. However, lively discussion of these classification schemes established that for any new one to be accepted it will have to (1) be based on measurements that can be made by numerous investigators, (2) not rely on inferred processes, and (3) not include unsavory terms (you had to be there). It is clear that further development work will be necessary here.

COLLECTION OF IDPs

At present, IDPs are actively being collected in the stratosphere, from polar ices, and within impact features on spacecraft. Abstracts by Maurette, Zolensky, and C. Dardano cover basic aspects of these efforts. It is fair to say that all techniques being used are complementary, and that no one is clearly superior in all aspects. The stratospheric collections provide the least contaminated and heated particles, but recovered particles are generally less than 70 mm in diameter. Particles from polar ices can be larger than the stratospheric particles, but are more contaminated and heated, and may actually represent a different population of objects. Particles collected in space can be collected with velocity and trajectory information, unlike those collected at Earth, but are generally highly shocked and/or melted at best, and at worst are vaporized. All these collection techniques are being improved, as resources permit. In the stratosphere collection with a medium other than silicone oil has being attempted (so far without success). Cleaner equipment is now being used in the Antarctic to collect particles. Better capture media are being developed for less disruptive collections in space. Future flight opportunities for these collectors include LDEF II, EURECA II, MIR, and the U.S. space station.

Abstracts

FURTHER ANALYSIS OF REMNANTS FOUND IN LDEF AND MIR IMPACT CRATERS. S. L. Berthoud and J. C. Mandeville, CERT-ONERA/DERTS, 2 Av. E. Belin, 31400 Toulouse, France.

This study is the further investigation of space-exposed samples recently recovered from the American satellite LDEF and the Franco-Soviet Mir "Aragatz" experiment. Some interesting impact features have been selected as examples to demonstrate various findings. Part of the objective of the experiments was to determine the nature and origin of particles in low Earth orbit (LEO). Observations show that the "multiple foil detectors" appear to be an effective way of retaining impactor residues of larger particles. They provide a "witness" foil that shows the shape and dimensions of the impacting particle. Several low-velocity (<4 km s^{-1}) oblique craters containing significant quantities of impactor residue have been identified. Energy dispersive spectrometer (EDS) analyses of the residues show evidence of micrometeoroid and debris compositions. Similarities between the meteoroid signatures and those of Brownlee particles have been noted. Evidence of at least two different grain compositions in one impacting particle is shown. The discovery of debris impacts on the trailing edge of LDEF demonstrates that artificial debris may be found, not just in circular orbits, but also in elliptical orbits.

Introduction: One of the objectives of retrievable experiments flown in LEO is the identification of the particles responsible for the formation of craters on surfaces exposed to the LEO particulate environment. In this work, particle identification was achieved by EDS of particle residues in and around the craters. Residues were classed as being of natural origin if they had a high Mg, Al, Si, Fe, Ca content. They were classed as being of man-made origin if they had a high O (for Al_2O_3), Ti and Si (paint flakes), Fe, Cr, Ni, Cu, Zn (stainless steel and alloys) content. Analysis efforts were handicapped by alloy inclusions, organic contamination containing Na, Cl, K, S (which occurred before, during, and after space exposure), and the shadowing effect caused by crater geometry. For a summary

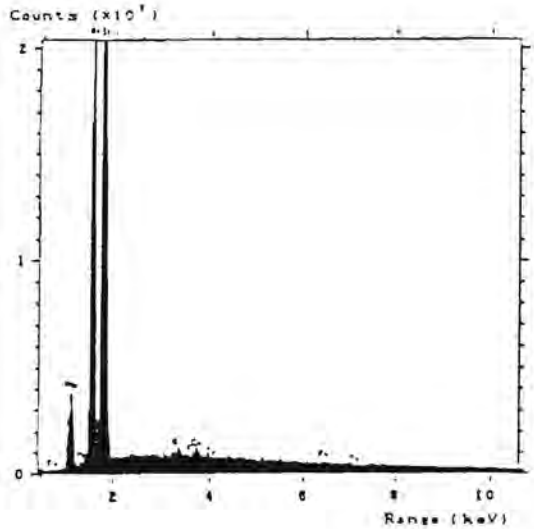

Fig. 1. LDEF D11/2 multiple foil detector. (a) Perforation (55×40 µm) of 5-µm-thick Al top foil. (b) Star-shaped crater distribution around crystalline fragment on 125-µm Al bottom foil. (c) EDS spectrum of crystalline fragment (20 keV).

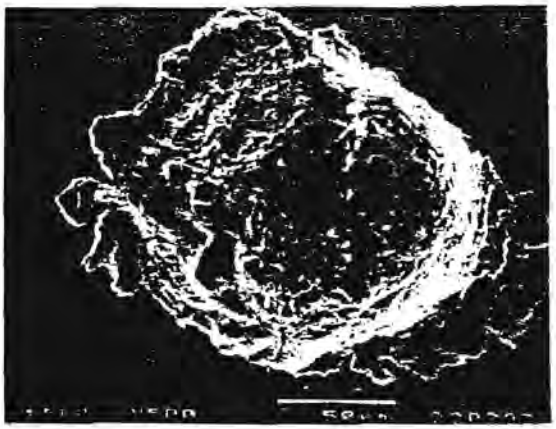

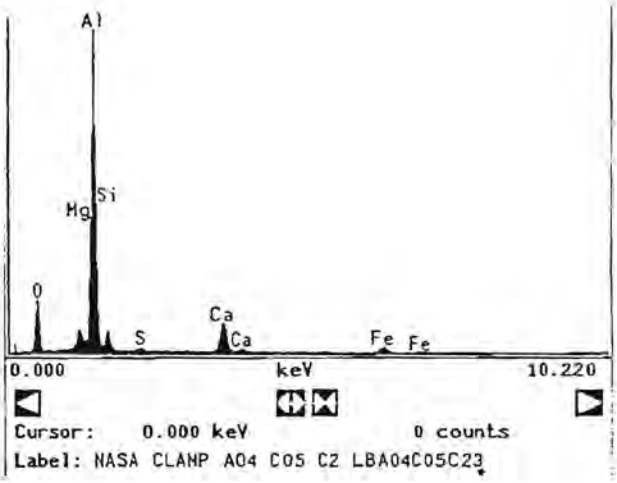

Fig. 2. Meteoroid impact on LDEF clamp A04 C05. (a) Oblique impact (135 × 125 μm). (b) Detail of molten residues on shelf. (c) EDS spectrum of residues (15 keV).

of the observed meteoroid vs. debris proportions for several experimental surfaces and a discussion of the importance of particle velocity and experiment position (with respect to the leading edge of the spacecraft), see Hörz [1] and Berthoud and Mandeville [2].

Impact Features: *Multiple foil detectors.* Examination of the space-exposed detectors (see [3] for a full description) revealed several instances of perforation by large particles. The particles leave a perforation with barely perceptible lip formation the same shape and size as themselves, which avoids the necessity for conversion between crater size and particle diameter—a process fraught with pitfalls [4]. An example from the LDEF FRECOPA experiment is shown in Fig. 1. The particle perforated the top foil and then fragmented, causing a star-shaped distribution of secondary craters on the target below. Analysis of the central crystalline fragment and of secondary craters revealed the presence of Si, Na, Ca, Fe, and Mg, indicating a particle of natural origin.

LDEF clamps (described in [5]). Figure 2 shows an oblique impact average depth-to-diameter ratio P/D = 0.41) on clamp A04 C05. The characteristic shelf formation has been observed to occur at impact angles >60° (to normal) in simulation experiments by the authors. The jet of projectile ejecta produced by hypervelocity impact frequently leaves projectile fragments on these shelves. EDS analysis of the molten fragments revealed the presence of Al, Mg, Si, and Fe—a classic signature for a particle of natural origin (see W7027F11 in [6]). Figure 3 shows an impact on clamp A06 C06. Unmelted fragments of the impacting particle are clearly visible inside the crater. EDS spectra of different areas of the fragments showed a wide range of proportions of the elements Al, Mg, Si, Ca, Fe, and Cr (Cr probably comes from the chromic acid anodization). We deduce that the impactor was a "fluffy" meteoroid consisting of an aggregate of at least two different minerals of different compositions.

LDEF FRECOPA (trailing edge). Figure 4 shows a crater (P/D = 0.3) found on the trailing edge of LDEF. EDS analysis of the melted residues shows a micrometeoroid signature—Al, Mg, Si, Fe, O, S, Ca, and Cr. Figure 5 shows an impact found on the trailing edge of LDEF that demonstrates that debris exists in elliptical orbits around the Earth, not just in circular orbits as was previously thought. The impactor appears intact although fractured. The image strongly resembles that produced by a laboratory simulation experiment [7]. EDS analysis revealed the presence of Al, Fe, and Va, indicating stainless steel, which explained the above similarity.

Conclusions: Chemical identification of residues is easier for low-velocity impacts. This means that oblique impacts and multiple foil detectors, which both slow down the impacting particle, are more likely to retain impactor residues than normal impacts onto thick

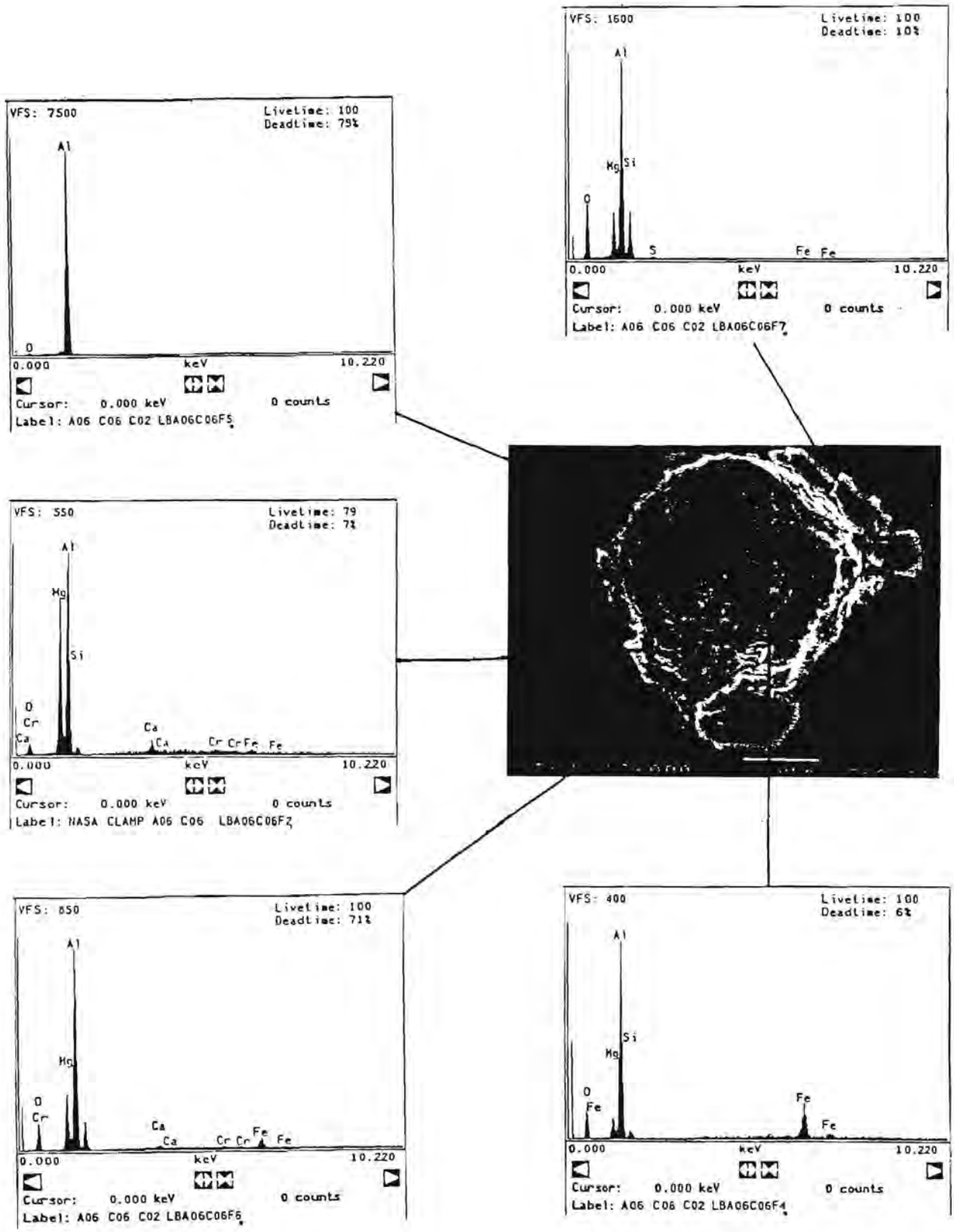

Fig. 3. Low-velocity impact (33 μm) in LDEF clamp A06C06 with spectra from different areas of the residues to show different grain compositions.

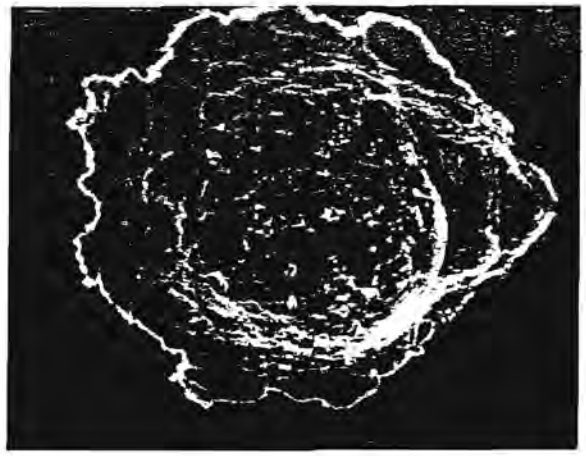

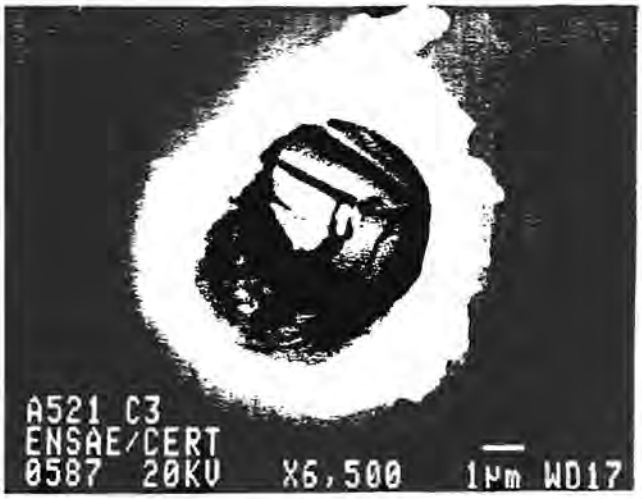

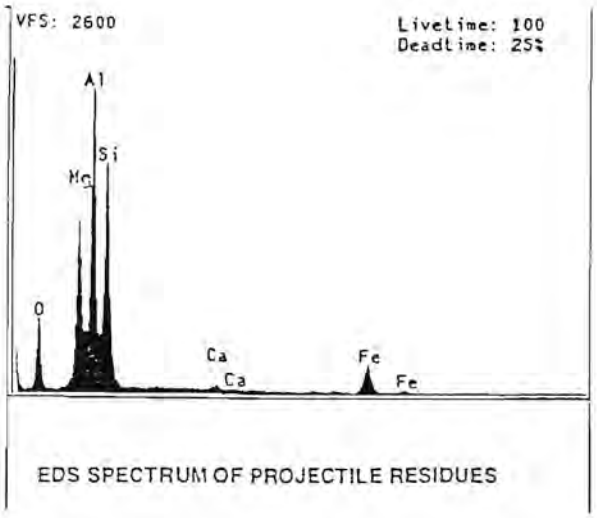

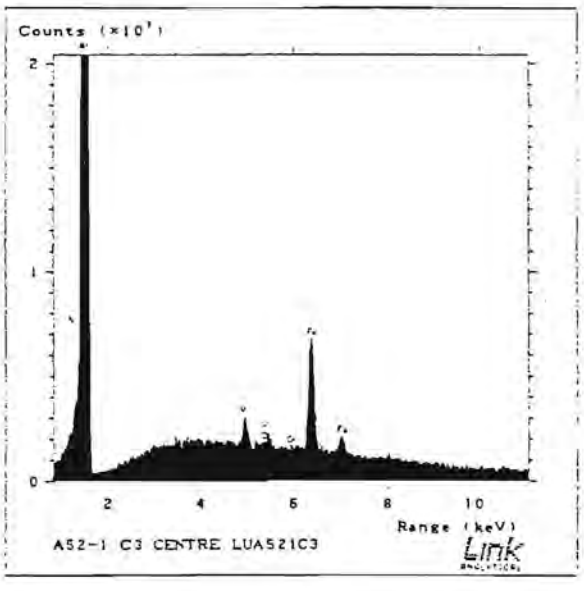

Fig. 4. Meteoroid impact on LDEF FRECOPA (03) "Ecran Rigide." (a) Oblique impact (235 × 176 µm) on Al alloy experiment support surface. (b) Detail showing molten residues. (c) EDS spectrum of residues (15 keV).

Fig. 5. Debris impact on LDEF FRECOPA. (a) Oblique impact (6.6 × 5.4 µm) on 99% pure Al experiment surface. (b) Simulation experiment using Al_2O_3 particle impacting stainless steel target at 2 km s^{-1}. Crater measures 9.3 × 8 µm. (c) EDS spectrum of (a) residues (20 keV).

targets. Indeed, meteoroids travel at higher velocities than debris and are thus more likely to vaporize and leave no residue. These methods therefore offer a rare opportunity to observe and analyze micrometeoroids that have caused craters in experimental surfaces. They provide ideas for the design of future detectors.

The meteoroid impacts are all relatively shallow (P/D varying from 0.3 to 0.52), which is commensurate with the high lateral velocity component for oblique impacts and with the low density of the impactors (assumed to be around 2–3 g cm^{-3} from the compositions). The examination of unmelted meteoroid fragments reveals their agglomerate nature and similarity to certain Brownlee particles.

References: [1] Hörz F. and Bernhard R.P. (1992) *NASA TM-104750.* (2) Berthoud L. and Mandeville J. C. (1993) in press. [3] Mandeville J. C. (1990) *Adv. Space Res., 10,* 3397–3401. [4] Berthoud L. and Mandeville J. C. (1993) *Proc. Conf. Space Debris*, Darmstadt, submitted. [5] See T. et al. (1990) *MDSIG Preliminary Report,* 24, NASA Publ. 84, JSC 24608. [6] *NASA Cosmic Dust Catalog* (1983) Vol. 4, No. 2, NASA Publ. 65, JSC 18928. [7] McKay D. et al. (1986) *LPI Tech. Rpt. 86-05,* 72–75.

SOLAR ENERGETIC PARTICLE TRACK DENSITIES AS AN INDICATOR OF THE ORIGIN OF INTERPLANETARY DUST.

G. E. Blanford, University of Houston–Clear Lake, Houston TX 77058, USA.

Sandford [1] theoretically explored the use of track densities from solar energetic particles in interplanetary dust grains (IDPs) to distinguish whether they were of cometary or asteroidal origin. He determined that there were differences in the characteristic distributions of track densities that would occur from these two possible sources. Flynn [2,3] examined the heating of IDPs on atmospheric entry and concluded that IDPs must be predominantly from asteroidal sources because these asteroidal particles would have sufficiently low velocities to survive atmospheric heating with little or no modification whereas cometary particles would ordinarily have velocities that are much higher. Blanford [4] combined these approaches to show that most low-velocity particles would have similar track densities regardless of origin. We have continued to examine the relation of track densities to the orbital elements of source bodies and we will report on the positive and negative aspects of using track densities to determine the origin of IDPs.

Determining the buildup of tracks in an IDP follows the procedure of Sandford [1]. He used the formulas derived by Wyatt and Whipple [5] to follow the change in eccentricity and semimajor axis of a particle under the influence of radiation pressure and Poynting-Robertson drag. We have modified these formulas to include solar wind drag as 30% of Poynting-Robertson drag [6]. The modified formula for the time to go from eccentricity e_j to eccentricity e_j+1 ($e_j > e_j+1$) is given by

$$\tau_j = 9.58\times10^6 \frac{s\rho C^2}{\upsilon}\int_{e_{j+1}}^{e_j}\frac{e^{0.762}de}{(1-e^2)^{1/2}}$$

where s is the radius, ρ is the density (ρ = 1 g/cm^3 was used here), and υ is the absorption coefficient of the particle in cgs units. Burns et al. [7] have shown that a Mie coefficient should be used in general rather than an absorption coefficient. However, IDPs that are large enough to handle and analyze fall in a size range in which geometrical optics should apply and an absorption coefficient approximates the Mie coefficient. The constant C is given by

$$C = a_0 e_0^{-0.881}(1-e_0^2)$$

where a_0 and e_0 are the initial semimajor axis and eccentricity of the particle. The track density is then given by

$$\rho_{track} = \sum_{i,j} A\left[\frac{\Delta p_i}{r_i^{\beta}}\right]\tau_j$$

where A is the track production rate at 1 AU, which is assumed to follow an inverse square law from the Sun such that ß = 2. The

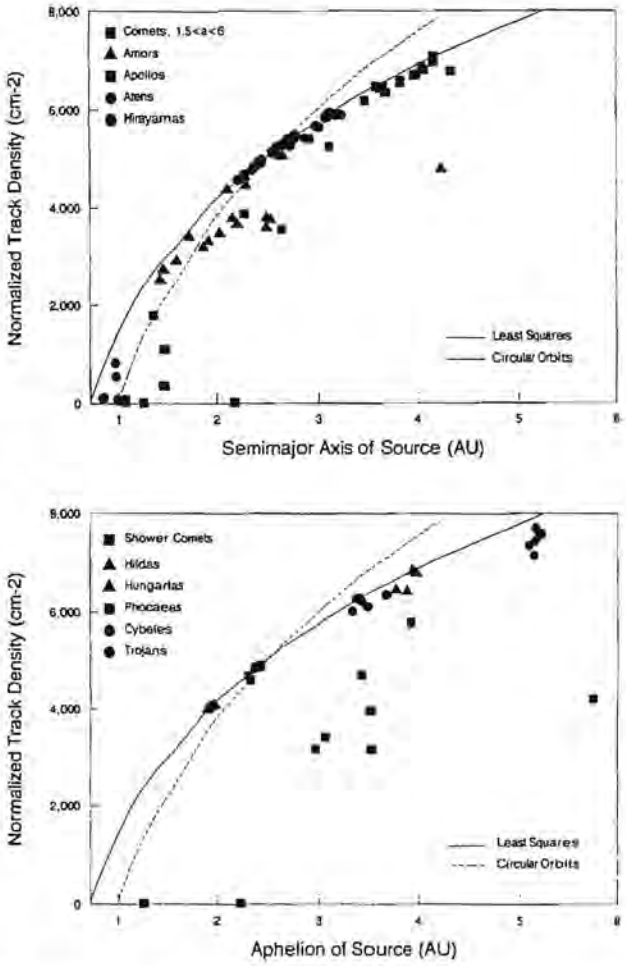

Fig. 1. Normalized theoretical track densities in 5 μm radius interplanetary dust particles (IDPs) graphed vs. the semimajor axis of the source body. The black line represents the lower limit of the semimajor axis of the source body for a particle of a given track density. It was found by taking a least squares fit of the track density as a logarithmic function of the semimajor axis for those bodies that appeared to define this lower limit curve. The red line is a similar line that can be derived analytically for particles in circular orbits (see text). Normalized track densities result from using a track production rate of 1 track/cm^2/yr.

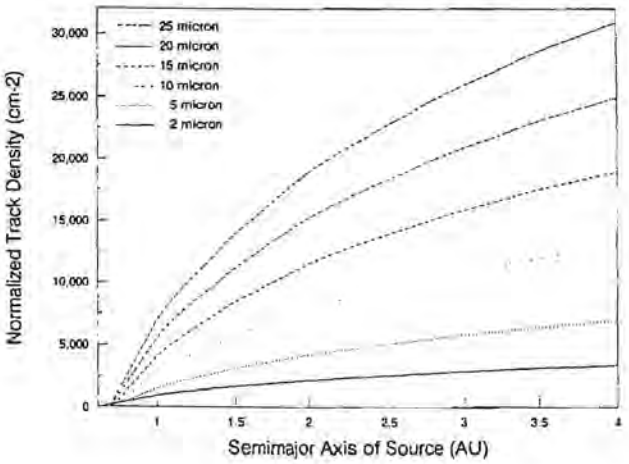

Fig. 2. This graph shows the calculated lower limit curve for track densities in IDPs of different radii. For a particle of a given size and track density the curves can be used to find the lower limit of the semimajor axis of the source body of the particle.

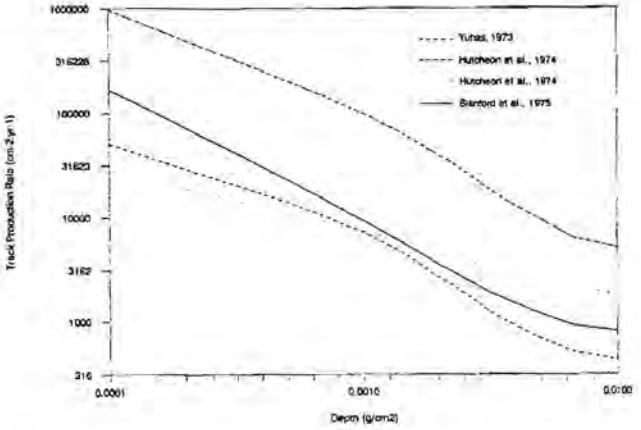

Fig. 3. The track production rate 1 AU as a function of depth in a 100 μm radius, spherical IDP derived from the measurements of three different groups of scientists [14,10,11]. These track production rates were made in lunar rocks that are >2 × 10^5 years old. These long-term average track production rates are probably better choises than the measurements made in the Surveyor glass [15-17]. Nevertheless, they give widely discrepant results. Zinner [12] concluded that the measurement of Blanford et al. [11] was probably correct to within 30%.

fraction of an orbital period Δp_i between r_i and r_i+1 ($r_i > r_i+1$) is given by

$$\Delta p_i = \frac{1}{\pi}\left\{\sin^{-1}\left(\frac{r-a}{ae}\right) - \frac{1}{a}\left[a^2e^2-(r-a)^2\right]^{1/2}\right\}^{r_i}$$

These formulas were coded such that Δp_i was calculated in steps of $r_i/100$ and time intervals were calculated for steps of $a/100$ or $\Delta e = 0.0001$, whichever was greater. The integration was finished when the line of nodes reached values of 1.017 AU and 0.983 AU. The geocentric velocities of the particle were also calculated at the nodal crossings.

The track production rate at 1 AU, A, must be integrated from the differential energy spectrum of solar energetic particles and the geometry of irradiation according to the formula given by Fleischer et al. [8]. Values for the differential energy spectrum of solar energetic particles have been extrapolated to the appropriate energy from measurements made in lunar samples by [9–11]. An important parameter in the integration is the observable track length ΔR. We have attempted to measure ΔR and have obtained a preliminary value of 0.475 μm. J. P. Bradley (private communication) believes the true value may be 1–2 μm. We will report on the correlation of predicted track densities derived from reported differential energy spectra with measured values [12].

We have found that from our calculations that predicted track densities for a particle of given size are related logarithmically to the minimum semimajor axis of the source body. Zook (private communication) has verified that this will be true for a particle in circular orbit decaying by Poynting-Robertson drag. Consequently, although track densities measurements may not be capable of distinguishing cometary from asteroidal sources, they should give us information on the minimum semimajor axis of the originating bodies.

It is known that high-velocity particles will volatilize in the atmosphere [e.g., 2,3]. For this reason we would not expect IDPs to come significantly from Apollo, Aten, from most of the Amor asteroids, and comets responsible for meteor showers [13]. The following obstacles will otherwise limit the usefulness of track densities in predicting the origin of IDPs. (1) We have very uncertain knowledge

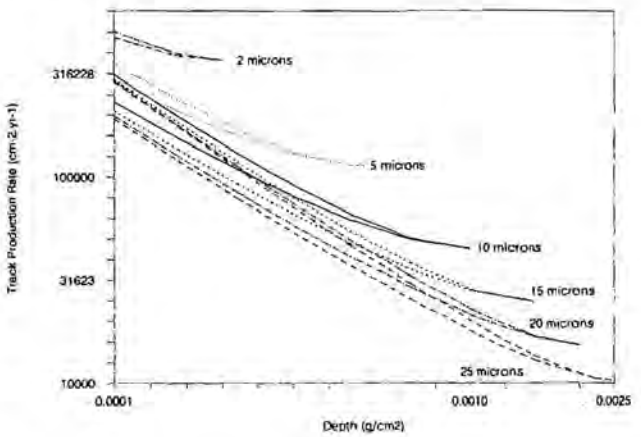

Fig. 4. The track production rate in spherical particles varies as a function of the depth in a particle, the size of the particle, and the orientation of the surface observed relative to the nearest surface of the particle. This graph gives the track production rate as a function of depth for particles of 6 diffferent radii. The upper curve in each pair is for a surface oriented parallel to the particle surface and the lower curve for a surface perpendicular to the particle surface. The track production rate of Blanford et al. [11] was used for the graph.

of the long-term average differential energy spectrum of solar energetic particles. The measured values [9–11] are all extrapolated to ranges appropriate for IDPs and none of the extrapolations agree with the others. (2) It is quite important to know the geometrical position of a grain with measurable tracks. We will show that track densities can easily differ by over an order of magnitude depending

on the grain's location in the IDP. (3) Statistical uncertainties arising from the relative low count of tracks in individual grains will severely limit our ability to determine the origin of an IDP. (4) IDPs that are ≥30 μm in radius will frequently achieve resonant orbits [6]. Track densities will indicate that they have been in resonant orbits, but otherwise they will be unrelated to the origin of the IDP.

References: [1] Sandford S. A. (1986) *Icarus, 68,* 377–394. [2] Flynn G. J. (1989) *Icarus, 77,* 287–310. [3] Flynn G. J. (1990) *Proc. LPSC 20th,* 363–371. [4] Blanford G. E. (1993) *LPS XXIII,* 131–132. [5] Wyatt S. P. and Whipple F. L. (1950) *Astrophys. J., 111,* 134–141. [6] Jackson A. A. and Zook H. A. (1992) *Icarus, 97,* 70–84. [7] Burns J. A. et al. (1979) *Icarus, 40,* 1–48. [8] Fleischer R. L. et al. (1975) *NuclearTracks in Solids: Principles and Applications,* Univ. of California. [9] Walker R. and Yuhas D. (1973) *Proc. LSC 4th,* 2379–2389. [10] Hutcheon I. D. et al. (1974) *Proc. LSC 5th,* 2561–2576. [11] Blanford et al. (1975) *Proc. LSC 6th,* 3557–3576. [12] Thiel K. et al. (1991) *Nucl. Tracks Radiat. Meas., 19,* 109–716. [13] Sandford S. A. and Bradley J. P. (1989) *Icarus, 82,* 146–166.

DESCRIPTION OF THE COMRADE EXPERIMENT

J. Borg[1], C. Maag[2], J.-P. Bibring[1], W. Tanner[3], and M. Alexander[3], [1]Institut d'Astrophysique Spatiale, Bat. 121, 91405 Orsay Cedex, France, [2]Science Applications International Corporation, Glendora CA 91740, USA, [3]Department of Physics, Baylor University, Waco TX 76798, USA.

The COMRADE experiment is designed to return minimally degraded particles to Earth along with complete *in situ* information concerning mass, velocity, and trajectory of encountered particles. The objectives of the program are very diverse. A set of flight-tested active detectors will be combined in an array to identify some of the physical properties of an incident grain, e.g., velocity vector, momentum, and mass. The use of passive detectors gives access to the chemical and isotopical properties of the grains in the micrometer size range. We are concerned simultaneously with a destructive capture, using metallic collectors, and a nondestructive capture, using a new low-density target in which the impacting grains stop, practically intact.

Introduction: The main scientific interest in the analysis of extraterrestrial particles, more commonly called interplanetary dust particles (IDPs), is due to the fact that some of these particles could be of cometary origin and thus contain information on the origin of the solar system. A second minor component is also present, originating from the asteroid belt. The smaller size fraction (grains less than 10 μm in diameter) is supposed to be enriched in grains of cometary origin. Also present is orbital debris with velocities of the same order and resulting from man-made activities (paint flakes, aluminum oxide spheres, etc.). The small-sized grains are the ones most frequently orbiting the Earth, man-made debris having, for all sizes, much larger fluences than extraterrestrial grains.

The Collection of Micrometeorites, Residue, and Debris Ejecta (COMRADE) experiment has been selected as a proposal for the EURECA pre-Columbus flight in order to gain information on all sizes of particles present in low Earth orbits, including submicrometer grains. We are concerned, simultaneously, with a destructive capture of orbiting grains using metallic collectors, improved since the COMET-1 experiment, and a nondestructive capture, using new low-density targets in which the impacting grains stop, practically intact. The advantage of the first type of capture is twofold: it allows us to gain information on the smallest size fraction and to detect the presence of light elements such as C. The interest in the second type of capture is to allow the extensive study of intact IDPs. Grains a few micrometers in size can be stopped in those low-density materials and recovered for further studies. Our COMRADE experiment will be the first one purposely coupling the two techniques. The proposed investigation, which will collect micrometer/submicrometer particles with a minimum of particle degradation, will at the same time measure the dynamic particle parameters (determination of its mass, velocity, trajectory, and, for some, charge) with a high degree of confidence.

Scientific Objectives: The primary objectives for this mission are (1) to identify the particle remnants of the micrometer-sized grains having impacted on purposely designed metallic collectors, for complete and detailed chemical, isotopic, and organic analysis, thereby determining grain composition as well as the existence of organic and inorganic molecules, to be related with the possible cometary origin of the grains showing an extraterrestrial signature; (2) to return captured intact particles to Earth for complete and detailed chemical, isotopic, spectral, mineralogical, and organic analysis, thereby determining grain composition as well as the existence of organic and inorganic molecules; and (3) to capture micrometer/submicromter dust grains in a manner that ensures minimal particle degradation and guarantees state-of-the-art confidence in measurement of the *in situ* particle parameters including trajectory, velocity vector, mass, and flux distributions.

Capture of Remnant Particles for Chemical Analysis: High-purity metallic surfaces are used for the collection of all grains down to submicrometer sizes. During the impact of a high-density impactor, a characteristic crater is formed, with rounded features and a depth-to-diameter ratio characteristic of the encountered metal, the velocity and size of the impacting particles. The particle is destroyed and the remnants are mixed with the target material, concentrating in the bottom of the crater or on the surrounding rims. Its chemical and isotopic properties can be identified by analyzing the rim material. In the case of impacting aggregates of very low density, it seems that the particle sticks to the collector, much less melted.

The major strength of the metallic collectors lies in the fact that these analytical techniques can be applied without modification to craters ranging from tens of nanometers up to millimeters in size, limited only by the thickness of the plate. Also, identification of C and organic material is made possible, which is essential for the study of extraterrestrial material in search of particles of cometary origin. Gold and Ni are metals suitable for such collectors; the evaporation of 50 nm of Au on the exposed surface noticeably increases the identification of the impacting position, as the tear of the film creates a decoration of the impact position, allowing it to be found more easily.

The collectors, after their exposure in space, are brought back in clean, sealed boxes to the clean rooms of the lab. There, the impact positions of the grains are identified directly on the surface of the collectors, either by optical microscopy for the larger ones or by using a scanning electron microscope for the micrometer-sized impacts, at a magnification that allows the identification of crater features down to diameters of 1 μm. We can thus analyze the size distribution of the impact features down to these sizes, allowing the evaluation of the incident microparticle flux in the near-Earth environment. In a second step, it is possible to determine, for each

selected crater, the chemical composition down to C of the impacting particles, generally physically destroyed and mixed with target material in the process of crater formation. For grains identified on a chemical basis as being of extraterrestrial origin, this analytical step is to be followed by a high-resolution analytical protocol including Field Emission Scanning Electron Microscopy (FESEM) imagery, and molecular and isotopic identification.

Intact Capture of Hypervelocity Impact Particles: The return of extraterrestrial material to the laboratory is a primary goal of this investigation. The proposed investigation intends to retrieve relatively unshocked material by impacting three types of "underdense" capture devices. Shuttle experiments (STS 41-B, 41-D, and 61-B) have shown that both organic foam and aerogel materials can be successfully used to capture intact particles. These underdense capture devices will also be complemented by the well-established technique of successive foils. A high-density impactor on a low-density target will experience the lowest level of damage.

Polymer foams will be currently employed for capturing particles with minimum degradation. The manufacture of extremely low-bulk-density (<0.1) materials is usually achieved by the introduction of voids into the material base. Polymer foam has been used to collect material on various STS flights. Intact particles, mainly of terrestrial origin, as small as 0.4 μm in size have been recovered. They are often recovered by encrusted pyrolized foam easily removed, leaving an undegraded specimen.

Measure of Fundamental Particle Parameters: The reliable determination of the trajectory of each individual dust particle is a high priority of the proposed investigation. Particle trajectories (as well as particle time of flight) can be determined using the thin film/plasma technique, which is based on the fact that a dust particle that impacts an extremely thin film will create a minute plasma cloud. The collection of this plasma cloud then allows for the analytic determination of dynamic particle parameters. The use of multiple thin films thereby yields a method whereby particle trajectories and time of flight can be determined.

In addition to the particle trajectory, it is vital that dynamic particle parameters also be measured with a high degree of reliability. The basic parameters that the proposed experiment will measure and/or determine are the particles' velocity and mass. The particle charge and time of flight can be measured by examining the thin film/plasma technique discussed previously. Also, by examining the amplitude of the plasma pulse produced, the kinetic energy of the particle can be obtained, which in turn enables a determination of the particles' mass. Since one of the major goals of the proposed instrument is to capture the particle while causing minimum particle degradation, it is necessary that extremely thin films be used in this sensor. The thinner the foil, the smaller the plasma produced and the more difficult it is to capture the signal produced.

Conclusion: It is in the context of research of cometary particles down to submicrometer sizes that our proposal of exposing materials in LEO must be perceived. The detection of these particles combines active detectors to determine the physical properties of the grains in LEO, with types of passive detectors (metallic collectors and low-density material). Any collection facility designed for a long-term exposure should contain some high-purity metallic targets for chemical and isotopic identification of particles. The coupling of metallic collectors and low-density material is a unique opportunity to complete information on all sizes of grains from submicrometer sizes to a few micrometers.

All grains down to submicrometer sizes can be collected on our metallic targets. Because of their high relative velocity (≥5 km s^{-1}), the impacting grains are physically destroyed, leaving a melted remnant that is mixed with the crater material. This process is more favorable for the smaller grains, with sizes in the micrometer range; the larger grains can vaporize, leaving no analyzable remnant. Our previous results have shown that Au and Ni collectors are favorable for the collection and analysis of the small-sized grains orbiting Earth. For the less frequent larger grains, their collection is possible on large surfaces of low-density material.

The analysis of the grains, either remnants or entire, will be performed with the high-resolution instruments we have access to (optical microscopy, SEM, EDS, FESEM, ion probe). By the time the collectors will be back from space, new techniques will have been developed and accessible for our analysis, for instance, IR spectroscopy of individual grains or double laser probe, promising techniques for identifying eventual organic molecular species present inside the grains. The possibility, offered for the first time with the EURECA platform to recover IDPs of cometary origin, in which the organic phase can be analyzed, is a very exciting one, as the comet grains remain privileged witnesses of the beginning of the solar system.

The COMRADE proposal expands upon a program initiated a few years ago with the COMET-1 experiment. It provides the collections of cometary dust and space debris as well as the characterization of their dynamic properties. It will consist of exposing a variety of detectors and captors on board spacecraft orbiting Earth. The opportunities in the future might include EURECA-2, LDEF-2, and possibly the MIR station to which an improved version of the COMET experiment could be attached. The latter flight opportunity would open the possibility to collect material at any given period and for any duration chosen.

WHAT DOES THE FINE-SCALE PETROGRAPHY OF IDPs REVEAL ABOUT GRAIN FORMATION AND EVOLUTION IN THE EARLY SOLAR SYSTEM?

J. Bradley, MVA, Inc., 5500/200 Oakbrook Parkway, Norcross GA 30093, USA.

The most widely studied interplanetary dust particles (IDPs) are those with bulk compositions that are approximately chondritic. Within the chondritic subset, there are believed to be at least three distinct mineralogical classes of IDPs, referred to as "pyroxene," "olivine," and "layer silicate" [1]. Infrared (IR) and analytical electron microscope studies indicate that most IDPs fall within this classification scheme [1,2], although there are exceptions. Collectively, chondritic IDPs have yielded information about grain formation and evolution, together with evidence of postaccretional processes. Since the three classes of chondritic IDPs yield somewhat different types of petrographic information, it is necessary to consider each class separately.

"Pyroxene" IDPs exhibit highly specific evidence of grain-forming reactions, which may have occurred early in the solar nebular or even in presolar interstellar environments. Gas-to-solid condensation is the fundamental grain-forming mechanism throughout the galaxy, and gas phase reactions have been a recurring theme among petrographic studies of pyroxene IDPs. For example, the most distinctive and easily recognized crystals in pyroxene IDPs, enstatite

($MgSiO_3$) whiskers and platelets, were probably formed by high-temperature (>1000°C) condensation in a relatively low-pressure nebular gas [3]. Some whiskers contain screw dislocations, resulting from spiral growth, and they have not been found in any other class of meteoritic materials. In a study of FeNi grains and carbonaceous material, a low-temperature carbide (ε $[FeNi]_3C$) was identified in several IDPs [4]. Epsilon carbide has been synthesized in the laboratory only by Fischer-Tropsch type (FTT) reactions between finely divided metal grains and C-containing gases (e.g., CO and CH_4). The presence of ε carbide in IDPs suggests that some of the carbonaceous material was emplaced by low-temperature (~200°C) catalytic reactions between metal grains and a C-containing gas (e.g., CO or CH_4). It has been suggested that FTT catalytic reactions played a role in the formation of organic compounds in chondritic meteorites [5]. A study of the crystal chemistry of Mg-rich olivines and pyroxenes in IDPs has shown that some of them contain unusually high levels of Mn (up to 5 wt%). Klöck et al. [6] have suggested that the Mn abundances can be explained in terms of condensation of olivines and pyroxenes from a gas of solar composition.

Pyroxene IDPs also contain fine-grained aggregates. In some IDPs, aggregates can account for >75% of the particle volume. At least three mineralogically distinct types of aggregates have been identified, whose mineralogy and petrography reflect significantly different formation/accretion environments or postaccretional histories. They have been referred to as unequilibrated, equilibrated, and reduced aggregates (UAs, EAs, and RAs) [7]. Some of these (0.1–0.3-μm-diameter) aggregates exhibit major-element compositions that are similar to the bulk composition of the IDP in which they reside. It is possible that they are agglomerates of submicrometer meteorites, some with solar compositions, which now form the matrixes of pyroxene IDPs.

"Layer silicate" IDPs are typically compact (nonporous) particles that contain (hydrated) phyllosilicates and sometimes Mg-Fe carbonates. Since it appears that they have undergone varying degrees of postaccretional alteration, evidence of earlier accretional mechanisms may be have been obscured or even erased completely. It has been suggested that layer silicate IDPs are probably derived from parent bodies similar to those of type CI and CM carbonaceous chondrites. This idea is supported by two tochilinite-containing layer silicate IDPs that have been linked directly to type CI petrogenesis [8,9], and one mixed layer silicate has been linked to type CI meteorites [10]. However, there are important petrographic differences between most layer silicate IDPs and the fine-grained matrixes of CI/CM meteorites [11]. Irrespective of their origins, most layer silicate IDPs exhibit evidence of postaccretional (aqueous) alteration, and evidence of primordial grain-forming reactions may have been obscured or even erased. Petrographic studies of the layer silicates and other secondary minerals may provide insight into the parent body regolith(s) of layer silicate IDPs.

"Olivine" IDPs are an enigma. Whereas solar flare tracks have now been found in many particles from the pyroxene and layer silicate classes, tracks are conspicuously absent in many of the olivine IDPs studied to date. Some olivine IDPs exhibit igneous textures and equilibrated silicate mineralogy and Fe-sulfides are commonly decorated with magnetite rims. These observations suggest that this class of chondritic IDPs is dominated by strongly heated objects. The absence of solar flare tracks leaves open the possibility that the heating is occurring during atmospheric entry. Pulse-heated IDPs are clearly unsuitable for petrographic studies aimed at investigation of primordial grain-forming reactions. However, since tracks have been observed in two olivine-rich IDPs [12], the olivine class may include IDPs from more than one genetic group. Future noble gas measurements may help clarify the thermal histories of olivine IDPs [13].

Summary: The "pyroxene" IDPs may be the best samples for investigation of primordial grain-forming reactions because they appear to have experienced negligible postaccretional alteration. They are likely to continue to yield information about gas-to-solid condensation and other grain-forming reactions that may have occurred either in the solar nebular or presolar interstellar environments. An immediate challenge lies in understanding the nanometer-scale petrography of the ultrafine-grained aggregates in "pyroxene" IDPs. Whether these aggregates contain components from diverse grain-forming environments may ultimately be answered by systematic petrographic studies using electron microscopes capable of high-spatial-resolution microanalysis. It may be more difficult to decipher evidence of grain formation and evolution in "olivine" and "layer silicate" IDPs because they appear to have experienced postaccretional alteration. Most of the studied "olivine" IDPs have been subjected to heating and equilibration, perhaps during atmospheric entry, while the "layer silicate" IDPs have experienced aqueous alteration.

References: [1] Sandford S. A. and Walker R. M. (1985) *Astrophys. J., 291*, 838. [2] Bradley J. P. et al. (1989) *EPSL, 93*, 1. [3] Bradley J. P. et al. (1983) *Nature, 301*, 473. [4] Christoffersen R. and Buseck P. R. (1983) *Science, 222*, 1327. [5] Hayatsu R. and Anders E. (1981) *Top. Curr. Chem., 99*, 1. [6] Klöck W. et al. (1989) *Nature, 339*, 126. [7] Bradley J. P. (1993) *LPS XXIV*, 171. [8] Bradley J. P. and Brownlee D. E. (1992) *Science, 251*, 549. [9] Reitmeijer F. J. M. (1992) *LPS XXIII*, 1153. [10] Keller L. P. (1992) *GCA, 56*, 1409. [11] Zolensky M. E. and McSween H. Y. (1988) in *Meteorites and the Early Solar System*, 114–143, Univ. of Arizona, Tucson. [12] Christoffersen R. and Buseck P. R. (1986) *EPSL*, 78, 53. [13] Nier A. O. and Schlutter D. J. (1993) *LPS XXIV*, 1075.

THE ORIGIN AND ROLE OF DUST IN THE EARLY SOLAR SYSTEM. D. E. Brownlee, Department of Astronomy, University of Washington, Seattle WA 98195, USA.

Dust was the primary building material of the solar nebula planetesimals that accumulated to form minor planets, solid planets, and the cores of giant planets. The original dust was of interstellar origin that initially formed circumstellar environments and was modified both in the interstellar medium and the local environments that preceded the formation of the Sun and planets. In the solar nebula the initial grains were modified by a variety of processes including heating, collisions, irradiation, accretion, adsorption, condensation, and chondrule formation, processes that occurred after accumulation into larger planetesimals (parent bodies). The effects of these processes had a wide range of severity that presumably varied with both the time and location of exposure of the grains to nebular conditions. In some cases it is likely that the primordial grains survived with little modification while in others the grains were totally reworked.

Collected IDP samples probably contain preserved samples of nebular dust that formed over a wide range of radial distance. There are two general source regions of IDPs, the asteroid belt and the

short-period comets. The collected asteroid particles are likely to be rather representative samples of material that accreted into planetesimals in the 2.2–3.3-AU region. The comet samples are likely to be representative samples of grains that accreted in the Kuiper belt region between 20 AU and some hundreds of AU. Many of the solar system effects on grains should have been more pronounced or even restricted to the <5-AU region where the asteroids formed. Evidence from meteorites indicates that there were highly complex processes and conditions in this region that produced diverse materials represented by the different meteorite classes. In the asteroid region there were transient heating effects that melted grains to form chondrules, there were high-velocity collisions, there was enhancement of nebular H_2O/H_2 ratio above solar values, there was ice condensation in at least the outer parts of the region, and there were "parent-body effects" that produced heating inside planetesimals that ranged from room temperature to >1300°C. As the Kuiper belt region is roughly an order of magnitude further from the Sun than the main-belt asteroids, it is likely that many of the previously discussed effects did not play significant roles in modifying cometary matter. The radial variations of spectral reflectance classes among the asteroids support the notion that many of the more destructive alteration processes were confined to the inner solar system.

A major goal of IDP research is to try to identify typical asteroidal and cometary IDPs and to study their properties. If successful this will provide fundamental insight into both the initial solids in the solar nebula and materials modified by a variety of important nebular processes.

LDEF METEOROID AND DEBRIS DATABASE. C. B. Dardano[1], T. H. See[1], and M. E. Zolensky[2], [1]Lockheed Engineering and Sciences Co., Houston TX 77058, USA, [2]NASA Johnson Space Center, Houston TX 77058, USA.

The Long Duration Exposure Facility (LDEF) Meteoroid & Debris Special Investigation Group (M&D SIG) database is maintained at the Johnson Space Center (JSC), Houston, Texas, and consists of five data tables containing information about individual features, digitized images of selected features, and LDEF hardware (i.e., ~950 samples) archived at JSC. About 4000 penetrations (>300 μm in diameter) and craters (>500 μm in diameter) were identified and photodocumented during the disassembly of LDEF at the Kennedy Space Center (KSC) [1], while an additional 4500 or so have subsequently been characterized at JSC. The database also contains some data that have been submitted by various PIs, yet the amount of such data is extremely limited in its extent, and investigators are encouraged to submit any and all M&D-type data to JSC for inclusion within the M&D database.

Digitized stereo-image pairs are available for ~4500 features through the database. However, because of the magnitude of image data (i.e., ~8.8 gigabytes), it cannot be stored online for direct user access. Presently these images reside on a set of 12 Maxtor OC-800 Laser Optical Disks, which can be made available on a loan basis. However, the M&D SIG is currently investigating the possibility of transferring these images to standard RCD CD-ROMs. If and when this occurs, a set of CD-ROMs would also be made available for temporary loan to interested investigators. Although the images are not stored on line, the database contains the file name and optical disk number on which the images can be found. A few images may be made available for downloading at the user's request.

Data Tables: The M&D database is broken into five major data tables in order to facilitate data entry and retrieval, yet information can be obtained from more than one data table simultaneously. These five data tables are the Primary Surfaces, Features, Cores, Digital Images, and Allocation History Tables. The Primary Surfaces, Cores, and Allocation History Tables are used for keeping track of the samples controlled by JSC, although they do contain additional information about the nature of the samples. The Features Table is the heart of the database, on which the other tables are based. This table contains one record for every feature that has been identified either at KSC, JSC, or by contributing investigators. The Digital Images Table serves as an index for retrieving digitized images of features.

Sample Numbering Scheme: The feature numbers recorded in the database represent a combination of the surface ID and a unique feature number for that surface. (The surface ID consists of four parts: the LDEF bay and row numbers, and the component type and number.) The bay and row numbers are the same as those initially assigned to the satellite grids, while the component type is a one-letter code that translates to a particular piece of hardware [e.g., "E" for experiment trays, "C" for tray clamps, "F" for frame pieces (intercostals and longerons), etc.]. The component number is a sequential number assigned to differentiate separate pieces of the same component type taken from the same bay and row location. (Note: Subsequent divisions of components, following their initial scan at KSC, are assigned two-letter subsurface designations for purposes of maintaining uniqueness of individual surface pieces.) Specific feature numbers are assigned sequentially as they are identified; numbers begin with "1" for each surface. These unique feature numbers remain with the individual feature, even if the initial component is subdivided at some later date.

Cores, which represent features that have been physically removed from a surface with part of the surrounding substrate, are numbered sequentially as they are generated. All LDEF cores are prefixed with the characters "LD-" to differentiate LDEF cores from those of other spacecraft hardware.

Primary Surfaces Table: The Primary Surfaces Table contains one record for each surface (and subsurface) on which features have been identified. The table contains fields for the origin, shape, orientation, surface area, substrate, location, and comments. These fields contain the following types of information:

Origin: LDEF experiment number, intercostal, longeron, thermal blanket, etc.

Shape: Rectangle, dimensions.

Orientation: Left, right, center, or position.

Surface Area: Area of the exposed surface in mm^2 (excluding overlaps and bolt holes).

Substrate: Material type (e.g., aluminum, Teflon, steel, gold, etc.).

Location: JSC location, PI (locations are recorded only for those surfaces controlled by JSC).

Features Table: The Features Table contains one record for each feature that has been identified, with each record containing fields for the site of identification, x and y coordinates, diameters, depth, impact type, and the presence of material and/or residues associated with the feature.

Site of Identification: KSC, JSC, or PI name.

x and y Coordinates: Two sets of coordinates are recorded; one set represents the coordinates relative to an origin assigned when the surface was originally scanned at KSC (see [1] for details on these procedures and the location of this origin). The other set represents the coordinates as recorded during any subsequent scanning of the surface at other facilities; offsets are calculated so that the data can be converted to the KSC coordinate values.

Diameters: Diameters for both the major and minor axes are recorded for noncircular features. The diameters currently recorded in the database represent center-of-lip-to-center-of-lip diameters. Analysis of the digital images is in progress at JSC and should provide diameters of the features as determined at the original target surface.

Depth: Depth information is presently recorded for only a few features; this information was provided by D. Humes and D. Brownlee. Analysis of the digital images will also provide depth information for features as determined from the original target surface.

Impact Type: Crater, hole or penetration, other (spray pattern, etc.).

Material Presence: Yes, no, and sometimes the quantity of material.

Cores Table: The Cores Table contains one record for each feature/core combination. In some instances, there may be more than one feature present on a given core because the close proximity of several features made it difficult or impractical to generate separate cores. In such cases, there are two (or more) records entered; both records have the same core number but different feature numbers. Additionally, there may be several records for different core numbers with the same feature number. This situation usually arises when the surface is made up of more than one layer of material and the feature is present on several layers (e.g., multilayer thermal blankets). This table contains fields for the core number, feature number, subsurface, layer, substrate type, and location.

Core Number: Sequentially assigned, unique integer prefixed by the characters "LD-". Core numbers are assigned in order, regardless of the surface on which they were identified.

Feature Number: Corresponds to the number of the feature (or features) physically present on the sample.

Subsurface: Additional designator for surfaces physically separated from original surfaces.

Substrate: Material type (e.g., aluminum, steel, Teflon, gold, etc.).

Location: JSC Lab or PI Name

Digital Images Table: The Digital Images Table contains one or more records for each image file name. Duplicate records with the same file name are allowed in order to accommodate images recorded at KSC and subsequent images recorded at JSC with the same name. Fields are included for the left and right image filenames, feature number, magnification, station number, disk number, and image date.

Left Image File or Right Image File: The image file names are constructed so that the feature number is contained in the file name, and so that these file names conform to the DOS standard of eight characters for the file name and three characters for the extension. For the first image pair of each feature the first character of the left image file is "L", while "R" is the first character for the right image file. Subsequent files are identified by consecutive alphabetic characters beginning with "A" and "B" for the left and right images, respectively. A potential third set of images would begin with the letters "C" and "D" respectively, and so forth. Characters 3–5 of the filename indicate the component type and number of the surface ID, while characters 6–9 represent the specific feature number (with embedded zeros for numbers less than 1000). The file extension indicates the LDEF bay and row grid location (e.g., A03, F10, etc.).

Feature Number: The feature number is included for the convenience of the user. It corresponds to the feature number in the Features Table, which may be derived from the image file name, in most instances.

Magnification: Represents the magnification at which the images were acquired.

Station Number: There were several scanning and imaging stations at KSC, and each one was assigned a separate number. All images acquired at JSC use station 7.

Disk Number: Represents the disk number (i.e., Maxtor Laser Optical Disk) on which the image resides. The characters "A" or "B" represent the front or back of the disk respectively.

Image Date: Indicates the date on which the images were acquired.

Allocation History Table: The Allocation History Table is used for recording the history of movement for primary surfaces and cores controlled by JSC. Every time a surface or core changes custody, an entry is made in this table. It contains fields for surface number, core number, investigator or site, and the date allocated.

Surface Number: Corresponds to the surface ID recorded in the primary surfaces table. Data is contained in this field only if the sample represents a primary surface.

Core Number: Corresponds to the core number (not the feature number) recorded in the cores table. Data is contained in this field only if the sample represents a core.

Investigator/Site: Either a NASA site or an investigator's name.

Date Allocated: Date the sample was allocated or returned to JSC.

Database Access: The LDEF database may be accessed via NSI/DECNET, Internet, or a modem. The results of searches can be downloaded to the user's local computer via FTP, Kermit, or e-mail. A small number of image files may be downloaded via FTP and, less efficiently, Kermit. The image files do not stay on line, but a limited number may be made accessible upon request. Procedures for accessing the M&D database are:

Via NSI/DECNET:

1. Log onto local host computer.
2. Type **set host 9300.**
3. Type **pmpublic** at the "Username:" prompt.

Via Internet:

1. Type **telnet 146.154.11.35** or **telnet curate.jsc.nasa.gov.**
2. Type **pmpublic** at the "Username:" prompt.

Via Modem:

The modem may be 300, 1200, or 2400 baud; no parity; 8 data bits; 1 stop bit. The area code is 713 for long distance calls.

1. Dial 483-2500.
2. Type **sn_vax** in response to the "Enter Number:" prompt.
3. Hit <CR> 2 or 3 times after the CALL COMPLETE message.
4. Type **j31x** in response to the "#" prompt.
5. Type **c curate** in response to the "Xyplex>" prompt.
6. Type **pmpublic** at the "Username:" prompt.

References: [1] See T. H. et al. (1990) *Meteoroid and Debris Features Documented on the Long Duration Exposure Facility: A Preliminary Report,* NASA JSC Publ. No. 24608, 586 pp.

DETECTION OF ASTEROIDAL DUST PARTICLES FROM KNOWN FAMILIES IN NEAR-EARTH ORBITS.

S. F. Dermott and J. C. Liou, University of Florida, Gainesville FL 32611, USA.

Introduction: Eos, Koronis, and Themis are the most prominent families in the asteroid belt. They are quite distinguishable in their ($e\cos\varpi$, $e\sin\varpi$) and ($I\cos\Omega$, $I\sin\Omega$) phase spaces. Naturally the dust particles produced from these families will have quite distinguishable initial orbital elements. However, when the dust particles spiral in toward the Sun due to Poynting-Robertson light drag, planetary perturbations and passages through resonances may cause their orbital elements to change to such an extent that they are no longer distinguishable when they reach the Earth. Secondly, forced inclinations and eccentricities are imposed on their orbits with the result that the osculating orbits in the vicinity of the Earth are quite different from those in the asteroid belt. The questions we would like to answer in this paper are (1) When dust particles arrive at the near-Earth orbit, is there still any difference between the orbits of the different families and (2) Can we still recognize the different family members from their orbits alone?

Method: We have studied the orbital evolution of dust particles with two different sizes (diameters equal to 4 μm and 9 μm) originating from the Eos, Koronis, and Themis asteroidal families. We first wind the solar system (without Mercury and Pluto) back in time numerically so that the dust particles being released from their origin will reach the Earth in 1983. We calculate the initial forced elements for each family (by using the orbital elements of seven planets at the time of release) and combine these with the proper elements to determine the starting orbital elements using the "particles in a circle" method [1]. We then numerically integrate 249 particles in each family using RADAU [2] on an IBM ES/9000. All the planetary perturbations, radiation pressure, Poynting-Robertson light drag, and corpuscular solar wind effect are included in the calculation. We record the orbital elements of each particle while they are moving toward the Sun and analyze the data.

Results: *4-μm particles.* We analyze the dust particles as they approach and pass the Earth. In Fig. 1 we plot the positions of dust particles for all three families in the ($I\cos\Omega$, $I\sin\Omega$) phase spaces every 300 years while they are Earth crossers. It is obvious that the Eos particles are quite distinguishable from the Themis and Koronis particles in inclination space. The proper inclinations of the dust particles are unchanged by orbital evolution [1]. On the other hand, all three families are no longer distinguishable in eccentricity space. This is primarily due to the fact that the radiation pressure and Poynting-Robertson drag change the eccentricities of dust particles, both from the very beginning when they were released and throughout their orbital evolution. Passage through mean motion resonances with Jupiter/Earth and trapping in the near-Earth resonances are not significant for particles with this size (the drag rate is too high).

The off-center distributions of Themis and Koronis particles in inclination space leads to another interesting result, the seasonal variation of particles being collected by an Earth-orbiting detector. In Fig. 2 we show the variation in terms of number of particles that intersect the Earth at their ascending nodes during different months in 1983 for Themis particles. The difference between the maxima and minima is larger than a factor of 3. The seasonal variation for Eos particles, which has a larger proper inclination, is not so obvious.

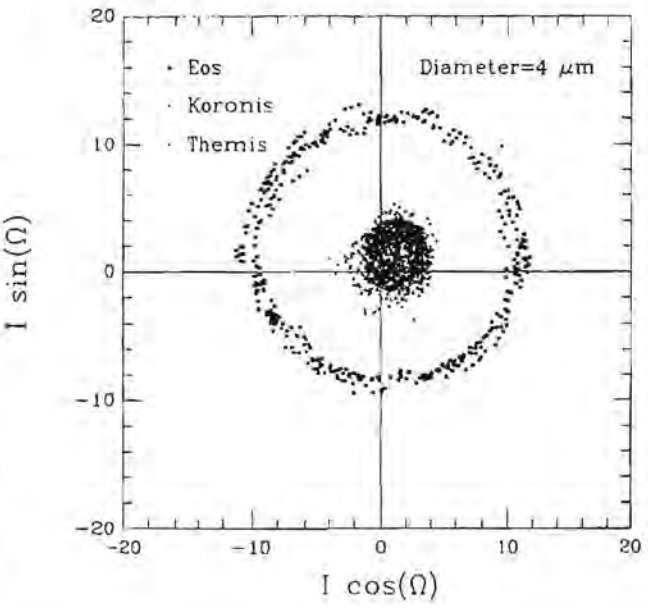

Fig. 1. The positions in ($I\cos\Omega$, $I\sin\Omega$) of 4 μm particles from all three families for every three hundred years when they become Earth crossers.

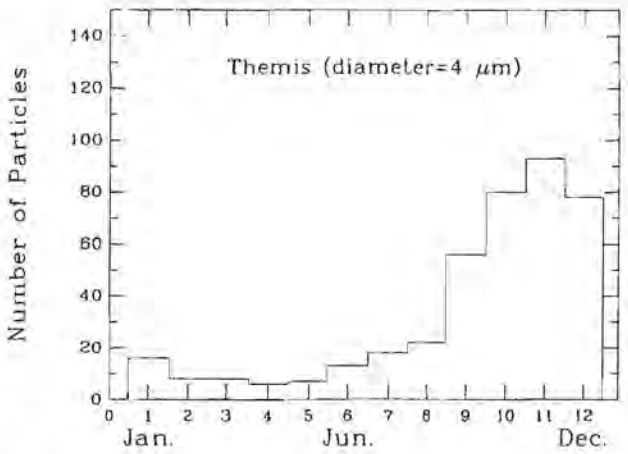

Fig. 2. The number of 4-μm Themis particles that intersect the Earth during the course of one year.

9-μm particles. These are the main contributor to the zodiacal cloud observed by the Infrared Astronomical Satellite (IRAS) at 25 μm wavelength [3]. These 9-μm particles move approximately twice as slow as 4-μm particles. Thus the number of particles being trapped in the near-Earth resonance increases somewhat. However, the overall trapping in resonance is still not significant. In the eccentricity space, dust particles from all three families mix up in the area between zero eccentricity and 0.1 eccentricity. In the inclination space, Eos particles are still quite distinguishable from the Koronis and Themis particles (Fig. 3). The off-center distribution for Koronis and Themis particles again results in the seasonal variation similar to Fig. 2.

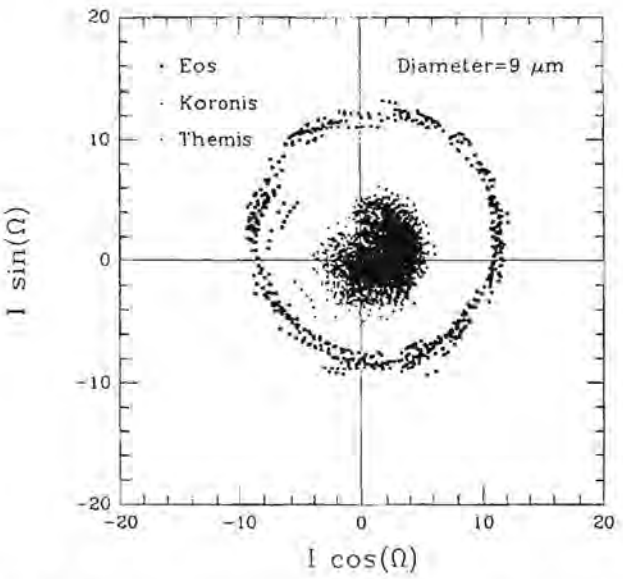

Fig. 3. The positions in (I cos Ω, I sin Ω) of 9 μm particles from all three families for every three hundred years when they become Earth crossers.

Discussion: From the distribution of dust particles in the inclination space we can clearly see that some families are distinguishable from one another. By knowing the position and velocity vectors of dust particles being collected at the near-Earth orbits, we can place them in the (I cos Ω, I sin Ω) space, and relate them to their possible origins. The off-center distribution in the inclination space of the dust particles is caused by the gravitational perturbation of planets. It produces two observational consequences: the first is the seasonal variation of the number of dusts intersecting the Earth and the second is the seasonal variation in the osculating inclination of particles from the same family. In Fig. 4 we show the results for two different size particles. From the diagrams we can see that even though the inclinations of particles vary a lot (for Eos particles, the inclinations vary from 7° to 12°; for Koronis and Themis particles they vary from 0° to 6°), Eos particles are well separated from Koronis and Themis particles. Furthermore, if we have an estimate of the size of the particle, then both the proper and the forced orbital elements can be calculated and these lead to an identification of the family members in near-Earth orbit.

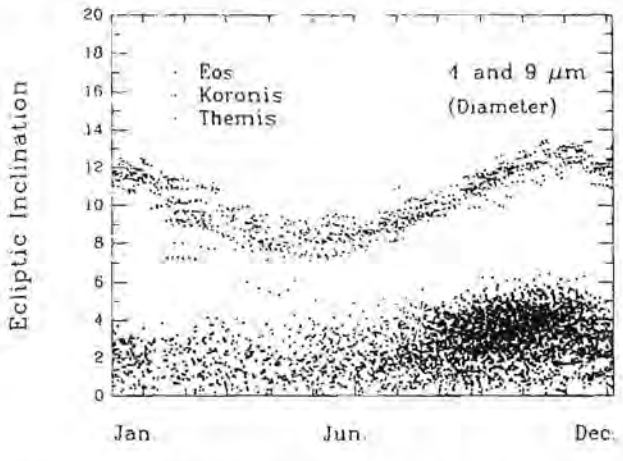

Fig. 4. The variation in osculating inclinations for both 4- and 9-μm particles with ascending nodes during the course of one year.

The differences in orbital elements of dust particles will cause different encounter velocities with the Earth, hence the difference in peak temperature on atmospheric entry. All these an be calculated from our results. Based on our study here, we conclude that for particles having diameters ranging from 4 μm to 9 μm, Eos particles are quite different in orbital elements from Themis and Koronis particles. For Koronis and Themis particles, the best times to collect them are around April and October.

References: [1] Dermott S. F. et al. (1992) In *Chaos, Resonance, and Collective Dynamical Phenomena in the Solar System* (S. Ferraz-Mello, ed.), Kluwer, Dordrecht. [2] Everhart E. (1985) In *Dynamics of Comets: Their Origin and Evolution* (A. Carusi and G. B. Valsecchi, eds.), 185–202, Reidel, Boston. [3] Dermott S. F. et al. (1993) *Proc. Slovak Acad. Sci.*, in press.

MODERN SOURCES OF DUST IN THE SOLAR SYSTEM.

S. F. Dermott, D. D. Durda, B. Å. S. Gustafson, S. Jayaraman, J. C. Liou, and Y. L. Xu, Department of Astronomy, University of Florida, Gainesville FL 32611, USA.

We have used the observed size-frequency distributions of the main-belt and family asteroids and the results of an analysis of the IRAS data on the zodiacal background and the solar system dustbands to estimate the extent of the contribution of asteroidal dust to the zodiacal cloud. In order to estimate the area of dust associated with the main-belt asteroids we must use the observed number of small asteroids as a basis for extrapolating to dust size particles. Although the discovery rate for asteroids has increased in recent years, the main-belt population of asteroids is complete with respect to discovery down to a diameter of only about 30 km, a very large size for our purposes. We have therefore used data from the McDonald and Palomar-Leiden Surveys (MDS and PLS respectively) [1,2] to extend our description of the size-frequency distribution to diameters nearly an order of magnitude smaller. We also demonstrate the validity of extending the distribution to yet smaller sizes by a power-law distribution expected for a collection of particles in collisional equilibrium [3]. We note that the observed slope of the asteroidal size-frequency distributiuon is in good agreement with the results of collisional models incorporating a size-dependent impact strength. However, we do need to know the strength of asteroidal grains to extrapolate the distribution of the sizes that determine the effective cross-sectional area of the dust. Without that knowledge, an uncertainty factor as large as 5 or 10 is introduced. Particles are also lost from the main belt by Poynting-Robertson (PR) light drag and there may be collisional loss due to fast-moving cometary particles. We conclude from the data on large asteroids alone that although asteroids could account for the whole of the zodiacal cloud, there is no way of proving it at present. The arguments with respect to a likely cometary component are even weaker and we do not attempt to discuss that source using similar arguments.

The IRAS (and COBE) data provide much stronger lines of argument. The survey of the sky made by IRAS in 1983 revealed the complex structure of the zodiacal cloud. We now know the inclina-

tion and nodes of the plane of symmetry of the cloud with respect to the ecliptic. Of even more interest is the discovery by IRAS of prominent dust bands that circle the Sun in planes near parallel to the ecliptic. In 1984 we suggested that the solar system dust bands discovered by IRAS are produced by the gradual comminution of the asteroids of the major Hirayama asteroid families [4]. The confirmation of this hypothesis has involved (1) the development of a new secular perturbation theory that includes the effects of PR light drag on the evolution of the dust particle orbits; (2) the production of a new high-resolution Zodiacal History File by IPAC (the Infrared Processing and Analysis Center at Caltech); and (3) the development of the SIMUL code, a three-dimensional numerical model that allows the calculation of the thermal flux produced by any particular distribution of dust particle orbits. SIMUL includes the effects of planetary perturbations and PR drag on the dust particle orbits and reproduces the exact viewing geometry of the IRAS telescope. These tools allow us to account in detail for the observed structure of the dust bands and to demonstrate that asteroids are indeed a significant source of zodiacal dust [5].

The dust bands evident in the IRAS data have very small amplitudes—not greater than a few percent of the ecliptic amplitude of the large-scale background signal. This does not imply that the asteroid families responsible for the the bands contribute only a few percent of the dust particles in the zodiacal cloud. The bands evident in the data are only the tip of the iceberg and, in fact, most of the flux derived from the dust generated by the family asteroids goes into the large-scale background. We use the observed dust band profiles and our modeling techniques based on SIMUL to estimate the total contribution of flux from the families and conclude that the families alone provide about 10% of the observed ecliptic flux. From the observed ratio of the number of family to main-belt asteroids, we conclude that the total asteroidal contribution to the zodiacal signal is probably 40% of the total flux.

Thus, some 60% of the flux probably derives from a nonasteroidal source, that is, a source other than main-belt asteroids (we have yet to investigate near-Earth asteroids). This conclusion is supported by a second independent line of argument based on the observed shape of the large-scale background cloud. It would appear that an asteroidal model alone cannot account for the large flux intensities observed near the ecliptic poles—flux from an asteroidal source is very much confined to near-ecliptic latitudes. Again, a cometary source could be the answer, but other sources, including interstellar dust, need to be investigated.

This work is supported in part by NASA through grants NAG 9-40 and NAGW-1923 and under the ADP program through NAG 5-1725. It was also supported in part by the University of Florida and the IBM Corporation through their Research Computing Initiative at the Northeast Regional Data Center.

References: [1] Kuiper G. P. et al. (1958) *Astrophys. J. Suppl., 3*, 289–334. [2] Van Houten C. J. et al. (1970) *Astr. Astrophys. Supp., 2*, 339–448. [3] Dohnanyi J. S. (1969) *JGR, 74*, 2531–254. [4] Dermott S. F. et al. (1984) *Nature, 312*, 504–509. [5] Dermott S. F. et al. (1992) In *Chaos, Resonance, and Collective Dynamical Phenomena in the Solar System* (S. Ferraz-Mello, ed.), 333–347, Kluwer, Dordrecht.

AN ASSESSMENT OF THE CONTAMINATION ACQUIRED BY IDPs DURING ATMOSPHERIC DECELERATION.

G. J. Flynn, Department of Physics, State University of New York–Plattsburgh, Plattsburgh NY 12901, USA.

The E-layer of the terrestrial mesosphere, between 80 and 110 km altitude, is derived from meteoric ablation [1]. Concentrations of Na and Fe, contributed by meteoric vapor have been monitored in the mesosphere, and both individual meteors and average concentration profiles have been measured [1].

Individual IDPs entering the Earth's atmosphere must pass through the mesospheric layers rich in meteoric volatile elements. Limits on the extent to which individual IDPs can be contaminated by meteoric volatile elements during deceleration in the upper atmosphere can be established by considering the extreme cases: the direct passage of an IDP through a meteoric vapor trail or the passage of an IDP through the mesospheric layer rich in meteoric volatiles.

The worst case for contamination would occur if an IDP were to pass directly through a meteoric vapor trail. In this case the local concentration of meteoric material is maximized. Peak densities of 10^4 atoms/cm^3 for Na and 10^5 atoms/cm^3 for Fe have been measured in meteor vapor trails [1]. However, these trails are small (~100 m wide) and persist for only a short period of time (typically a few minutes or less) [1].

During the direct passage of a 10-μm-diameter IDP through a 100-m-diameter vapor trail having a Na ion density of 10^4 atoms/cm^3 and an Fe density of 10^5 atoms/cm^3, the IDP would directly collide with only 80 Na ions and only 800 Fe atoms. This level of possible contamination is far below the indigenous Na and Fe contents of a chondritic IDP.

Kane and Gardner [1] have used Lidar to monitor an area of the sky for meteor vapor trails. They detected 89 meteor events in 450 hours of data aquisition. Assuming an average trail duration of 1 minute, a meteor trail appeared within the field of view of their instrument for about 0.0033 of the observing time. Thus, events in which a decelerating IDP passes through a meteor trail must be quite rare.

Alternatively, contamination could occur as the IDP passed through the mesospheric layer of vapor accumulated from many individual meteors. The effectiveness of this mechanism to produce IDP contamination can be modeled using the terrestrial accretion rate of meteors and the mesospheric residence time of their debris. The terrestrial accretion rate of meteoritic particles from 10^{-13} to 10^6 g in mass is estimated to be 16×10^9 g/yr [2]. If each particle were to initially have a Zn content equal to the CI meteorite content (~300 ppm), then the terrestrial accretion rate of meteoritic Zn would be 4.8×10^6 g/yr. Although some particles in this size range are known to survive atmospheric entry with their Zn intact, we can obtain an upper limit on the addition to this meteoric vapor layer by assuming that all 4.8×16^6 g/yr of Zn is deposited into the upper atmosphere. The surface density of Zn in this atmospheric (i.e., the total mass density along a line from the top of the atmosphere to the surface) can then be calculated as the product of the Zn residence time (t_{Zn}) and the Zn accretion rate divided by the surface area of the atmosphere [$4\pi R^2 = 4\pi\ (6.4 \times 10^6\ \text{m})^2 = 5.1 \times 10^{14}\ \text{m}^2$]. Thus, the maximum surface density of Zn in this atmospheric layer would be 9.4×10^{-9} g/m^2 × yr × t_{Zn}.

If we then allow a 10-μm-diameter IDP to pass through this layer during atmospheric deceleration, the particle could accrete all the Zn encountered by its cross-sectional area ($\pi r^2 = 8 \times 10^{-11}$ m^2). Thus, the total Zn accretion possible in this model is 8×10^{-19} g/IDP$\times$ t_{Zn}. To aquire a chondritic Zn content (300 ppm) by this mechanism requires the addition of 1.5×10^{-13} g of Zn to a 10-μm-diameter, density 1 g/cm^3, spherical IDP. Thus the value of the Zn residence time (t_{Zn}) would have to be 2×10^5 yr for the meteoric layer to have a high enough Zn content for this mechanism to be viable. However, Hunten et al. [3] have modeled the deposition of meteoric material into the Earth's upper atmosphere. They suggest that meteoric vaporization products probably recondense into "smoke" particles with a mean size of about 1 nm at an altitude of about 80 km. Even employing a viscous settling model, which results in much longer residence times than for models permitting coagulation and eddy diffusion used by Hunten et al. [3], Sutton and Flynn [4] calculate the descent of the 1-nm meteoric smoke from 80 km to 40 km takes no longer than 50 yr, far short of the 2×10^5 year Zn residence time required for the IDP to encounter a chondritic amount of Zn during deceleration in the mesosphere.

Alternatively, we could allow the IDP to collect Zn over a much larger area than its physical cross section. However, even if the 50-yr Zn residence time is assumed, each particle would require a effective Zn accretion cross section 4000 times its physical cross section. No mechanism by which a hot, high-speed IDP decelerating through the upper atmosphere could collect Zn (or other volatiles) over a cross section so much larger than the physical cross section of the particle has been suggested.

It appears the interaction of IDPs with meteoric vapor during deceleration in the upper atmosphere does not produce significant contamination of IDPs as they decelerate in the upper atmosphere.

References: [1] Kane T. J. and Gardner C. S. (1993) *Science, 259*, 1297–1299, Wiley. [2] Hughes D. W. (1978) in *Cosmic Dust*, 123–185. [3] Hunten D. M. et al. (1980) *J. Atmos. Sci., 37*, 1342–1357. [4] Sutton S. R. and Flynn G. J. (1990) *Proc. LPSC 20th*, 357–361.

CHANGES IN IDP MINERALOGY AND COMPOSITION BY TERRESTRIAL FACTORS.

G. J. Flynn, Department of Physics, State University of New York–Plattsburgh, Plattsburgh NY 12901, USA.

Major objectives in the study of interplanetary dust particles (IDPs) are to constrain the physical and chemical conditions in the early solar system, to characterize the particles making up the zodiacal cloud, and to infer the physical, chemical, mineralogical, and isotopic properties of the IDP parent bodies—the comets and the asteroids. However, the effects of terrestrial interactions alter the properties of some IDPs from those of the zodiacal cloud particles. The interactions can be separated into four distinct phases: near-Earth gravitational segregation, atmospheric entry deceleration, stratospheric residence, and the collection/curation process.

Near-Earth Gravitational Segregation: Gravitational focusing strongly biases all near-Earth collections in favor of IDPs derived from main-belt asteroids over those from comets [1]. Jackson and Zook [2] found that some 10-μm-radius IDPs from main-belt asteroids have geocentric velocities as low as 1 km s^{-1} (prior to acceleration by Earth's gravity) at the Earth capture opportunity. For an IDP with a 1 km s^{-1} encounter velocity the effective Earth capture cross section is 126$\times$ the physical cross section of the Earth [1]. By comparison, the Earth capture cross section for a particle derived from Comet Encke is only 1.15$\times$ the physical cross section. If IDPs of both types were equally prevalent in the zodiacal cloud, the low-velocity, asteroidal IDPs would outnumber the IDPs from Encke by a factor of 109 in Earth collections. Even if the mean velocity (4.79 km s^{-1}) of the main-belt asteroidal IDPs from Jackson and Zook [2] is used, the effective Earth capture cross section is 7$\times$ the physical cross section.

Atmospheric Deceleration: A 20-μm-diameter IDP experiences noticeable deceleration at altitudes above 175 km, and atmospheric deceleration continues until the IDP has slowed to atmospheric settling speeds (a few meters per second or less) at about 80 km altitude [3]. The duration of the atmospheric deceleration phase is generally less than a minute, though, in rare cases, IDPs can be captured into Earth orbit and experience repeated gentle decelerations of much longer durations [4].

Atmospheric Entry Heating: A procedure to model the heating pulse experienced by an IDP on atmospheric entry was developed by Whipple [5] and extended by Fraundorf [6]. Flynn [7] developed a computer simulation of the atmospheric entry heating and deceleration process, allowing the actual atmospheric density profile to be incorporated. This model predicts substantially less heating for small particles and for particles encountering the Earth at grazing incidence. Love and Brownlee [4] have extended these calculations with a computer simulation that includes the effects of partial vaporization.

However, these calculations all rest on assumed values for three parameters never measured experimentally: the IDP emissivity at temperatures from a few hundred degrees to the silicate melting temperature (~1600 K), the IDP drag parameter at gas densities appropriate for the upper atmosphere, and the degree of elasticity of the collisions. Following the arguments of Whipple [5], Flynn [3] has described the rationale for selecting values for these parameters. However, Fraundorf [6] suggested the blackbody emissivity assumption might break down for small particles, and Rizk et al. [7] have repeated the calculations using a theoretical expression for the emissivity. For spheres of forsteritic olivine ≥10 μm in diameter they found peak temperatures that agreed within 100 K with the predictions using a blackbody emissivity [7]. However, they predict peak temperatures of IDPs <10 μm several hundred degrees higher than those calculated by the blackbody assumption [7].

Mineral Transformations: The most obvious mineralogical alteration of IDPs on heating is the production of magnetite or maghemite, which has previously been observed in natural and artificially produced meteorite fusion crusts [8]. Studies on IDPs show the development of a magnetite rim correlates well with other indicators of severe atmospheric entry heating [9]. Magnetite rims are observed on both anhydrous and hydrated IDPs [10]. However, pulse heating studies have not yet been conducted on IDPs to determine the magnetite formation temperature, or the variation of this temperature with the initial IDP mineralogy. In studies on analog materials, magnetites form on layer silicates heated to 1100°C within 25 s [11].

Sandford [12] has shown that a layer-silicate IDP, pulse heated in steps from 190°–1200°C, showed pronounced changes in the depth of the 3.0-μm water band in its infrared absorption spectrum. This feature disappeared completely at 560°C. The alteration tem-

perature measured by Sandford [12] by infrared absorption cannot be correlated directly with changes, such as the alteration of a lattice spacing, visible in the TEM.

Although olivine and pyroxene, the dominant minerals in the anhydrous IDPs, are more stable than layer silicates, Keller et al. [9] report the alteration of olivine to laihunite in an IDP, and attribute this to high-temperature oxidation of the olivine.

Volatile Element Loss: Fraundorf et al. [13] showed that S was lost from chondritic IDPs heated to simulate the atmospheric entry thermal pulse. The S depletion became severe above 800°C, and they suggested a chondritic S/Si ratio was probably incompatible with an IDP having been heated above 800°C for even a few seconds [13]. However, they suggested some chondritic IDPs might have low intrinsic S/Si ratios (i.e., the distribution of S-bearing phases might be inhomogeneous in the parent body), thus low S/Si should not necessarily be interpreted as indicating severe heating [13].

Flynn [14] suggested that Zn, which is generally more volatile than S in meteorite heating experiments, could also serve as an indicator of IDP heating. Flynn and Sutton [15] have identified a subset of the chondritic IDPs that exhibit Zn depletions to less than 0.1 × CI. Flynn et al. [16], Thomas et al. [10], Klöck et al. [17], and Keller et al. [9] have demonstrated that Zn depletions correlate well with mineralogical evidence and He inferences of substantial atmospheric entry heating. However, pulse heating experiments on IDPs have not yet been performed to establish the Zn mobility temperature.

Fraundorf et al. [13] suggested that C, not measured in the pulse heating experiments, might be lost at low temperature. However, Thomas et al. [10] have identified both anhydrous and hydrated IDPs that have low Zn abundances and well-developed magnetite rims, but carbon contents of about 2× the CI abundance. The mobility of C in IDPs has yet to be established.

For the elements from Cr to Br, Flynn et al. [18] suggest that the mobility sequence is Zn, followed by Br, followed by Ge. However this mobility sequence rests on the assumption that both the severely heated and the less-heated IDP groups started out with the same average chemical compositions. Since cometary IDPs are expected to be heated to significantly higher temperatures, on the average, than main-belt asteroidal IDPs [14], compositional differences between the severely heated and the less-heated IDPs might reflect differences in the source compositions as well as the effects of element mobilities.

Solar Flare Track Annealing: Fraundorf et al. [19] have shown that fresh Fe ion tracks are annealed in olivine by a 25-s heating pulse at 572°C, while tracks in enstatite were annealed by heating to 705°C. Track annealing experiments have not been performed on actual solar flare tracks in IDP silicates, though these tracks are less stable in the TEM than fresh Fe tracks.

Loss of Solar-implanted Noble Gases: Nier and Schlutter [20] have demonstrated that implanted solar He is released from lunar grains and IDPs during heating pulses comparable to those experienced on atmospheric entry, and they suggest the release profile indicates the peak temperature.

Consistency of Thermal Indicators: Klöck et al. [17] have compared the heating inferences from a chemical indicator (degree of Zn depletion), a mineralogical indicator (the formation of a magnetite rim), and a noble gas indicator (the abundance and minimum release temperature of He) in a set of IDPs each of which was examined by three different techniques. Klöck et al. [17] found the three indicators provided a consistent picture of the degree of heating experienced by individual IDPs. However, Flynn et al. [21] found that two chemical indicators, Zn and S, gave contradictory indications of the degree of heating in 14 of the 30 IDPs for which both elements were measured, and that the Zn content agreed with other indicators of heating (magnetite and/or He content) in 6 of the 7 cases for which independent evidence of heating was available.

Particle Fragmentation: Particle fragmentation during entry could produce more extreme heating than calculated for the resulting fragments since a large particle penetrates more deeply into the atmosphere prior to deceleration. Fragmentation can also alter the distribution of densities, since particles are likely to fragment into their strongest subunits. However, Love and Brownlee [4] suggest few IDPs experience fragmentation because even fragile cometary IDPs melt before the dynamic pressure is sufficient for fragmentation.

Isotopic Fractionation: The large Zn depletions in some IDPs (≤0.01× CI in one IDP [10]) suggest vaporization of a substantial fraction of the starting Zn. If so, then large mass fractionations would be expected in the residual Zn due to Rayleigh fractionation.

Significant mass fractionations (up to 32‰amu) have been observed for Ni and Fe in magnetite-wüstite spherules recovered from the sea floor. Davis and Brownlee [22] infer the pre-atmospheric mass of these spherules from the fractionation.

Contamination During Entry: The Na- and Fe-layers of the terrestrial mesosphere, between 80 and 110 km altitude, are derived from meteoric ablation [23]. The passage of IDPs through these layers, rich in meteoric volatile elements, during atmospheric deceleration suggests two possible contamination mechanisms: IDP passage through a fresh meteoric vapor trail or IDP passage through the layer of meteoric material. Flynn [24] modeled the interaction of IDPs with mesospheric meteoric vapor, and concluded the fraction of IDPs that experience significant contamination by meteoric vapor during the deceleration process is very small.

Ion Implantation: During the initial stage of the deceleration the individual air molecules strike the surface of the IDP with energies ranging from about 4 eV amu^{-1} at a 30 km s^{-1} velocity to about 1 eV amu^{-1} at a 10 km s^{-1} velocity when viewed in the rest frame of the IDP. Thus the air molecules may penetrate several atomic layers into the IDP surface before stopping [5]. The low N content of IDPs suggests few if any of these air molecules are retained.

Stratospheric Residence: Typical IDPs spend weeks to months in the stratosphere, with settling rates of a few centimeters per second in the lower stratosphere [13]. Zolensky and Mackinnon [25] calculate the time between collisions for particles >1 μm is 5 × 10^9 yr, and for particles >0.1 μm is 10^8 yr, suggesting contamination by solid particles during stratospheric residence is small.

Chemical Contamination: Aerosol particles, predominantly H_2SO_4 droplets, are abundant in the Earth's stratosphere. Three stratospheric particles analyzed for surface chemistry by Auger spectroscopy showed a thin (~150 Å thick) S-rich layer, suggesting contamination by stratospheric H_2SO_4 aerosols. Because the contamination layer is thin, its effects on bulk particle chemistry are small, contributing <1 wt% S [25].

Halogens (particularly Br and Cl) are abundant in the stratosphere. Rietmeijer [28] has shown a correlation of particle settling time with Br abundance, and Flynn et al. [21] have reported enrichments of Br in IDPs with otherwise CI-like volatile element abundances, both suggesting the possibility of Br contamination.

Mineralogical Contamination: Rietmeijer [29] has detected silica-rich glass and trydimite in an IDP. He suggests these fragments are terrestrial volcanic debris, incorporated into the IDP during stratospheric residence.

Collection and Curation: The IDPs are collected into a layer of silicone oil. Despite efforts to remove this oil by cleaning, Sandford [30], using infrared absorption, and Rietmeijer [31], using analytical transmission electron microscopy, have demonstrated that silicone oil contamination remains.

Interactions on the collector surface may also cause contamination. IDPs may impact the collector near or on top of stratospheric H_2SO_4 droplets or terrestrial particles. Contamination might explain the unusual chemical contents, such as high Cd, measured in rare cases in otherwise chondritic IDPs.

The possibility of alteration induced by terrestrial factors is particularly important in cases where the the measured properties of the IDPs differ from what might be expected based on their general similarity to chondritic meteorites.

References: [1] Flynn G. J. (1990) *Proc. LPSC 20th*, 363–371. [2] Jackson A. A. and Zook H. A. (1992) *Icarus, 97*, 70–84. [3] Flynn G. J. (1989) *Proc. LPSC 19th*, 673–682. [4] Love S. G. and Brownlee D. E. (1991) *Icarus, 89*, 26–43. [5] Whipple F. L. (1950) *Proc. Nat. Acad. Sci., 36*, 687–695. [6] Fraundorf P. (1980) *GRL, 10*, 765–768. [7] Rizk B. et al. (1991) *JGR, 96*, 1303–1314. [8] Browlee D. E. et al. (1975) *JGR, 80*, 4917–4924. [9] Keller L. P. (1992) *LPS XXIII*, 675–676. [10] Thomas K. L. et al. (1992) *LPS XXIII*, 1427–1428. [11] Flynn G. J. et al. (1993) *Proc. NIPR Symp. Antarct. Met.*, in press. [12] Sandford S. A. (1986) *LPS XVII*, 754–755. [13] Fraundorf P. et al. (1982) in *Comets*, 383–409, Univ. of Arizona. [14] Flynn G. J. (1989) *Icarus, 77*, 287–310. [15] Flynn G. J. and Sutton S. R. (1992) *Proc. LPS, Vol. 22*, 171–184. [16] Flynn G. J. et al. (1992) *LPS XXIII*, 375–376. [17] Klöck W. et al. (1992) *Meteoritics, 27*, 243–244. [18] Flynn G. J. et al. (1993) *LPS XXIV*, 495–496. [19] Fraundorf P. et al. (1982) *Proc. LPSC 13th*, in *JGR, 87, A409–A412*. [20] Nier A. O. and Schlutter D. J. (1993) *LPS XXIV*, 1075. [21] Flynn G. J. et al. (1993) *LPS XXIV*, 497–498. [22] Davis A. M. and Brownlee D. E. (1993) *LPS XXIV*, 373–74. [23] Kane T. J. and Gardner C. S. (1993) *Science, 259*, 1297–1300. [24] Flynn G. J., this volume. [25] Zolensky M. E. and Mackinnon I. D. R. (1985) *JGR, 90*, 5801–5108. [26] Mackinnon I. D. R. and Mogk D. W. (1985) *GRL, 12*, 93. [27] Mogk D. W. et al. (1985) *LPS XVI*, 569–570. [28] Rietmeijer F. J. M. (1992) *Meteoritics, 27*, 280–281. [29] Rietmeijer F. J. M. (1986) *LPS XVII*, 708–709. [30] Sandford S. A. and Walker R. M. (1985) *Astrophys. J., 291*, 838. [31] Rietmeijer F. J. M. (1987) *LPS XVIII*, 836–837.

COMETARY DUST: A THERMAL CRITERION TO IDENTIFY COMETARY SAMPLES AMONG THE COLLECTED INTERPLANETARY DUST.

G. J. Flynn, Department of Physics, State University of New York–Plattsburgh, Plattsburgh NY 12901, USA.

The relative proportions of the cometary and the asteroidal contributions to the interplanetary dust have not yet been definitively established. These proportions may vary with time as a result of major catastrophic disruptions in the main belt [1] or the appearance of fresh, active comets [2]. Dermott et al. [3] and Reach [4] suggest the debris from catastrophic collisions in the main belt can account for most of the zodiacal cloud particles. Earth collection of these asteroidal particles is strongly favored by near-Earth gravitational enhancement [5]. However, comets are observed to produce interplanetary dust particles (IDPs), and the identification of cometary IDPs would allow inferences of the compositions, mineralogies, and physical properties of the comets.

Flynn [6] has shown that IDPs derived from main-belt asteroids, from comets with perihelia >1.5 AU, and from comets with perihelia ≤1.5 AU separate into three distinct velocity groups, as shown in Table 1. These velocities, calculated for nodal crossing at 1 AU in the absence of Earth's gravity, can be transformed into atmospheric entry velocities using energy conservation

$$v_{entry} = [(11.1 \text{ km s}^{-1})^2 + (v_{nodal\ crossing})^2]^{1/2}$$

Main-belt asteroidal particles, which encounter the Earth from nearly circular orbits, have entry velocities ranging from Earth's escape velocity (11.1 km s^{-1}) up to about 12.4 km s^{-1} (nodal crossing velocity = 5.5 km s^{-1}) in the model developed by Flynn [6].

Jackson and Zook [7] have modeled the evolution of dust grains released from 15 main-belt asteroids, 15 short-period comets with perihelia >1 AU, and 5 long-period comets with perihelia <1 AU. Their results, which include planetary gravitational perturbations, have confirmed the existence of the three velocity regimes, though there is some overlap, particularly among the two cometary groups (see Table 1). Almost all 10-μm-radius dust from main-belt asteroids had nodal crossing velocities at 1 AU ≤7.5 km s^{-1}, corresponding to atmospheric entry velocities ≤13.4 km s^{-1}, only slightly higher than the ≤12.4 km s^{-1} atmospheric entry velocity limit for dust from main-belt asteroids previously suggested [6].

A few main-belt asteroids, such as Hungaria and Phocaea, have unusually high orbital inclinations, approximately 23° in each case. These two asteroids, and other members of their families, produce IDPs indistinguishable from cometary dust based on their entry velocities. However, the dust contribution from these two main-belt asteroid families is likely to be small. The major dust bands detected by the IRAS satellite are associated with the Eos, Themis, and Koronis families of asteroids, all of which have much lower orbital inclinations and produce IDPs that are easily distinguished from cometary IDPs by the entry velocity criterion.

The peak temperatures reached by IDPs on atmospheric entry indicate the distribution of IDP velocities [6]. Each IDP contains many internal thermometers: minerals that transform above certain temperatures, volatile elements that are lost sequentially with increasing temperature, solar flare tracks that anneal at different temperatures in different minerals, and solar-implanted noble gases that outgas progressively with temperature. Thus limits on the peak temperature reached by each IDP on Earth atmospheric entry can be set.

On an individual particle basis, the separation of IDPs into cometary and main-belt asteroidal groups on the basis of heating is complicated because the peak temperature reached on entry depends on the entry angle [6]. Thus a cometary IDP entering at grazing incidence is heated less extremely than a main-belt asteroidal IDP with the same physical properties entering at normal incidence [6].

However, it is possible to distinguish some cometary IDPs from their main-belt asteroidal counterparts since the normal incidence case results in the most extreme entry heating. Thus IDPs can be separated into two groups: one group containing particles heated

TABLE 1. Velocity range at nodal crossing for 10-μm-radius IDPs.

Parent Body	Velocity Range at 1 AU Nodal Crossing (km s^{-1})	
	Flynn [6]	Jackson and Zook [7]
Main-belt Asteroids	0–5.5	1–7.5*
Comets		
Perihelia >1.5 AU (or >1 AU)†	5.5–11	5.3–17‡
Perihelia <1.5 AU (or <1 AU)†	>11	>11.8

* Except for IDPs derived from the Hungaria and Phocaea families, which have velocities up to 13.5 km s^{-1} at nodal crossing.

† Jackson and Zook [7] separate the comet groups at a perihelion of 1 AU, while Flynn [6] separates them at 1.5 AU.

‡ Except IDPs from one comet having 25.3 km s^{-1} at nodal crossing.

above the maximum temperature possible for main-belt asteroidal particles of that size and density, and a second group that is less heated. The first group contains only cometary particles (and a minor contribution from asteroids in highly elliptical or highly inclined orbits). The second group includes asteroidal particles and cometary particles having small incidence angles.

Using the atmospheric entry interaction model developed by Whipple [8] and extended by Fraundorf [9], the peak temperature reached during atmospheric entry was calculated for normal incidence at a velocity of 13.4 km s^{-1} for IDPs with diameters ranging from 1 to 50 μm and densities of 0.6, 1.0, 1.9, and 3.0 gm cm^{-3} (see Fig. 1). The 13.4 km s^{-1} entry velocity (nodal crossing velocity = 7.5 km s^{-1}) is the upper limit for main-belt asteroidal IDPs, except rare IDPs from asteroids in high inclination orbits.

These peak temperature predictions assume blackbody emissivity at temperatures up to the peak experienced by each IDP. Rizk et al. [10] performed entry heating calculations using a theoretical expression for the emissivity appropriate for spheres of forsteritic olivine. Their peak temperatures agree to within 100 K with predictions assuming a blackbody emissivity for particles ≥10 μm in diameter [10]. However, they calculated that particles significantly smaller than 10 μm are heated to peak temperatures several hundred degrees higher than predicted using the blackbody assumption. Thus the peak temperatures in Fig. 1 are likely to be valid for particles ≥10 μm in diameter, but the validity of these calculations for smaller particles (particularly those ≤5 μm in diameter) cannot be assessed because the actual emissivity of silicate grains in a high C matrix has not been determined.

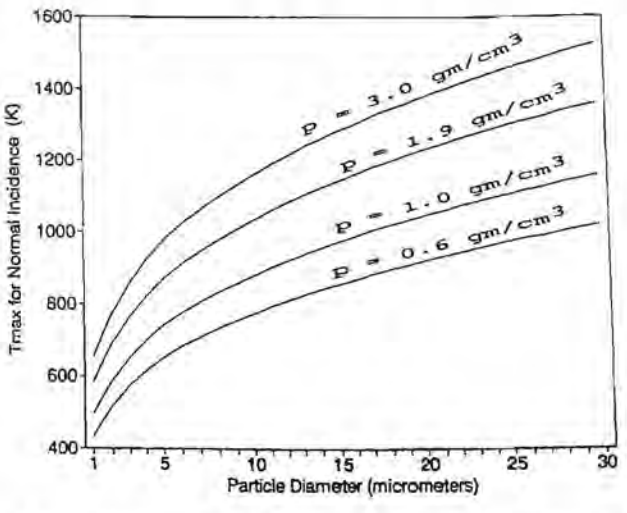

Fig. 1. Peak temperature (T_{max}) reached by main-belt asteroidal IDPs (v_{entry} = 13.4 km/s, normal incidence,) during atmospheric entry vs. particle diameter and particle density (p).

The collection of small cometary particles at Earth is hampered because solar radiation pressure imposes a lower limit on the size of cometary particles that remain bound by solar gravity [11]. For example, dust ≥8 μm in diameter emitted by comet Giacobini-Zinner near perihelion is expelled from the solar system (see tabulation in reference [6]). This minimum diameter decreases for particles emitted at larger distances from the Sun; however, the dust production by comets peaks near perihelion.

Because of the uncertainty in the peak temperature calculations for particles ≥10 μm in diameter, and the likelihood that most of the small particles emitted by the major dust producing comets are ejected from the solar system, cometary IDPs can best be distinguished from main-belt asteroidal IDPs near 10 μm in diameter. A program of study of heated IDPs, including sequential measurements of major- and trace-element contents, particle densities, mineralogies, solar flare tracks, and He^4 content, has the potential of identifying a cometary subset of the IDPs.

References: [1] Sykes M. V. and Greenberg R. (1986) *Icarus*, 65, 5–69. [2] Whipple F. L. (1967) in *The Zodiacal Light and the Interplanetary Medium*, 409–426, NASA SP-150. [3] Dermott S. F. et al. (1992) in *Asteroids, Comets, and Meteors 91*, 153–156, LPI, Houston. [4] Reach W. T. (1991) in *Origin and Evolution of Interplanetary Dust*, 211–214. [5] Flynn G. J. (1990) *Proc. LPSC 20th*, 363–371. [6] Flynn G. J. (1989) *Icarus*, 77, 287–310. [7] Jackson A. A. and Zook H. A. (1992) *Icarus*, 97, 70–84. [8] Whipple F. L. (1950) *Proc. Nat. Acad. Sci.*, 36, 687–695. [9] Fraundorf P. (1980) *GRL*, 10, 765–768. [10] Rizk B. et al. (1991) *JGR*, 96, 1303–1314. [11] Burns J. A. (1979) *Icarus*, 40, 1–48.

CARBON IN COMET HALLEY DUST PARTICLES.

M. Fomenkova[1] and S. Chang[2], [1] California Space Institute, University of California–San Diego, La Jolla CA 92093-0216, USA, [2]NASA Ames Research Center, Moffett Field CA 94035, USA.

Comets are small bodies of the solar system containing primarily a mixture of frozen gases and carbonaceous and mineral grains. They are likely to preserve volatile material from cold regions of the protosolar nebula and remnants of interstellar dust and gas. More than 2500 mass spectra of cometary grains with masses in the range 5×10^{-17} to 5×10^{-12} g were measured *in situ* by PUMA 1 and PUMA 2 mass spectrometers on board the VEGA spacecraft during flyby missions to Comet Halley [1]. In this paper we discuss different organic and inorganic C-containing components discovered so far in comet Halley dust particles, the nature and abundance of which provide information about possible astrophysical sources of C and constrain models of interstellar grains.

[C] Phases: Among the grains analyzed, 97 in PUMA 1 data and three in PUMA 2 data contain ~99% C [3]. These particles comprise about 6% of the total C abundance in dust grains of comet Halley. All [C] grains contain some minor abundances of rock-forming elements. Specific [C] phases known in meteorites and

interplanetary dust particles—diamonds, graphite, or amorphous carbon—cannot be identified in cometary particles because mass spectra do not provide information about the structure of grains. In the Murchison carbonaceous meteorite, however, characterized [C] phases represent a small fraction of the total ~2% noncarbonate carbon: graphite ~10^{-4} and diamond ~10^{-2} [4].

[C] Particles: These were most abundant at the outbound segment of the VEGA 1 trajectory and uniformly present otherwise (Fig. 1). Comparison of the distribution of intervals between occurrences of the [C] grains with a Poisson law (Fig. 2) shows that the [C] grains were encountered as clusters along the trajectory and suggests there was a mechanism for disaggregating or disintegrating clusters of grains or larger grains in the coma. Chemical transformations or evaporation seem to be less probable than physical destruction (e.g., electrostatic disruption [6]) because known [C] phases are chemically stable and involatile.

The [C] particles prevail among small grains (Table 1; [7]). This is consistent with estimates of the sizes of circumstellar and interstellar C particles [8]. Mass loss from C stars may have contributed up to 50% of all matter injected into interstellar medium. Interstellar grains are believed to represent a major fraction of cometary dust [9]. In terms of their size and spatial distribution the [C] particles differ from other classes of comet Halley dust particles, and they probably represent a special population of preserved interstellar C grains.

Hydrocarbons: In PUMA 1 and PUMA 2 data, respectively, 42 and 6 particles contain primarily C and H, of which only 4 from PUMA 1 are "pure" [H,C] particles lacking any other elements. The class of [H,C] grains implies the presence of C-H bonds [3]. Such bonds exist in hydrogenated amorphous carbons and in polycyclic aromatic and highly branched aliphatic hydrocarbons, which are thought to occur in comets and interstellar clouds [10] and have been observed in carbonaceous chondrites [11]. Anomalously high D/H ratios in meteoritic hydrocarbons signify their interstellar origin. Based on H/C ratio, subgroups of the [H,C] class of comet Halley, dust particles were identified as mixtures of C phases and hydrocarbons in various proportions. About 10% of total C is contained in these grains, which are uniformly distributed in all mass ranges.

Complex Organic Matter: This material occurs in 145 particles of PUMA 1 data (of which 25 are "pure" CHON) and 26 particles of PUMA 2 data. Classes of CHON particles such as [H,C,N], [H,C,O], and [H,C,N,O] were supposed [3] to be mixtures of various carbons and organic components rather than a single component species. These particles are more abundant among large grains (Table 1), which also suggests they may be composed of "building blocks" of smaller size observed in other mass groups.

The bulk composition of these complex organic grains is ~$C_{100}H_{115}N_9O_{65}S_1$ (~$C_{100}H_{90}N_8O_{45}S_1$ if [C] grains and hydrocarbons were included) and they contain about 25% of the total C content. This compares with the 20–30% of meteoritic C extractable as relatively involatile organic compound and the 70–80% in the form of insoluble kerogen [11]. Abundances of H and O relative to C are higher in these cometary grains than in meteoritic kerogen ~$C_{100}H_{71-48}N_{1-3}O_{12}S_2$. Some of the cometary grains may contain water ice mixed with organic matter or, alternatively, H and O could have been chemically bonded to C and lost along with water as a result of depletion of volatiles from meteorite parent bodies. Bulk meteoritic kerogen samples are actually made up primarily of minute particles 0.1–0.01 μm [12], about the size of comet Halley CHON grains. The isotopically anomalous H and N in kerogens signify interstellar origins, and meteoritic kerogens can be mixtures of cometary CHON grains of interstellar origin. Despite the aqueous alteration and mild thermal evolution, relic cometary grains may well be discernible in kerogens extracted from meteorites.

There are also 22 grains in PUMA 1 data representing ~1% of the total C that contain [C,O] and [C,N] polymers [3]. These may be related to compounds identified as cyanopolyynes and multicarbon monoxides in the interstellar media.

Mixed Particles: In PUMA 1 and in PUMA 2 data, respectively, 897 and 255 particles were classified as mixed. By definition [5], in these grains the ratio of C to rock-forming elements is in the range 0.1–10 and they comprise about 40% of the total C abundance. The mixed particles were assumed to consist of various Mg/Fe silicates and organic matter (which is consistent with an increase of

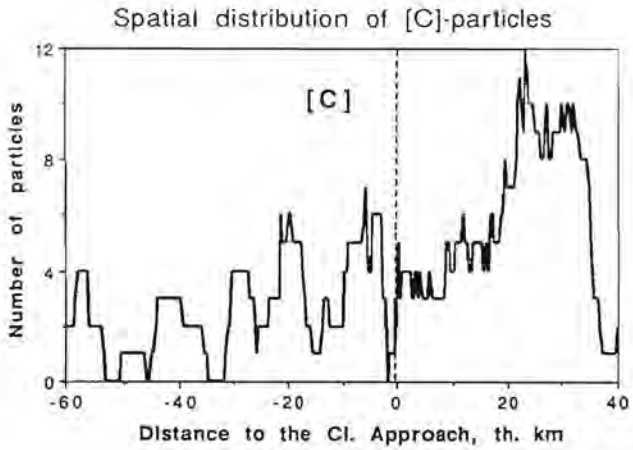

Fig. 1. PUMA 1 data. The number of encountered [C] grains was averaged with a 60-s moving window. At the closest approach the distance to the nucleus was ~8900 km.

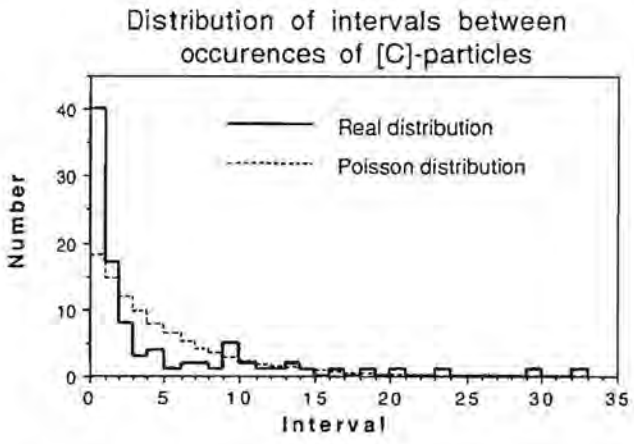

Fig. 2. Intervals between occurrences of the [C] grains in the coma are not randomly distributed. A Poisson law approximates random occurrences. A high peak at the interval equal to 1 indicates that frequently several grains followed closely upon each other. The long tail of the distribution indicates that such clusters were separated by relatively large distances.

their proportion among larger grains; Table 1), but we cannot exclude the possibility that a fraction of C can be bonded in minerals with rock-forming elements. More detailed analysis and/or classification of the organic part of the mixed particles has not been done yet.

Mg-Carbonates: The presence of Mg-rich grains in Comet Halley was previously noted [13]. Mg-carbonates were tentatively identified [5] in 77 particles of PUMA 1 data and 33 particles of PUMA 2 data. The presence of carbonates was also inferred from the weak 6.8-μm emission feature in the infrared spectrum [14]. The fraction of the total C in carbonates is estimated as 4%. In meteorites ~2–10% of C is in carbonates that are thought to be products of aqueous alteration that occurred in a parent body [15]. Carbonates are also minor, but persistent phases in anhydrous chondritic porous IDPs [16], which supposedly originated from short-period comets.

Carbonates in Comet Halley dust could have formed *in situ* by hydrocryogenic alteration. Such activity in nuclei of active short-period comets has been hypothesized [16] to take place in interstitial water layers at dust/ice interfaces below the melting point of water ice. On the other hand, the 6.8-μm feature was observed in protostellar spectra and the interstellar occurrence of carbonates has been suggested in [17].

Carbides: So far, SiC has not been identified among Comet Halley dust particles. Grains containing C, Si, and no Mg were considered as possible candidates, but all of them contain at least H and O, and sometimes also minor quantities of Na, Al, S, Cl, Fe, thus prohibiting unambiguous identification. The absence of SiC in comet Halley data probably can be explained by a statistical lack of data. In meteorites the proportion of SiC grains is ~6–8 ppm [18]. If the proportion of SiC in cometary solids were the same, then we would expect to discover one spectrum out of 10^5, while only 2500 spectra were measured by the PUMA 1 and PUMA 2 instruments and 3000 spectra were measured by the PIA instrument. The probability of one of them being SiC is ~0.05. The presence of FeC, however, can be suggested in 2–3 spectra.

Rock Particles: The analysis [5] revealed 430 grains in the PUMA 1 and 161 grains in the PUMA 2 data in which the ratio of C to rock-forming elements is <0.1. They contain <1% of the total C, which is below the level of measurement uncertainty. The proportion of rock particles decreases with an increase of the particle mass (Table 1). Cometary grains were suggested [3] to be built of small silicate grains embedded in a matrix of carbonaceous material.

[H] and [O] Grains: These particles (158 in the PUMA 1 and 16 in the PUMA 2 data) contain ~13% of the total C. The nature of these grains remains a mystery because the abundance of H and O is too high for chemically reasonable interpretation. Excess of H was explained by release of H dissolved in the target material [19] and the abundance of O in spectra may be strongly influenced by hypervelocity impact ionization processes [20]. On the other hand, the overabundance of H and O in some spectra may indicate the presence of water ice in these particles.

TABLE 1. Mass distribution of C-containing components of Comet Halley dust.

Mass Range	$<10^{-15}$		10^{-15}–10^{-13} g		$>10^{-13}$ g	
	N	%	N	%	N	%
[C] grains	51	9	33	3	16	2
Hydrocarbons	17	2–3	18	2	13	2–3
Complex organic	20	3–4	84	7–8	67	11
[C,N],[C,O] polymers	8	1	10	1	4	<1
Mixed particles	193	33	601	50	358	57
Mg carbonates	20	3–4	44	4	46	7
Rock particles	237	40	291	25	63	10
[H] and [O] grains	44	7–8	71	6	59	9
All	590	100	1152	100	626	100

PUMA 1 and PUMA 2 data are combined together. N = number of spectra. Percentages are the total number of spectra in each mass range.

References: [1] Kissel J. et al. (1986) *Nature, 321*, 280–282, 336–338. [2] Sagdeev R. Z. et al. (1986) *Proc. 20th ESLAB Symp. on the Exploration of Halley's Comet*, 349–352, ESA SP-250. [3] Fomenkova M. N. et al. (1993) *Science*, submitted. [4] Lewis R. S. et al. (1987) *Nature, 326*, 160–161; Blake D. F. et al. (1988) *Nature, 332*, 611–613; Zinner E. et al. (1990) *LPSC XXI*, 1379–1380. [5] Fomenkova M. N. et al. (1992) *Science, 258*, 266–269. [6] Mendis D. A. (1991) *Astrophys. and Space Sci.* [7] Fomenkova M. N. and Chang S. (1993) *LPSC XXIV*, 501–502. [8] Jura M. (1987) in *Carbon in the Galaxy*, 39–45, NASA CP-3061. [9] Greenburg J. M. and Hage J. I. (1990) *Astrophys. J., 361*, 260–266. [10] Encrenaz T. and Knacke R. (1991) in *Comets in the Post-Halley Era* (R. L. Newburn et al., eds.), 107–130, Kluwer; Colangeli L. et al. (1990) *Astrophys. J.*, 348, 718–726; Allamandola L. J. et al. (1989) *Astrophys. J. Suppl. Ser., 71*, 733–781. [11] Cronin J. R. (1988) in *Meteorites and the Early Solar System* (J. F. Kerridge and M. S. Matthews, eds.), 819–857, Univ. of Arizona, Tucson. [12] Reynolds J. H. et al. (1978) *GCA, 42*, 1775–1789. [13] Clark B. C. (1987) *Astron. Astrophys., 187*, 779–784; Mukhin L. M. et al. (1991) *Nature, 350*, 480–481; Halliday I. (1987) *Astron. Astrophys., 187*, 921–924. [14] Bregman J. D. et al. (1987) *Astron. Astrophys., 187*, 617–619. [15] Zolensky M. and McSween H. Y. (1988) in *Meteorites and the Early Solar System* (J. F. Kerridge and M. S. Matthews, eds.), Univ. of Arizona, 114–143, Tucson; Bunch T. E. and Chang S. (1980) *GCA, 44*, 1543–1577. [16] Rietmeijer F. J. (1991) *EPSL, 102*, 148–159. [17] Sandford S. A. and Walker R. M. (1985) *Astrophys. J., 291*, 838–844. [18] Zinner E. et al. (1991) *Meteoritics, 26*. [19] Jessberger E. K. et al. (1988) *Nature, 332*, 691–695. [20] Evlanov E. N. et al. (1991) in *Chemistry in Space* (J. M. Greenberg and V. Pirronello, eds.), 383–397, Kluwer.

REMOTE SENSING OF COMETARY DUST AND COMPARISONS TO IDPs.

M. S. Hanner, Jet Propulsion Laboratory, California Institute of Technology, Pasadena CA 91109, USA.

Comets are the best link we have to the composition of the primitive solar nebula. They have remained relatively unaltered since their formation in the outer, colder parts of the solar nebula.

***In Situ* Sampling:** We have *in situ* sampling of the dust composition of only one comet, from the impact ionization time-of-flight mass spectrometer on the Halley probes [1]. The composition of the major rock-forming elements is chondritic within a factor of 2, but the comet dust is enriched in the elements H,C,N,O compared to carbonaceous chondrites, implying that the dust is more volatile rich and more "primitive" [2]. Within the so-called CHON particles, there is a wide spread in the abundance ratios, a result that is not consistent with the proposal that there is a refractory organic component consisting mainly of polyoxymethelenes. Among silicate

particles, the Fe/(Fe + Mg) ratio ranges from 0 to 1, with Mg-rich silicates predominating. The wide distribution of Fe/(Fe + Mg) does not agree with the narrow range measured in carbonaceous chondrites, but does resemble anhydrous IDPs [3].

Infrared Spectroscopy: Infrared spectroscopy is the best means of remotely studying the composition of cometary solids. The spectra can help to establish links to interstellar grains and to identify classes of IDPs likely to originate from comets. Vibrations within various organic molecules produce features in the 3-μm region, while the 10-μm spectral region contains information about the mineral content of the grains.

Spectral features from organic molecules. A broad emission feature at 3.36 μm was discovered in Comet Halley (Fig. 1) [4–8]. It has subsequently been detected in every bright comet observed in the 3-μm region [9–14]. The feature is generally assigned to a C-H stretch vibration, but it is not obvious from the shape of the feature whether it originates in the gas or in small grains. The detailed structure varies among comets, with secondary peaks at 3.28 μm, 3.41 μm, and 3.52 μm having differing strengths relative to the main 3.36-μm peak; the 3.28-μm peak is particularly visible in the long-period comet Levy 1990 XX [13]. The 3.28-μm peak resembles one of the set of unidentified infrared bands seen in H II regions, planetary nebulae, and a few young stellar objects, but there is no analogous 3.36-μm emission feature in any astronomical source [14].

Because the feature is seen in both new and evolved comets, it cannot be the result of cosmic ray irradiation of ices in the outer few meters of Oort Cloud comets. Brooke et al. [12] demonstrated that the strength of the 3.36-μm band emission correlates better with the gas production rate than with the dust continuum, implying a gas phase carrier. The 3.52-μm feature is consistent with the ν3 band of methanol (CH_3OH) [15]. But CH_3OH also has bands at 3.3–3.4 μm.

Reuter [16] has computed the contribution of methanol to the main 3.36-μm feature. Depending on how one normalizes the 3.52-μm feature, the accompanying contribution to the 3.36-μm feature ranges from 10% to 50%. Thus, the spectral shape and the heliocentric distance dependence of the residual "unidentified" 3.36-μm feature may be somewhat different from the total observed flux and we are back to the question whether the carrier is in the gas or solid phase.

Silicates. A broad emission feature near 10 μm is observed in intermediate bandpass filter photometry of most dynamically new and long-period comets [17,18]. The strength of the feature is quite variable, being strongest in "dust-rich" comets with a strong scatare reasonable.

Spectra at 8–13 μm with high signal/noise now exist for eight comets. Four are dynamically new comets (that is, thought to be coming in from the Oort cloud for the first time), two are long-period comets, and two (Halley and Brorsen-Metcalf) have periods ~70 yr. (These eight spectra will be analyzed in more detail in [19]).

The spectrum of Comet Halley is shown in Fig. 2, from [20]. There is a broad maximum at 9.8 μm and a narrower peak at 11.25 μm. A Halley spectrum from the Kuiper Airborne Observatory [21] shows similar peaks. The 11.25-μm peak agrees with that seen in olivine IDPs [22]. (1985), as illustrated in Fig. 2, and crystalline olivine is the probable source of the cometary peak. Other possible explanations for the peak at 11.25 μm, such as SiC or an organic component, can be ruled out from the width of the peak, abundance arguments, or for lack of any corresponding features, such as the 7.7–8.6-μm features present when an 11.3-μm feature is associated with

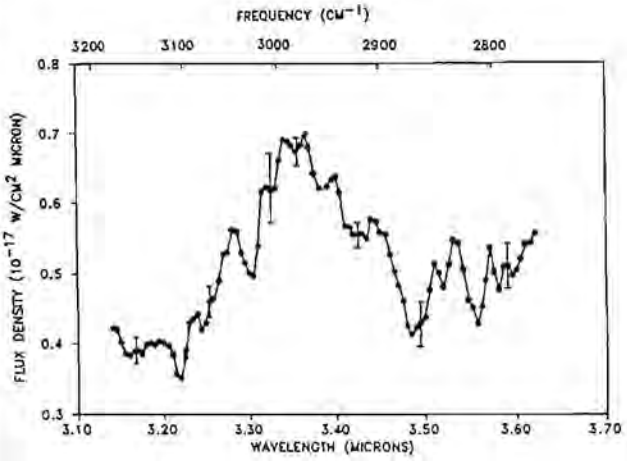

Fig. 1. 3-μm spectrum of Comet P/Halley on 25 April 1986 at r = 1.54 AU [7].

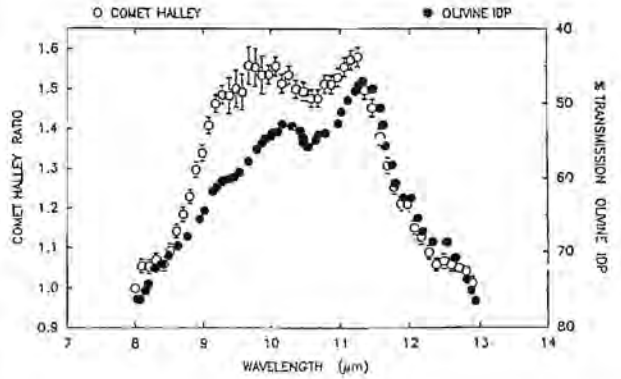

Fig. 2. 8–13-μm spectrum of Comet Halley at r = 0.79 AU [20] compared with olivine IDP [22].

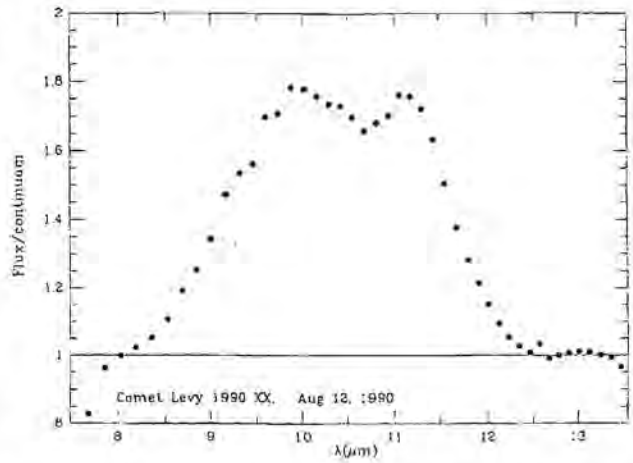

Fig. 3. 8–13-μm spectrum of Comet Levy 1990 XX at r = 1.56 AU perihelion [25]. The total flux has been divided by 270 K blackbody continuum.

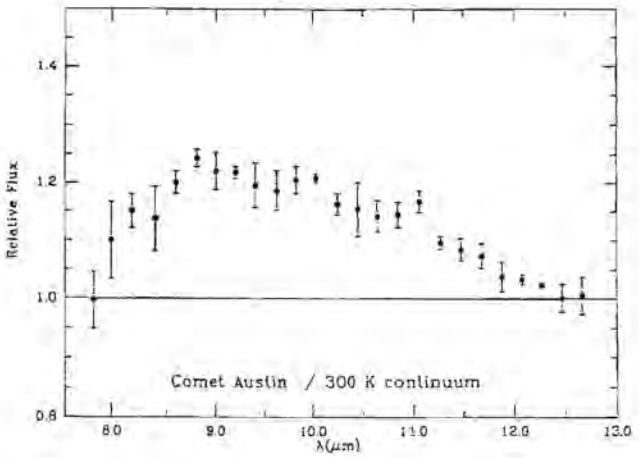

Fig. 4. 8–13-μm spectrum of Comet Austin 1990 V at 4 = 0.78 AU [19]. The observed flux has been divided by 300 K blackbody continuum.

the set of unidentified interstellar emission bands. Two long-period comets, Bradfield 1987 XXIX [23,24] and Levy 1990 XX [25] have similar double-peaked spectra. Levy's spectrum is shown in Fig. 3.

Koike et al. [26] have obtained infrared transmission spectra of olivine samples with differing Mg/Fe abundance. They find that the peak lies at 11.3 μm for Mg/(Mg + Fe) = 0.9 and shifts toward 11.5 μm as the Mg abundance decreases. The 11.25-μm position in the comets implies a high Mg/Fe abundance, a conclusion consistent with the dust analyses from the Halley probes [2,3].

However, another component must give rise to the broad maximum near 9.8 μm. There are three main possibilities [24]:

1. *Mix of crystalline minerals.* The IDPs examined in [22] can be classified by their 10-μm transmission spectra as olivines, pyroxenes, or hydrated silicates. A mix of these three grain types can approximately fit the Halley spectrum [21]. This approach has the advantage of relating the comet dust directly to IDPs. However, not all of these grain types necessarily originate from comets.

2. *Glassy silicates.* Interstellar silicate grains are thought to be amorphous because of their broad, structureless 10-μm feature. From the emission spectra measured in [27], amorphous olivine can explain the 9.8-μm cometary peak, while a mixture of amorphous olivine and amorphous enstatite can account for the rise between 8 and 9 μm. This explanation is attractive because it requires the least alteration of interstellar silicates before their incorporation into comets. A component of glassy silicate particles has recently been identified among the chondritic IDPs [28]. The spectrum of a thin section of a glass-rich IDP [28] resembles the comet spectra.

3. *Hydrated silicates.* Type II carbonaceous chondrites have about equal proportions of hydrated silicates and olivine. Their spectra actually look rather similar to the comet spectra [29]. Nelson et al. [30] suggested that amorphous silicate grains on the surface of a comet nucleus could absorb one or more monolayers of water molecules from the outflowing gas and could be converted to hydrated silicates if exposed to temperatures of 300 K or above for a few weeks. Yet, the silicate feature was strongest in Halley at times of strong jet activity when the silicate dust appeared to be emanating from deep vents in the nucleus rather than the surface. Moreover, the Mg/Fe/Si distribution in carbonaceous chondrites does not resemble the Halley dust [3].

Of the four new comets for which good quality spectra are available, each has a unique spectrum that differs from that seen in Comets Halley, Bradfield, and Levy. Kohoutek [31] has a strong emission feature similar to that in Halley, except that the 11.3-μm peak is lacking. Wilson 1987 VII [23] showed a broader emission feature with an unidentified peak at 12.2 μm. Okazaki-Levy-Rudenko 1989 XIX [32] had a weak feature with a maximum between 10.5 and 11.5 μm, while Austin 1990 V [33] showed a weak feature with a possible small peak at 11.1 μm (Fig. 4). Comets OLR and Austin were both dust-poor comets, based on the strength of their scattered and thermal continuum radiation; that is, the total dust cross section was low, but not necessarily the total dust mass, if the dust is concentrated in larger particles.

P/Brorsen-Metcalf showed the danger of generalizing. With a 70.6-yr period and perihelion at 0.48 AU, P/Brorsen-Metcalf has an orbit similar to that of P/Halley and one might have expected their spectra to be similar. Yet, Brorsen-Metcalf showed no emission feature at all in six days of observing [34].

Clearly, then, there is not a single kind of "cometary" silicate dust. Our sample of comets is too small to generalize about the characteristics of new vs. evolved comets. Spectra of one or more "dusty" new comets will be needed before we can conclude whether small crystalline olivine grains are ever present in new comets.

Acknowledgments: This research was carried out at the Jet Propulsion Laboratory, California Institute of Technology, under contract with NASA.

References: [1] Kissel J. et al. (1986) *Nature, 321*, 280, 336. [2] Jessberger E. K. et al. (1988) *Nature, 332*, 691. [3] Lawler M. E. et al. (1989) *Icarus, 80*, 225. [4] Combes M. et al. (1986) *Nature, 321*, 266. [5] Wickramasinghe D. and Allen D. (1986) *Nature, 323*, 44. [6] Knacke R. F. et al. (1986) *Astrophys. J., 310*, L49. [7] Baas F. et al. (1986) *Astrophys. J., 311*, L97. [8] Danks A. C. et al. (1987) *Astron. Astrophys., 184*, 329. [9] Allen D. and Wickramasinghe D. (1987) *Nature, 329*, 615. [10] Brooke T. Y. et al. (1989) *Astrophys. J., 336*, 971. [11] Brooke T. Y. et al. (1990) *Icarus, 83*, 434. [12] Brooke T. Y. et al. (1991) *Astron. J., 101*, 268. [13] Davies J. K. et al. (1991) *MNRAS, 251*, 148. [14] Green S. F. et al. (1992) in *Asteroids, Comets, Meteors 91* (A. W. Harris and E. Bowell, eds.), 211. [15] Hoban S. et al. (1991) *Icarus, 93*, 122. [16] Reuter D. C. (1992) *Astrophys. J., 386*, 330. [17] Ney E. P. (1982) In *Comets* (L. L. Wilkening, ed.), 323, Univ. of Arizona. [18] Gehrz R. D. and Ney E. P. (1992) *Icarus, 100*, 162. [19] Hanner M. S. et al. (1992) in preparation. [20] Campins H. and Ryan E. V. (1989) *Astrophys. J., 341*, 1059. [21] Bregman J. et al. (1987) *Astron. Astrophys., 187*, 616. [22] Sandford S. A. and Walker R. M. (1985) *Astrophys. J., 291*, 838. [23] Lynch D. K. et al. (1989) *Icarus, 82*, 379. [24] Hanner M. S. et al. (1990) *Astrophys. J., 348*, 312. [25] Lynch D. K. et al. (1992) *Icarus, 100*, 197. [26] Koike C. et al. (1993) *MNRAS*, in press. [27] Stephens J. R. and Russell R. W. (1979) *Astrophys. J., 228*, 780. [28] Bradley J. P. et al. (1992) *Astrophys. J., 311*, L97. [29] Zaikowski A. et al. (1975) *Astrophys. Space Sci., 35*, 97. [30] Nelson et al. (1987) *Proc. LPSC 17th*, in *JGR, 92*, E657. [31] Merrill K. M. (1974) *Icarus, 23*, 566. [32] Russell R. W. and Lynch D. K. (1990) in *Workshop on Recent Comets* (Huebner et al., eds.), 92, SWRI Albuquerque. [33] Hanner M. S. et al. (1993) *Icarus, 101*, 64. [34] Lynch D. K. et al. (1992) *Icarus, 97*, 269.

SOME CONSIDERATIONS ON VELOCITY VECTOR ACCURACY IN DUST TRAJECTORY ANALYSIS. A. A. Jackson[1] and H. A. Zook[2], [1]Lockheed Engineering and Sciences Company, Houston TX 77058, USA, [2]Solar System Exploration Division, NASA Johnson Space Center, Houston TX 77058, USA.

Introduction: The relative contributions of comets and asteroids to the reservoir of dust in the interplanetary medium is not known. There are direct observations of dust released from comets and there is evidence to associate the IRAS dust bands with possible collisions of asteroids in the main belt [1]. A means to sorting out the parent sources has been proposed in the establishment of a dust collector in orbit about the Earth [2]. The purpose of such a facility would be to collect not only cosmic dust particles intact but also the state vectors [3] as they arrive at the detector, the idea being that one may combine analytical laboratory analysis of the physics and chemistry of the captured particles with orbital data in order to help distinguish between bodies and identify parent bodies. The theoretical study of dust particle orbits in the solar system takes on greatly more importance if we use collected trajectory data. The orbital motion of dust when radiation and forces alone are acting is well understood [4]. When gravitational forces due to the planets are included, the motion can become quite complex [5– 7].

In order to characterize the orbits of particles as they crossed the Earth's orbits, a study of the long-time dust orbital evolution was undertaken. We have considered various parameters associated with these dust orbits to see if one may in a general way discriminate between particles evolved from comets and asteroids.

Preliminary Accuracy Considerations: We proceed in this study as we have done previously [7], that is, we consider the dust particles as ideal black bodies, with a density of 1 gm cc^{-1}, and spherical with radii between 10 and 100 μm. Particles of this size are effected by radiation forces, photon pressure, and Poynting-Robertson drag. Account was also taken of solar wind drag, which amounts to about 30% of the Poynting-Robertson drag negligible. The gravitational forces due to the planets are included, unlike in our previous study, and the planetary orbits are those of true n-body interaction so that the possibility of secular resonance is included. Our method was to calculate explicitly by a numerical procedure the orbits of dust particles after they left their parent bodies. The motion is determined numerically with the implicit Runge-Kutta integrator using Gauss-Radau spacings.

Particles are ejected from comets or asteroids at perihelion. This will happen due to some outgassing process on the comet or meteoric impact on an asteroid. Particles feel the immediate effect of radiation pressure and move on radiation-modified orbits that have new semimajor axis and eccentricity. Then the particle orbit was followed until it was well inside Mercury's orbit.

When the ascending or descending node of a test particle fell within the range of 0.983–1.017 AU from the Sun, a collision with a spacecraft in the same orbit as the Earth's becomes possible. The Earth is not a target for right now since we did not include the effects of its gravitational acceleration. Two orbital parameters proved useful for the characterization of parent body origin, orbital eccentricity e, and magnitude of relative velocity u, of intersection at the

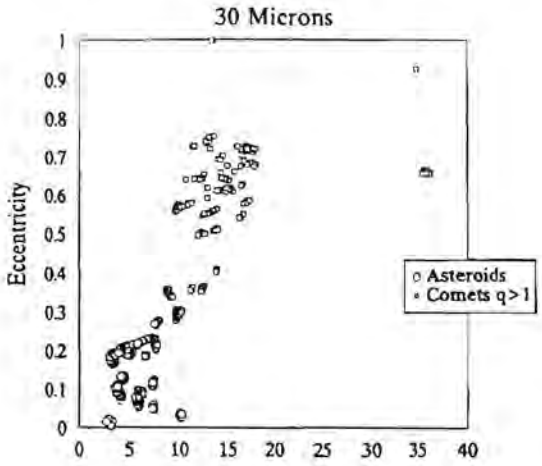

Fig. 1. Magnitude velocity at ascending node (km/s).

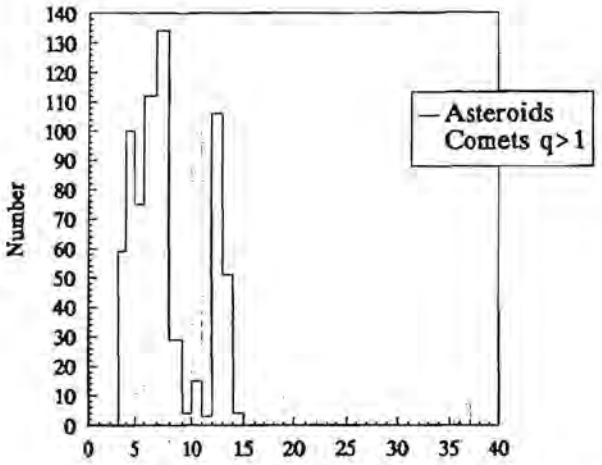

Fig. 2. Magnitude of relative velocity at ascending node (km/s) 30 μm.

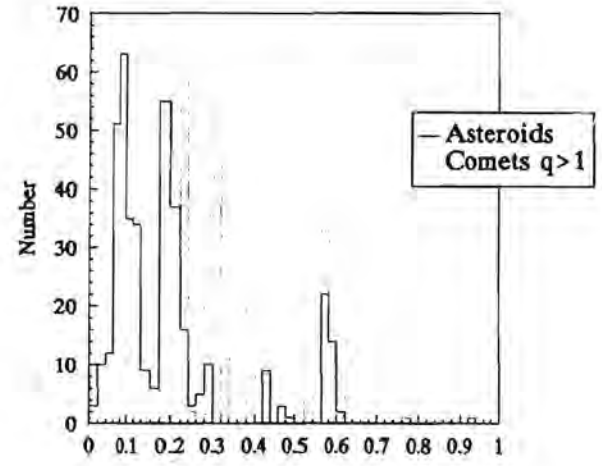

Fig. 3. Eccentricity at ascending node 30 μm.

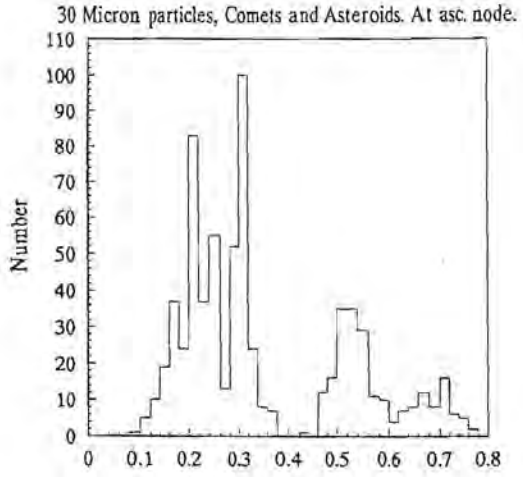

Fig. 4. Accuracy in magnitude of difference of velocities.

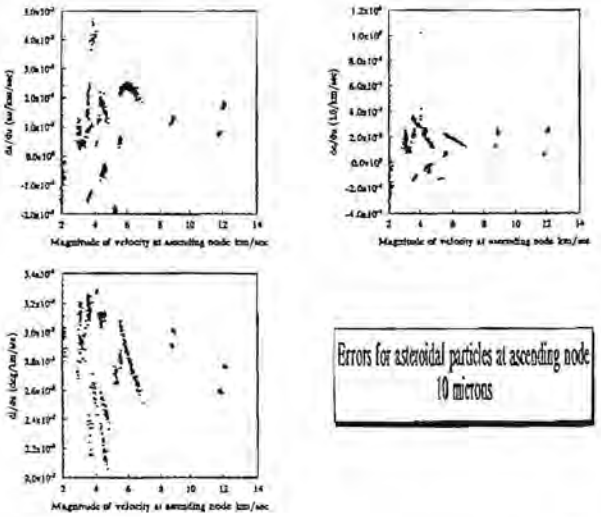

Fig. 6. Errors for asteroidal particles at ascending node 10 μm.

node.

For illustration we plot u vs. e in Fig. 1 for 30-μm particles. The circles are particles from asteroids and the squares are particles from comets. As might be expected, dust particles from the comets retain their high eccentricities, while asteroidal grains are of low eccentricity.

However, there is some overlap in eccentricity and velocity. Figures 2 and 3 show histograms of the magnitude of the velocity and eccentricity of the particle orbits from comets and asteroids at nodal crossing.

We considered as a measure of accuracy the following quantity

$$\mathrm{Acc} = (\delta v_r^2 + \delta v_t^2 + \delta v_n^2)^{1/2}|v|$$

where δv_r is the magnitude of the difference between the relative radial velocities of the asteroid and comet, δv_t is the magnitude of the difference between velocities tangential to the Earth's orbit, and δv_n is the magnitude of the difference between the velocities normal to the Earth's orbit. "Relative" here means the relative velocity between the dust particle and a hypothetical spacecraft in a circular orbit at the Earth's orbit.

Figure 4 shows the results of taking pair-wise for each 30-μm dust asteroid particle with each comet particle and keeping only the minimum value of the accuracy that results.

Error Analysis: We take the following as a simple model of the effect of measurement error on the determination of dust orbits by a detector. In order to make the problem tractable, take the dust detector to be in a circular heliocentric orbit with dust particles striking it. Such acceleration processes as the gravitational field of the Earth (important for a spacecraft orbiting the Earth) are not considered here.

We also take the collision to occur with the detector spacecraft at the dust particle orbit ascending node. Let there be a coordinate system x, y, z erected at the instantaneous position of the spacecraft and the intersection point of the dust particle. Where x is in the radial direction away from the Sun, y points tangent to the velocity vector of the circular spacecraft orbit, and z is along the angular momentum of the spacecraft orbit. Öpik (1963) then gives the components of

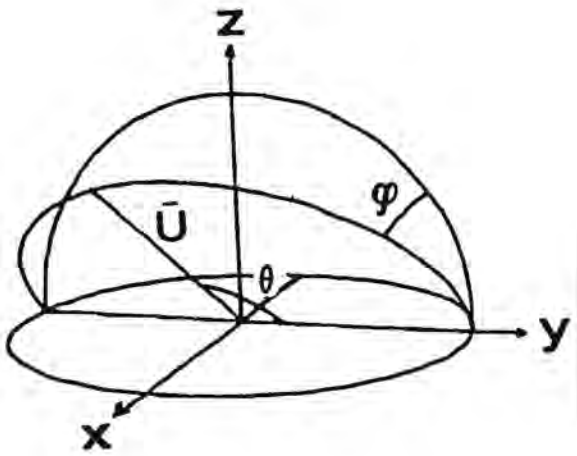

Fig. 5.

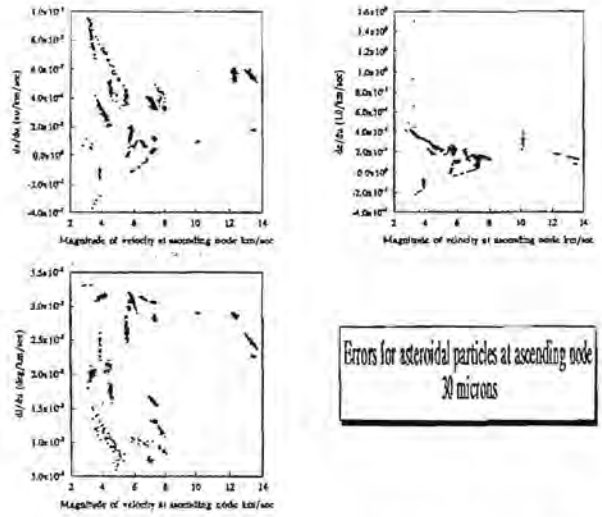

Fig. 7. Errors for asteroidal particles at ascending node 30 μm.

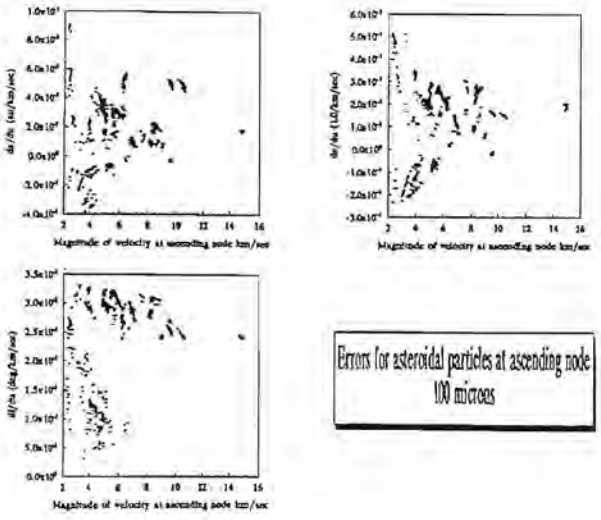

Fig. 8. Errors for asteroial particles at ascending node 100 μm.

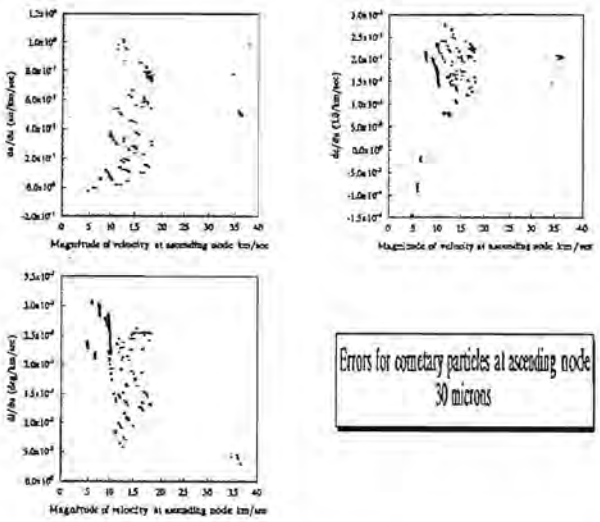

Fig. 10. Errors for cometary particles at ascending node 30 μm.

particles velocity vector u by the following

$$u_x^2 = (2 - a(1 - e^2) - 1/a)$$
$$u_y = [(a(1 - e_2)]^{1/2}\cos i - 1$$
$$u_z^2 = a(1 - e^2)\sin^2 i$$

In the above, orbital elements are computed relative to a "radiation"-modified gravitational potential. That is, if β = force of radiation/force of gravity then the potential is of the form $(1-\beta)\mu/r$, if μ and r are usual gravitational parameter distance from the Sun.

Where a (in units of the spacecraft orbit semimajor axis) is the semimajor axis of the particle orbit, e is its orbital eccentricity, and i is its inclination to plane of the spacecraft's orbit.

Conversely one may write

$$a = (1 - u^2 - 2u)^{-1}$$
$$1 - e^2 = (2 - a^{-1} - u_x^2)a^{-1}$$
$$\tan i = u_z/(1 + u_y)$$

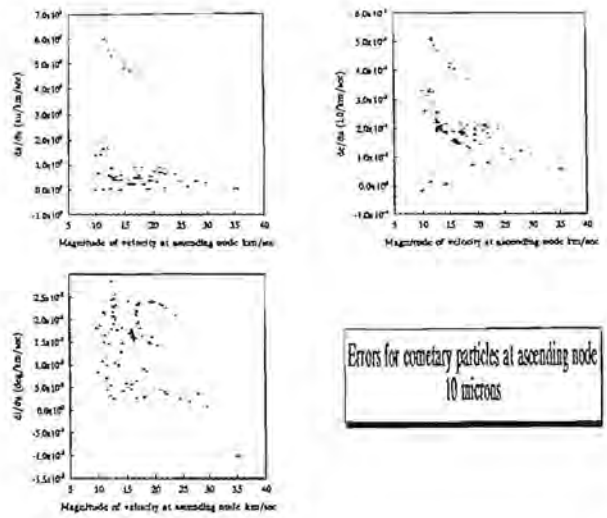

Fig. 9. Errors for cometary particles at ascending node 10 μm.

which give orbital elements as a function of the velocity components.

Let the detector measure the magnitude of the particle velocity and two angles θ the angular distance from the positive y axis and ϕ the azimuth angle (see Fig. 5). Then the velocity components can be expressed as

$$u_x = u \sin\theta \sin\phi$$
$$u_y = u \cos\theta$$
$$u_z = u \sin\theta \cos\phi$$

so that

$$\cos\theta = u_y/u$$
$$\tan\phi = u_x/u_z.$$

Now consider another simplification. Take the angular measurements θ and φ to be perfect. Let an error occur in the measurement of magnitude of the relative velocity, u. Holding θ and φ constant we have

$$da/du = (2u + 2du_y/du)/(1 - u^2 - 2u_y)^2 \quad (1)$$
$$de/du = [(2 - a^{-1} - u_x^2)a^{-2}da/du + (a^{-2}/da/du +$$
$$2u_x du_x/du)a^{-1}]/2e \quad (2)$$
$$\sec^2 i\, di/du = du_z/du(1 + u_y)^{-1} - u_z du_y/du(1+u_y)^{-2} \quad (3)$$

Taking the data given at the ascending node from the computed orbital evolution of dust particles the dependence of da, de, and di on du are given in Figs. 6–8 for the asteroidal particles and Figs. 9–11 for the cometary particles.

Conclusions: The largest error incurred in semimajor axis determination arises in the case of 10-μm particles from comets, da/du ≈ 6 (see Fig. 9). This was a particle from comet Honda-Mrkos-Pajduskova, which had at the time of intercept a semimajor axis of approximately 8 AU and an eccentricity of about 0.87. One sees from equation (1), and noting that the magnitude of u is $3-2[a(1 - e^2)]^{1/2} - 1/a$, that for large a and e ~ 1 that da/du ~ a; thus for particles

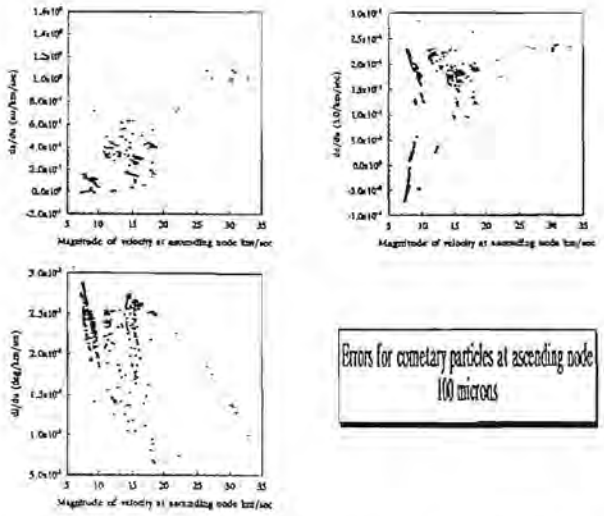

Fig. 11. Errors for cometary particles at ascending node 100 μm.

captured from large a and high eccentricity orbits the error in u can be substantial.

A value of de/du of nearly 1.5 occurs in a 30-μm asteroidal particle from asteroid Flora (Fig. 7). In this there is nothing unusual about the orbital elements at arrival, however, the particle has a low azimuth angle and high elevation of nearly 90° in this case de/du $\sim u^2$.

The errors incurred in measured orbital inclination were always smaller than those for the other orbital elements. The current error budget for CDCF has a candidate value of 1% [3]. In the worst case above this would result in an error of 0.07 AU in semimajor axis determination (can be higher for bigger cometary orbits) and 0.015 in eccentricity.

We will continue study of this problem, including efffects of the Earth's gravitation and errors in the measurement angles. We will present further results in a later report.

References: [1] Dermott S. F. et al. (1984) *Nature, 312,* 505–509. [2] Hörz F. et al. (1990) *NASA TM 102–160.* [3] Zook H. A. (1986) *LPI Tech. Rpt. 86-05,* 97–99. [4] Wyatt S. P. and Whipple F. L. (1950) *Astrophys. J., 111,* 134–141. [5] Gonzci R. et al. (1982) *Icarus, 51,* 633–654. [6] Gustafson B. Å. S. and Misconi N. Y. (1986) *Icarus, 66,* 280–287. [7] Jackson A. A. and Zook H. A. (1992) *Icarus, 97,* 70–84.

CARBON IN PRIMITIVE INTERPLANETARY DUST PARTICLES.

L. P. Keller[1], K. L. Thomas[1], and D. S. McKay[2], [1]Lockheed Engineering and Sciences Company, 2400 NASA Road 1, Houston TX 77058, USA, [2]Code SN, NASA Johnson Space Center, Houston TX 77058, USA.

Currently, one of the best sources of information regarding the nature and formation of carbonaceous materials in the early solar system comes from studies of primitive interplanetary dust particles. Carbon is a significant component of most IDPs, and the nature of the C-rich phases bears on the chemical and physical processes that have affected C from its nucleosynthesis to its incorporation into primitive solar system bodies. In this abstract we review the data regarding C in IDPs since ~1987. Brownlee [1] summarized the state of C in IDPs in a workshop held at Ames in 1987; other recent reviews have summarized the formation mechanisms that have been proposed for carbonaceous materials in primitive solar system materials [2,3]. We discuss here the abundance of C in IDPs, the nature and distribution of C, and topics and strategies for future work.

Abundance of C in IDPs: Blanford et al. [4] published the first quantitative bulk C analyses of IDPs and subsequent work has greatly expanded the initial observations to include analyses of ~20 anhydrous particles along with their detailed mineralogy [5]. Analyses of anhydrous IDPs show a range of C abundances from ~4 to 45 wt% with an average of ~13 wt%. Carbon abundance correlates with mineralogy such that pyroxene-rich IDPs tend to have the highest C contents, whereas olivine-rich particles have chondritic levels of C (<3× CI) [5]. The correlation of C abundance with the mineralogy of anhydrous IDPs is not an expected result, and the reasons for it are unclear, but may provide evidence for potential sources. Pyroxene-rich IDPs have been proposed as strong candidates for cometary particles based on their unusual mineralogy and high C contents [5]. The major-element compositions of anhydrous IDPs as a group are more primitive than the CI chondrites; anhydrous IDPs are also physically more primitive than CI chondrites.

Hydrated IDPs on average are also strongly enriched in C relative to CI chondrites. Carbon abundances in hydrated IDPs range from 5 to over 20 wt% with an average of 13 wt%, although nearly one-half of the hydrated IDPs analyzed have chondritic (<3× CI) C abundances [6]. The strong enrichment in C in hydrated IDPs as a group relative to the carbonaceous chondrites was not predicted, and suggests that most hydrated IDPs are derived from parent bodies that are more C-rich than the known carbonaceous chondrites, although the extent of aqueous alteration effects in hydrated IDPs is comparable to that in the CI chondrites.

Nature of the C-bearing Phases: A host of C-bearing materials are known from IDPs. The most abundant C-rich material is poorly graphitized or amorphous C that occurs as grain coatings, as a matrix in certain fine-grained aggregates (in anhydrous IDPs) [3], and as distinct "clumps" in anhydrous IDPs [5]. In high-C anhydrous IDPs, the amorphous carbon can be readily recognized by TEM examination of microtome thin sections, and the distribution of carbonaceous material can be documented [5]. Amorphous C is distributed throughout anhydrous IDPs and is not concentrated on the surfaces of the particles [5].

From the analyses of hydrated IDPs, it is now known that carbonates are only a minor component of most hydrated IDPs, and that the high C abundances in hydrated IDPs indicates that additional C-bearing phases are present in significant concentrations, probably in the form of amorphous or poorly graphitized C [6]. The distribution of these C phases in hydrated IDPs is not known because it is difficult to differentiate poorly ordered carbonaceous materials from fine-grained phyllosilicates, but is assumed to be homogeneously distributed.

From meteorite studies it is known that a large number of other organic compounds are present at individual concentrations typically <100 ppm. One might expect IDPs to contain a suite of organic compounds similar to those in carbonaceous chondrites, although the proportions may be dramatically different. Thomas et al. [7] note that in some anhydrous particles, the carbonaceous material is vesicular, a texture that is interpreted as a loss of hydrocarbons

during heating. In other IDPs, the carbonaceous material is featureless. Although is has been long been suspected that IDPs contain indigenous polyaromatic hydrocarbons (PAHs), the direct analysis of PAHs in IDPs has only recently been performed [8]. A variety of PAHs were observed in two IDPs, but apparently the mass distribution patterns are different from other analyzed extraterrestrial materials [8]. A careful evaluation of heating during atmospheric entry needs to be considered in these studies (see below).

The occurrence and concentration of refractory carbons such as silicon carbides and diamonds in IDPs have not been demonstrated. FeNi-carbides are a minor constituent of anhydrous IDPs, and are believed to have formed by catalytic reactions between metal grains and CO gas [3].

There is intriguing evidence that the carbonaceous material in IDPs is not all the same. Wopenka [9], using Raman spectroscopy, noted distinct differences in the degree of order exhibited by carbonaceous material in a group of 20 IDPs. She recognized that the interpretation of the degree of order is a complex function of the types of precursor organics and the metamorphic history of the particle, including atmospheric entry heating. However, solar flare tracks were observed in two of the IDPs that showed different degrees of order, indicating that they were not strongly heated during atmospheric entry. Wopenka speculated that the differences in these two particles reflected different organic precursor material. These differences could also indicate different levels of parent body thermal metamorphism. More measurements of this type in conjunction with detailed mineralogical studies to determine the atmospheric entry heating effects in a suite of well-characterized IDPs would be desirable. Major differences may indicate multiple sources and provide new information about the formation processes. The carbonaceous material in IDPs probably contains the main carrier phase for the large D enrichments, but the identity of the specific carrier phase(s) is not known.

Secondary processes such as aqueous alteration and atmospheric entry heating have modified the mineralogy and chemistry of many IDPs, and these processes may have modified the C phases in IDPs as well. Although the range of C abundances is similar in the anhydrous and hydrated IDPs, the aqueous alteration process has probably changed the C phases in hydrated IDPs (are there primary and secondary organics just like there are primary and secondary minerals?). There are basic differences in the amount and variety of organic compounds in anhydrous carbonaceous chondrites (e.g., Allende) and altered chondrites (e.g., Murchison) [2], and thermodynamic modeling suggests that reactions converting certain PAHs to amino and carboxylic acids are energetically favorable at the the conditions inferred from the mineral assemblages [10]. Thus, we would expect to see similar effects in cosmic dust particles.

Strategies for Future Work: Studies involving the structure of the carbonaceous component of IDPs or the molecular compounds in IDPs must select particles that are pristine and that have not been strongly heated during atmospheric entry (although this may induce a bias toward asteroid-derived particles). A major consideration in IDP studies is understanding how atmospheric entry heating has modified the C chemistry of IDPs. Analyses of C in hydrated IDPs shows that C abundance does not correlate with the degree of atmospheric entry heating estimated from mineralogical changes, even though ~75% of hydrated IDPs analyzed show evidence for entry heating [6]. There are indications that the form of C may change with entry heating, including the loss of low-mass PAHs [7] and increasing order in poorly graphitized C [9,11]. We need to be able to interpret results from heated particles, so laboratory pulse-heating experiments should be performed to understand mineralogical changes and changes in the C chemistry of IDPs as a function of heating.

One of the approaches to the unanswered questions regarding C in IDPs is to organize consortium studies on cluster particles. Cluster particles were originally 30- to 50-μm-sized particles that broke into several fragments on the collection surfaces. Cluster particles will be extremely valuable for multidisciplinary study because there are usually 3–6–10-μm-sized fragments available for a wide variety of investigations including mineralogical, chemical, isotopic, and spectroscopic measurements. Only with substantial cooperation among research groups will major advances be made in understanding the role of C in the early solar system.

Acknowledgments: This work was supported by NASA RTOP 15217-40-23 (PMG) and 199-52-11-02 (Exobiology).

References: [1] Brownlee D. E. (1990) *NASA CP-3061*, 21. [2] Cronin J. R. et al. (1988) in *Meteorites and the Early Solar System*, 819–860. [3] Bradley J. P. et al. (1988) in *Meteorites and the Early Solar System*, 861–898. [4] Blanford G. et al. (1988) *Meteoritics*, *23*, 113. [5] Thomas K. L. et al. (1993) *GCA*, *57*, in press. [6] Keller L. P. et al. (1993) *LPSC XXIV*, 785. [7] Thomas K. L. et al., this volume. [8] Clemett S. J. et al. (1993) *LPSC XXIV*, 309. [9] Wopenka B. (1988) *EPSL*, *88*, 221. [10] Shock E. and Schulte M. D. (1990) *Nature*, *343*, 728. [11] Reitmeijer F. (1992) *GCA*, *56*, 1665.

MINERALOGICAL AND CHEMICAL RELATIONSHIPS OF INTERPLANETARY DUST PARTICLES, MICROMETEORITES, AND METEORITES.

W. Klöck[1] and F. J. Stadermann[2], [1]Institut für Planetologie der Universität Münster, Wilhelm-Klemm-Strasse 10, D-4400 Münster, Germany, [2]Fachbereich Materialwissenschaft, Technische Hochschule Darmstadt, Hilpertstrasse 31, D-6100 Darmstadt, Germany.

Introduction: Cosmic dust particles are, in addition to meteorites and lunar rocks, a third class of extraterrestrial matter available for laboratory studies. Traditionally, dust particles less than 50 μm in size collected in the stratosphere are called interplanetary dust particles (IDPs) or Brownlee particles [1]. Larger dust particles, which settle too fast to be effectively collected in the stratosphere, are called micrometeorites. Recently, micro-meteorites were recovered in large numbers from polar regions on Earth [2,3], whereas in the past they have been extracted from deep sea sediments [4,5]. One important aspect in understanding the flux of cosmic dust onto the Earth, is the relationship of stratospheric dust to micrometeorites and meteorites. Therefore, we will outline some general properties of stratospheric dust particles and unmelted Antarctic micrometeorites including a few examples of mineralogical and chemical similarities or differences of IDPs to micrometeorites and to known meteorites.

General Mineralogical Properties of IDPs: Interplanetary dust particles were classified according to their IR spectral signatures into olivine-, pyroxene-, and layer-lattice-silicate classes [6]. In general, this division was confirmed by analytical electron microscopy of IDP thin sections [7,8]. In detail, it appears that particles of the olivine IR class still contain pyroxenes, and olivines are present in

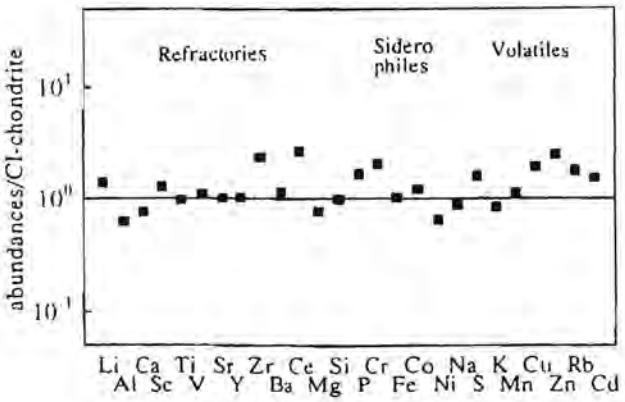

Fig. 1. Plot of major and trace elements of interplanetary dust particle "Nero." The data are normalized to CI chondrite abundances and silicon. The agreement (within a factor of 2) with average CI chondrite trace-element abundances for refractory, siderophile, and volatile elements is remarkable. The unfractionated-element pattern clearly supports an extraterrestrial origin of this stratospheric dust particle.

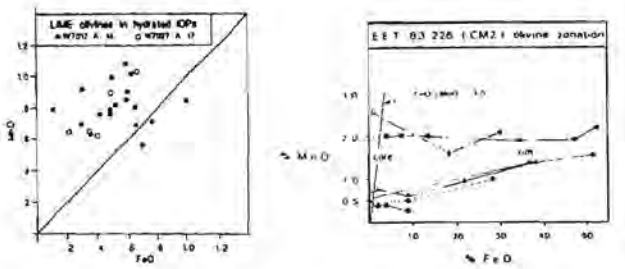

Fig. 2. Comparison of Fe and Mn contents of submicrometer olivines in hydrated IDPs and in the EET 83226 (CM2) meteorite. Forsterites in two hydrated IDPs have Fe/Mn ratios of about 1 and show no evidence of Fe enrichment from core to rim. High-Mn forsterites in accretionary dust mantles of EET 83226 show a prominent zoning in Fe contents. Core compositions of forsterites are comparable to IDP forsterites, but rims of forsterites are strongly enriched in Fe. This Fe enrichment is characteristic of CM2 submicrometer olivines and is absent in CI, CR, and Semarkona forsterites.

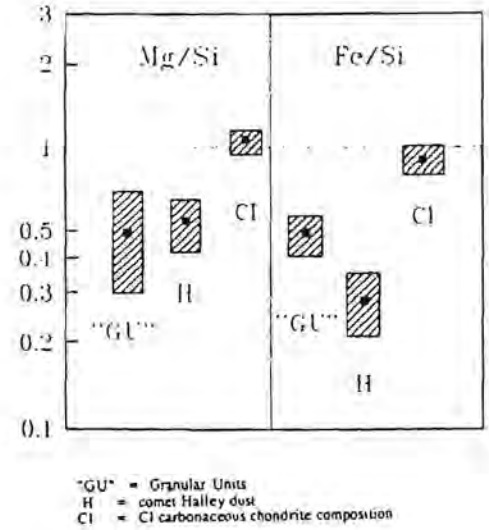

Fig. 3. Average Mg/Si and Fe/Si ratios of "microcrystalline aggregates" or "granular units" of eight anhydrous interplanetary dust particles are compared to elemental ratios of CI chondrites and Halley dust particles. Data are normalized to solar abundances. Mg/Si and Fe/Si ratios of "granular units" show a better match with Halley dust than to CI-chondrite values.

particles of the pyroxene IR class. The composition of these mafic minerals in anhydrous IDPs is a potential mineralogical indicator to distinguish primitive and processed dust particles [9,10].

A subset of the anhydrous class of IDPs consists of particles dominated by very-fine-grained material, so-called "microcrystalline aggregates" [11] or "granular units" [12]. These aggregates, having approximately chondritic major- and minor-element abundances, consist of 5–50-nm-sized grains of Mg-Fe silicates, Fe-Ni sulfides, and Fe-Ni metal embedded in a glassy matrix. Anhydrous IDPs of that subclass are strongly enriched in bulk C contents relative to CI-meteorite abundances [13]. High C abundances and additional mineralogical properties suggest that particles of this subclass are among the most primitive solar system material available for detailed laboratory studies [8,10,13].

A major portion of particles collected in the stratosphere belong to the layer-lattice-silicate class [6]. Among phyllosilicate IDPs, saponite particles dominate over serpentine particles [14]. Minor abundances include anhydrous mineral phases like Fe-Ni sulfides, Mg-Fe silicates, Mg-Fe carbonates, chromites, and magnetites. Surprisingly, at present, only two hydrated interplanetary dust particles were found with distinct mineralogical similarities to CI and CM meteorites [15,16]. Again, as is the case with anhydrous IDPs, major-element abundances of hydrated IDPs are also approximately chondritic, except for a sizable C enrichment of about 4× CI chondrite values [14]. The C overabundance could indicate that the supposedly asteroidal parent objects of hydrated IDPs are chemically and mineralogically unlike the asteroidal sources of CI and CM meteorites. Common to anhydrous as well as to some hydrated particles is the occurrence of olivines having a particular composition. They are forsteritic olivines characterized by Fe/Mn ratios of about 1. Olivines with an identical chemical signature also occur in the matrix of carbonaceous chondrites and in matrix of the unequilibrated ordinary chondrite Semarkona. Olivines with that unique composition provide a link between primitive meteorites, most likely derived from asteroids and cosmic dust and its sources.

Some Mineralogical Properties of Micrometeorites: Most micrometeorites in the 100–1000-μm size range are spherules, and their shapes and compositions indicate that they totally melted during atmospheric entry, in accordance with entry heating calculations [17,18]. A minor portion of these spherules contains relic refractory mineral phases like forsterites and enstatites, which survived melting, and their minor-element signatures suggest a link between deep sea spheres, melted polar micrometeorites, and CM chondrites [19]. Among micrometeorites in the 50–100-μm size range, recovered by Maurette from Antarctic ice [3], is a population of morphologically irregular and therefore probably unmelted micrometeorites. Their textures, mineral assemblages, and bulk

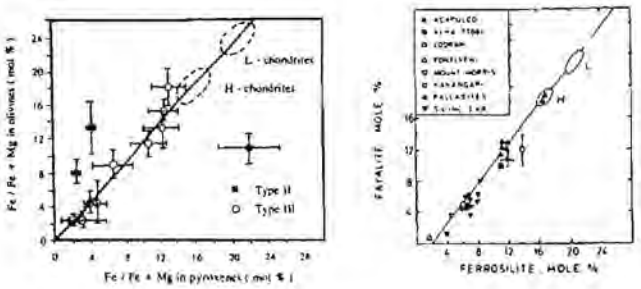

Fig. 4. Plot of fayalite (Fe_2SiO_4) content of olivine vs. ferrosilite ($FeSiO_3$) content of low-Ca pyroxene in anhydrous IDPs. Type III dust particles are relatively coarse-grained, compact objects. Iron contents of olivines and pyroxenes in these equilibrated particles are comparable to mineral compositions in acapulcoites, pallasites, and silicate inclusions in type IAB iron meteorites. The figure on the right is taken from Palme et al. (1981) *GCA 45*, 727–752.

chemical compositions are believed to be reminiscent of CI- meteorite matrix minerals [20]. Transmission electron microscope studies and IR spectroscopy of a number of irregular Antarctic and Greenland micrometeorites [21,22] have so far failed to identify layer-lattice-silicates by their characteristic basal spacings or IR spectral signatures. The supposedly unmelted micrometeorites appear to be heated to such an extent that the originally present phyllosilicates were transformed into assemblages of fine-grained olivines, pyroxenes, and magnetites embedded in a glassy matrix. The population of these polar micrometeorites, heated to various degrees, should, however, preserve even more relic phases and textures, and therefore important information about their source material compared to the melted micrometeorites. Interpretation of their minor- and trace-element patterns with respect to possible relationships with known meteorite classes turned out to be complicated by elemental loss and gain during residence in the Antarctic and Greenland ice [21,23,24]. A few examples are given below illustrating the possible relationships of stratospheric dust particles and larger extraterrestrial samples.

Mineralogical and Chemical Aspects of Primitive Anhydrous IDPs: Among the class of anhydrous stratospheric dust particles is a subset of dust particles having abundant fine-grained aggregates. The unequilibrated nature of these particles is documented by variable Fe contents of olivines dispersed throughout the fine-grained aggregates. In addition, particles of this subset are characterized by high ^4He abundances, relatively low ^4He release temperatures, chondritic levels of Zn, and the presence of solar flare tracks in Mg-Fe silicates [25]. These particles also have chondritic abundances of other volatile elements like Na, S, K, Mn, Cu, Rb, and Cd, as shown by Stadermann [26]. He reported trace-element analyses of IDP NERO (u44-m1-7), which is a typical example of that particle class, and found CI meteorite abundances (within a factor of 2) for all major, minor and trace elements analyzed (Fig. 1). The unfractionated trace element pattern suggests that this particle was not heated significantly above 600°C [26] arguing in favor of an asteroidal origin of that particle, though cometary sources with perihelia >1.5 AU [18,27] cannot be excluded.

Mn-rich Olivines in IDPs and Meteorites: A further argument supporting an asteroidal origin of primitive IDPs is the occurrence of Mn-rich forsterites in dust particles of the above-mentioned subset of the anhydrous class, as well as in several carbonaceous chondrites and in the unequilibrated ordinary chondrite Semarkona [28]. These Mn-rich forsterites in unequilibrated anhydrous IDPs and in different primitive meteorites show identical chemical signatures, suggesting that these Mn-enriched forsterites were present at the formation locations of meteorite parent bodies in the asteroid belt. Forsterites with that distinct chemical signature are also a minor component in some hydrated interplanetary dust particles (Fig. 2). Stratospheric dust particles dominated by phyllosilicates are believed to be genetically linked to the hydrous (CI, CM, CR) carbonaceous chondrites. Mn-rich forsterites in CM2 chondrites display a prominent Fe enrichment from core to rim (Fig. 2). This distinct zoning pattern could be used, in addition to the identification of the characteristic hydrated phases, to link hydrated IDPs to CM2 chondrites. Figure 2 clearly shows that the few hydrated interplanetary dust particles with Mn-rich forsterites studied so far are not genetically linked to CM2 meteorites.

Compositions of Microcrystalline Aggregates: The major building blocks of unequilibrated anhydrous IDPs are very-fine-

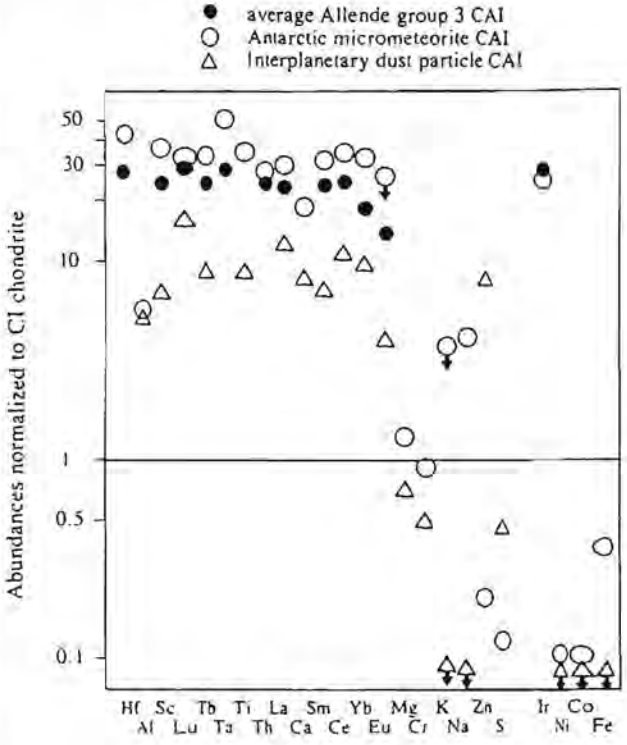

Fig. 5. Comparison of trace-element characteristics of calcium-aluminum-rich inclusions (CAIs) from different groups of extraterrestrial samples. CAI Didius is a stratospheric dust particle. Its extraterrestrial nature was confirmed by O isotopic measurements. Didius is enriched in ^{16}O and plots on the Allende mixing line in a three-isotope diagram. The refractory trace elements are about 10× enriched and nonrefractory siderophile elements are strongly depleted compared to CI chondrite trace-element abundances. The micrometeorite CAI, found among Antarctic unmelted particles, is chemically very similar, though the enrichment of refractories is somewhat higher. The slight negative Eu anomaly supports a relationship to group 3 Allende CAIs, which are shown for comparison as solid symbols.

grained components. Bradley [11] used the term "microcrystalline aggregates" and Rietmeijer [12] referred to them as "granular units" (GUs). On average, these aggregates are a few hundred nanometers in size. Individual crystallites are too small (5–50 nm) to analyze individually in TEM thin sections. Average bulk major elemental compositions of GUs of a number of primitive anhydrous IDPs point to a depletion of Mg and Fe relative to Si normalized to solar abundances (Fig. 3). Surprisingly, Halley dust particle compositions show similar elemental ratios [29,30]. Particles analyzed by Giotto and Vega mass spectrometers had masses of about 10^{-16}–10^{-10} g [31]. This mass range corresponds to particles in the size range from less than 100 nm to a few micrometers, which is compatible with sizes of fragments of "GUs" in unequilibrated IDPs. The wide compositional range of Halley dust particles is consistent with each dust particle analyzed by the mass spectrometers, being an agglomeration of many mineral grains of varying composition and size [30]. No single mineral grains (except iron-sulfides) were identified in the mass spectra. 10^{-16}-g agglomerates of several grains require sizes of individual minerals of less than 50 nm, which is consistent with the sizes of mineral grains in "microcrystalline aggregates" in primitive anhydrous IDPs. Compositions of GUs or "microcrystalline aggregates," silicate emission features [11] and other physical properties seem to suggest a cometary relationship of primitive unequilibrated IDPs; the presence of Mn-rich forsterites, however, indicates an asteroidal origin. This controversy can presently only be resolved if we assume that possible sources of primitive IDPs are long-period comets, and that these comets and primitive asteroids are compositionally alike.

IDPs with Links to Primitive Achondrites: In addition to porous, fine-grained particles, a number of rather compact and coarse-grained objects were identified among anhydrous IDPs. Their bulk chemical compositions are chondritic. Individual mineral grains of olivines and pyroxenes are micrometer sized and their textures suggest that these particles suffered intense thermometamorphism. Fe/Fe + Mg ratios of coexisting olivines and pyroxenes in these particles are given in Fig. 4. Olivines and pyroxenes in type III IDPs are equilibrated with respect to Fe and Mg. It is unlikely that flash heating during atmospheric entry causes complete Fe/Mg equilibration of micrometer-sized mineral grains. Therefore, Fe and Mg equilibration of olivines and pyroxenes in these particles requires metamorphism or melting on their parent objects. Ranges of Fe content in olivines and pyroxenes are comparable to ranges in Acapulcoites or silicate inclusions of IAB iron meteorites, which experienced intense heating and partial melting causing recrystallization of originally chondritic silicates (Fig. 4).

CAIs Among IDPs and Micrometeorites: Most interplanetary dust particles studied are roughly chondritic in composition. Zolensky [32] reported the identification of refractory dust particles and McKeegan [33] and Stadermann [26] characterized nonchondritic dust particles by their O isotopic composition and by trace-element abundances. Figure 5 is a comparison of trace-element contents of CAIs from three different sources. Didius (u47-m1-1a) is a refractory particle analyzed by Stadermann; the Antarctic CAI was analyzed by Lindstrom [24]. Their refractory and siderophile trace-element levels are compared to an average Allende CAI trace element pattern [34]. Common to all three objects is the enrichment of refractory elements. Didius is enriched by about a factor of 10, the Antarctic CAI by about a factor of 30. Non-refractory siderophile elements are strongly depleted in all CAIs compared to CI abundances. The slight negative Eu anomaly in Didius and possibly also for the Antarctic CAI suggests that these particles are chemically related to group 3 Allende CAIs [34]. This example illustrates that identical refractory components, primarily known from carbonaceous chondrites, are also present among micrometeorites and among stratospheric dust particles, indicating that at least some IDPs and micrometeorites are directly related to primitive carbonaceous chondrites and their asteroidal parent objects.

References: [1] Brownlee D. E. (1985) *Annu. Rev. Earth Planet. Sci., 13,* 147–173. [2] Maurette M. et al. (1986) *Science, 233,* 869–872. [3] Maurette M. et al. (1991) *Nature, 351,* 44–47. [4] Millard H. T. and Finkelman R. B. (1970) *JGR, 75,* 2125–2134. [5] Brownlee D. E. (1981) in *The Sea, Vol. 7* (C. Emiliani, ed.), Wiley, New York. [6] Sandford S. A. and Walker R. M. (1985) *Astrophys. J., 291,* 838–851. [7] Bradley J. P. (1988) *GCA, 52,* 889–900. [8] Germani M. S. (1990) *EPSL, 101,* 162–179. [9] Klöck W. et al. (1990) *LPSC XXI,* 637–638. [10] Klöck W. (1992) *Proc. 50th Ann. Meeting Electron Microscopy Soc. Am.,* 1718–1719. [11] Bradley J. P. et al. (1992) *Astrophys. J., 394,* 643–651. [12] Rietmeijer F. J. M. (1989) *Proc. LPSC 19th,* 513–521. [13] Thomas K. L. et al. (1993) *GCA,* in press. [14] Keller L. P. et al. (1993) *LPSC XXIV,* 785–786. [15] Bradley J. P. and Brownlee D. E. (1991) *Science, 251,* 549–552. [16] Keller L. P. et al. (1992) *GCA, 56,* 1409–1412. [17] Love S. G. and Brownlee D. E. (1991) *Icarus, 89,* 26–43. [18] Flynn G. J. (1989) *Icarus, 77,* 287–310. [19] Steele I. M. et al. (1985) *Nature, 313,* 297–299. [20] Kurat G. et al. (1992) *LPSC XXIII,* 747–748. [21] Flynn G. J. et al. (1993) *Proc. NIPR Symposium on Antarctic Meteorites,* in press. [22] Alexander C. M. O'D. et al. (1992) *LPSC XXIII,* 7–8. [23] Koeberl C. et al. (1992) *LPSC XXIII,* 709–710. [24] Lindstrom D. J. and Klöck W. (1992) *Meteoritics, 27,* 250. [25] Klöck W. et al. (1992) *Meteoritics, 27,* 243–244. [26] Stadermann F. J. (1990) Ph.D. thesis, University of Heidelberg. [27] Blanford G. E. (1993) *LPSC XXIV,* 131–132. [28] Klöck W. et al. (1989) *Nature, 339,* 126–128. [29] Jessberger E. K. et al. (1992) *EPSL, 112,* 91-99. [30] Lawler M. E. et al. (1989) *Icarus, 80,* 225–242. [31] Langevin Y. et al. (1987) *Astron. Astrophys., 187,* 761–766. [32] Zolensky M. E. (1987) *Science, 237,* 1466–1468. [33] McKeegan K. D. (1987) *Science, 237,* 1468–1470. [34] Kornacki A. S. and Fegley B. Jr. (1986) *EPSL, 79,* 217–234.

ANTARCTIC MICROMETEORITES. G. Kurat[1], C. Koeberl[2], T. Presper[1], F. Brandstätter[1], and M. Maurette[3], [1]Naturhistorisches Museum, Postfach 417, A-1014 Vienna, Austria, [2]Institut für Geochemie, Universität Wien, Dr. Karl-Lueger-Ring 1, A-1010 Vienna, Austria, [3]Centre de Spectrométrie Nucléaire et de Spectrométrie de Masse, Bat. 108, F-91405 Orsay Campus, France.

Introduction: Micrometeroids in the size range 50–500 μm dominate the flux onto the Earth [1]. Contrary to theoretical predictions [2,3] many of them survive atmospheric entry almost unchanged. Such micrometeorites can be collected from the Antarctic ice sheet where they account for a surprisingly large proportion of the total dust content of the ice [4–7]. Early studies of this important class of extraterrestrial material have revealed that some Antarctic micrometeorites are similar to CM chondrites in chemical bulk composition and mineral composition [e.g., 5,8–14], and a few seem to resemble CI chondrites [15]. However, none of the mi-

crometeorites investigated so far match CM or CI chondrites exactly, nor is there a match between average bulk micrometeorite composition and that of any other chondrite class. Also, the micrometeorite mineral chemistry is different from that of carbonaceous chondrites [e.g., 8–15]. Several elements are depleted in micrometeorites as compared to carbonaceous chondrites and some are enriched. The question arises whether these differences are pristine or if some of them are of secondary origin. On the basis of our data we will attempt to answer these questions, some of which have been adressed by us before [e.g., 1,12,14–18].

Samples and Methods: Two lines of analytical approach were followed: (1) Polished sections of selected dark micrometeorites from the 1987 and 1991 collections were investigated by analytical scanning electron microscopy (ASEM) and electron microprobe. (2) Individual large micrometeorites were selected from the 1991 collection and analyzed for trace-element contents by INAA [10]. Subsequently these samples were also studied by ASEM, then embedded into epoxy resin, polished, and analyzed by microprobe. The particle sizes varied between about 100 and 400 µm (mass range 1–49 µg). Analyses have been published in [5,10,12,14,15,19].

Besides nonchondritic paticles (which we preliminary bag as "terrestrial") there is a variety of extraterrestrial particles. Unmelted micrometeorites (UMMs) (although occasionally thermally metamorphosed) are particles representing the coarse (50–400 µm) particle size fraction. They consist of phyllosilicates or coarse-grained anhydrous silicates or mixtures thereof. We can distinguish phyllosilicate-dominated UMMs and anhydrous silicate-dominated, coarse-grained, crystalline UMMs. Phyyllosilicate UMMs can be thermally altered into partly melted, foamy, scoriaceous MMs that in turn grade into cosmic spherules (CSs) with increasing degrees of melting and degassing. In accordance with common usage we call stratosphric interplanetary dust particle IDPs, but keeping in mind that they represent just a tiny fraction of the interplanetary dust of the solar system.

Results: Selected bulk analyses of phyllosilicate UMMs as determined by EMP[19] are compared to CI composition (Fig. 1a). Compared to CI chondrites micrometeorites are depleted in Ca, Mg, Mn, Na, Ni, and S, and enriched in K. Compared to CI chondrites, CSs are depleted in NI (and S, not shown), Na, and K, but only occassionally depleted in Ca nd not depleted in Mg and Mn (Fig. 1b). Occassional enrichments are mainly confined to Ti and Al.

Refractory lithophile elements and Cr, Na, Zn, and Br in phyllosilicate UMMs [19] closely follow the CM compositional trend, except for K and Br, which can be enriched in MMs (Fig. 2). The refractory siderophile elements have, on average, CI-CM abundances. Nickel and Co are clearly depleted in UMMs, Au and As strongly enriched, and Se is at the CM level. Some occasional enrichment of Fe in UMMs is present.

Lithophile trace-element abundances in scoriaceous MMs are very similar to those in UMMs with the exception of Na, Zn, and Br,

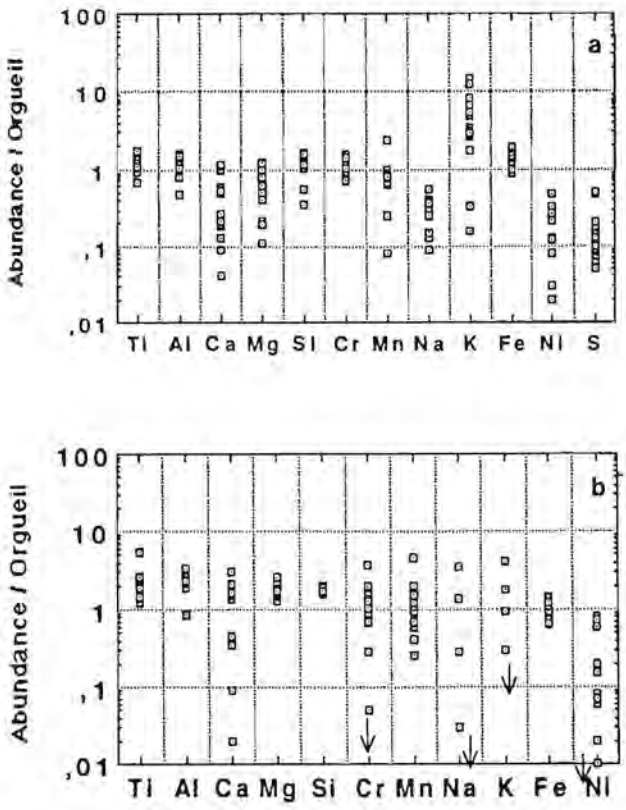

Fig. 1. Bulk major- and minor-element contents as determined by EMPA of (a) phyllosilicate UMMs and (b) CSs normalized to CI chondrites [20].

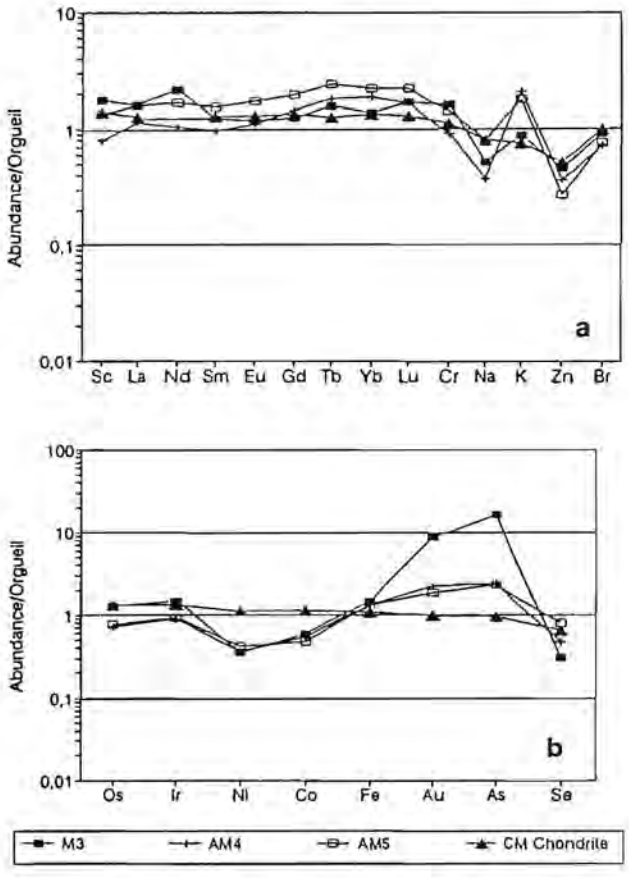

Fig. 2. Bulk trace-element contents of phyllosilicate UMMs compared to CM and CI chondrites [15,19,20,21]. (a) Lithophile elements, (b) siderophile elements.

which are mostly strongly depleted as compared to CM chondrites, and also K, which is—on average—enriched over CM levels. Occasional enrichments of Zn and Br are also present. Siderophile elements in scoriaceous MMs are generally unfractionated, but Fe, Au, and As tend to be enriched and Se is usually depleted as compared to CM abundances [19].

Discussion and Conclusion: Micrometeorites in the particle size range 50–500 μm probably are representative of almost 99% of today's interplanetary dust accreting onto Earth. About 60% are phyllosilicate-dominated objects, the remainder being coarse-grained low-Ca pyroxene and olivine particles. Such a mineralogical composition is comparable to that of CI and CM. However, the match between UMMs and CI/CM chondrites is not perfect. As compared to CM chondrites, UMMs have a very low olivine/pyroxene ratio [5,8,9,12,13,19], are depleted in Ca, Mg, Mn, Na, Ni, Co, and S, and are enriched in K, As, and Au.

The differences in mineral chemistry between UMMs (and scoriaceous MMs and CSs) and CM chondrites are mainly primary, but some differences can be ascribed to a secondary origin: UMMs lack carbonates and sulfates, which are very common in CM and CI chondrites.

However, some elemental depletions and enrichments observed in UMMs (and also IDPs [e.g., 22–28]) cannot have extraterrestrial causes. The volatile elements Na, K, Zn, Br, and Se are increasingly depleted with increasing degree of melting and degassing. This may simply reflect the increasing loss of volatiles with increasing temperature and/or duration of the melting event. The common depletions in Ca, Mg, and Mn of phyllosilicate-rich UMMs are not found in scoriaceous MMs and CSs (with a few expections for Ca among the CSs). This clearly demonstrates that the scoriaceous MMs and CSs had a parent that was not depleted in these elements. The same holds for Ni and Co, which are depleted in UMMs (and CSs), but not in scoriaceous MMs. The absence of carbonates and sulfates in phyllosilicate UMMs, as well as their depletions in Ca, Mg, Mn, Ni, Co, and S, indicates that the depletions were caused by the loss of carbonates (calcite, Mn-dolomite, and Mn-magnesite [e.g., 29–31]) and Ni-, Co-, and Na-bearing sulfates [11,14,19]. Because some IDPs have been reported to contain carbonates [32], the alteration of the UMMs probably took place in the Antarctic ice and/or the melt-ice water.

Enrichments in K, As, and Au found in UMMs and IDPs may also have terrestrial causes. As has been shown by [26] for Br, some of these enrichments could be the result of atmospheric contamination. Scoriaceous MMs are enriched in Br and Zn, but highly depleted in Na, probably resulting from recondensation of the most volatile elements from the atmosphere. The phase COPS [17] and the very common magnetite envelope around MMs [11] may also have resulted from this process. In summary, the whole family of dusty extraterrestrial matter ranging from unmelted micrometeorites to scoriaceous micrometeorite and cosmic spherules seems to have a common parent that is similar to, but not identical with, CM chondrites. It is interesting that the most common matter accreting onto the Earth today seems related to a rather rare meteorite class and probably forms a distinct subclass among them. The fairly common fine-grained anhydrous aggregates among the IDPs do not have any counterpart among the micrometeorites that are ~10× larger (10^3× more massive) than the IDPs.

Much more data are needed in order to unravel the complex relationships between dust particles of different mass and to answer the questions on their origin and history during the lifetime of the solar system.

Acknowledgments: This work was financially supported by FWF, Vienna, Austria (P-8125-GEO).

References: [1] Hughes D. W. (1978) In *Cosmic Dust* (J. A. M. McDonnell, ed.), 123–185, Wiley. [2] Kornblum J. J. (1969) *JGR, 74*, 1893–1907. [3] Love S. G. and Brownlee D. E. (1991) *Icarus, 89*, 26–43. [4] Maurette M. et al. (1989) *LPS XX*, 636–637. [5] Maurette M. et al. (1991) *Nature, 351*, 44–47. [6] Maurette M. et al. (1992) *LPS XXIII*, 859–860. [7] Maurette M. et al., this volume. [8] Christophe-Michel-Levy M. and Bourot-Denise M. (1992) *Meteoritics, 27*, 73–80. [9] Klöck W. et al. (1992) *LPS XXIII*, 697–698. [10] Koeberl C. et al. (1992) *LPS XXIII*, 709–710. [11] Kurat G. et al. (1992) *Meteoritics, 27*, 246. [12] Presper T. et al. (1992) *Meteoritics, 26*, 278. [13] Steele I. M. (1992) *GCA, 56*, 2923–2929. [14] Presper T. et al. (1993) *LPS XXIV*, 1177–1178. [15] Kurat G. et al. (1992) *LPS XXIII*, 747–748. [16] Maurette M. et al. (1992) *LPS XXIII*, 861–862. [17] Perreau M. et al. (1993) *LPS XXIV*, 1125–1126. [18] Engrand C. et al. (1993) *LPS XXIV*, 441–442. [19] Kurat G. et al. (1993) *Geol. Geofiz.*, in press. [20] Palme H. et al. (1981) In *Springer, Vol. 2* (Landoldt-Boernstein et al., eds.), 257–273. [21] Wasson J. T. and Kallemeyn G. W. (1988) *Phil. Trans. R. Soc. London, A325*, 535–544. [22] Flynn G. J. and Sutton S. R. (1987) *LPS XVIII*, 296–297. [23] Flynn G. J. and Sutton S. R. (1991) *Meteoritics, 26*, 334. [24] Flynn G. J. and Sutton S. R. (1992) *LPS XXIII*, 373–374. [25] Flynn G. J. and Sutton S. R. (1992) *Proc. LPS, Vol. 22*, 171–184. [26] Jessberger E. K. et al. (1992) *EPSL, 112*, 91–99. [27] Schramm L. S. et al. (1989) *Meteoritics, 24*, 99–112. [28] Thomas K. L. et al. (1992) *LPS XXIII*, 1427–1428. [29] Bostroem K. and Fredriksson K. (1966) *Smithson. Misc. Coll., 151/3*, 1–39. [30] Fredriksson K. et al. (1980) *Meteoritics, 15*, 291–292. [31] Brandstätter F. et al. (1987) *Meteoritics, 22*, 336–337. [32] Tomeoka K. and Buseck P. R. (1986) *Science, 231*, 1544–1546.

COLLECTION AND CURATION OF IDPs IN THE STRATOSPHERE AND BELOW. PART 2: THE GREENLAND AND ANTARCTIC ICE SHEETS.

M. Maurette[1], C. Hammer[2], R. Harvey[3], G. Immel[1], G. Kurat[4], and S. Taylor[5], [1]C.S.N.S.M., Batiment 108, 91405-Orsay, France, [2]Department of Geophysics, University of Copenhagen, Haraldsgade 6, DK 2200-Copenhagen, Denmark, [3]Department of Geological Sciences, University of Tennessee, Knoxville TN 37996, USA, [4]Mineralogisch Abteilung, Naturhistorisches Museum, Postfach 417, A-1014 Wien, Austria, [5]CRREL, Hanover NH 03755, USA.

Introduction: In a companion paper [1] Zolensky discusses interplanetary dust particles (IDPs) collected in the stratosphere. Here we describe the recovery of much larger unmelted to partially melted IDPs from the Greenland and Antarctica ice sheet ("polar" IDPs), and discuss problems arising in their collection and curation, as well as future prospects for tackling these problems. The collection of IDPs in other terrestrial sediments such as deep sea sediments has been well covered by Brownlee [2], and will not be reviewed here.

Stratospheric and polar IDPs are altered by space weathering in

the interplanetary medium, frictional heating upon atmospheric entry, atmospheric weathering during settling in the atmosphere, terrestrial weathering in their host sediments, and man-made collection procedures. As collection procedures and weathering processes can bias the type of dust particles recovered [3,4], comparison of very different collections of IDPs covering a wide range of particle sizes is required to identify characteristics that are independent of terrestrial processes.

Investigation of a few hundred polar IDPs indicate that IDPs up to sizes of ≈100 μm are remarkably well transmitted throughout the atmosphere [3,5], and that ≈50–400-μm-sized IDPs are mostly related to the rare meteorite class of CM chondrites. However, some features of these IDPs set them apart from CM chondrites [5–9]. First, their mineralogical composition is different in that IDPs have a low olivine/pyroxene ratio and would contain mainly smectite rather than serpentine. Second, the chemical composition of the nonhydrous phases (olivine and low-Ca pyroxene) is similar to that of CM chondrites, but IDPs seem to lack the refractory very-low-Fe isolated olivines that are very abundant in CM chondrites. Third, IDPs have bulk chemical compositions that differ somewhat from that of CM chondrites. These differences include a depletion in Ca, Ni, Co, and S, and sometimes also in Mg and Mn [5,10]; a higher content of carbonaceous material [11]; and an enrichment in K, Br, Au, As, and Fe [10,12,13]. The mineralogical and mineral chemical features of polar IDPs most probably are of primary origin, and clearly set them apart from the CM chondrites. But some bulk chemical features of IDPs appear to be probably of terrestrial origin, such as the elemental depletions, which are probably related to the dissolution of their constituent carbonates (Ca, Mg, Mn) and sulfates (Mg, S, Ni, Co), and some elemental enrichments, probably reflecting some forms of weathering and/or condensation during settling in the atmosphere [14]. All these investigations strongly suggest that polar-type IDPs of all sizes are the most common matter falling on the Earth today, and are not yet represented in meteorite collections.

Polar ices may be the most favorable collectors of large IDPs. The ice is ultraclean, and can be easily removed by melting. Furthermore, IDPs embedded in ice are shielded from both terrestrial weathering and other alteration processes operating on the ice surface. The major problem with the ice is the low concentration of IDPs. This concentration can be computed assuming that the micrometeorite (i.e., IDPs) flux given at ≈1 AU in the interplanetary medium [15] is the same as that for the Earth's surface (100% transmission efficiency), and that ice flow models properly determine where the host ice formed, and thus its accumulation rate, V(cm yr^{-1}). At the sites of our Greenland and Antarctic expedition V ≈ 50 and ≈ 20 cm, and concentrations of >50-μm-sized IDPs would be ≈3 and ≈10 grains per ton of ice respectively. At these low concentrations, a huge amount of ice has to be melted to get a reasonable number of IDPs. One has thus to find methods to melt these amounts of ice in the field, or to discover zones where local processes would drastically increase the concentration of IDPs. Such "accumulation" processes fortunately operate on both the Greenland and Antarctica ice sheets.

Mining of IDPs on the Melt Zone of the Greenland Ice Sheet: In the melt zone of the west Greenland ice cap, small seasonal lakes are formed during the short Arctic summer. They are fed by the melting of a ≈1-m-thick layer of ice, over collection basins that have diameters of a few kilometers. The amount of melt-ice water cycled each year through such a lake reaches ≈10^8 tons. Aerial photographs showed that these lakes contained dark patches of sediments (called "cryoconite"), and we hoped that IDPs were concentrated in the cryoconite of such "placer type" deposits.

At the site of our first expedition (Blue Lake 1), ≈20 km from the margin of the Sondrestromfjord ice field (latitude 67°08'N), ice flow models indicated that the ice surface was about ≈2000 years old. If the lakes form at about the same locations each year, because they reflect the much steeper and invariant "hill/valley" morphology of the basement rocks on which the ice flows, this yearly process of melting was in fact repeated over ≈2000 years, providing a gigantic amount of melt-ice water in excess of 10^{11} tons! In July 1984, we used a ≈500-g hand water pump to "vacuum-up" cryoconite first from a lake bottom (≈10 kg), and then ≈50 kg at other types of sites, including the bottom of the ≈20-cm-deep "cryoconite" holes that constitute most of the ice field surface.

We returned to Greenland in July and August 1987 to sample cryoconite at 30 different locations between ≈2 and 50 km from the margin of the same ice field, with the view of tracing back the past activity of the micrometeorite flux. In August 1984, 1985, 1987, and 1988 colleagues collected several ≈1-kg sample of cryoconite at higher latitudes including two sites of the Jakobshavn ice field (69° 20'N; ≈10 and ≈25 km from margin), and two sites near de Quervains Harbour (69°44'N; ≈5 and ≈9 km from margin). All expeditions yielded a total mass of wet cryoconite ≈200 kg, from about 50 distinct samples.

The cryoconite at all locations is essentially made of "cocoons" of filamentous siderobacteria [16] that tightly encapsulate a fine-grained mineral sand, predominantly terrestrial but containing a minor component of unmelted IDPs and cosmic spherules. The >100-μm size fraction (and occasionally the 50–100-μm fraction) from ≈100-g aliquots of the different samples was disaggregated using a stainless steel sieve and a hard nylon brush. Less than 10 g of sand per kilogram of wet cryoconite was recovered. The concentration of cosmic spherules (i.e., melted IDPs) in both this sand and its host cryoconite already leads to the following inferences:

1. About 800 cosmic spherules (and ≈200 unmelted IDPs) with sizes >100 μm are found per kilogram of (wet) cryoconite. This figure is independent of the type of deposit, the latitude of the ice field, and its distance to the margin. As argued elsewhere [3], this "saturation" concentration corresponds to a model where cryoconite holes act as IDPs collectors, while moving on the ice surface (over their "lifetime" of about 250 yr), between their formation near the limit of the melt zone (at about 50 km from the margin), until they are destroyed by flooding, or the opening of a crevasse.

2. In sharp contrast, the concentration of ≈100-μm-sized cosmic spherules, C_{cs}, measured in the residual sand extracted from ≈100 g of cryoconite, is dependent on the location of the collecting site. Indeed, C_{cs} scales the "purity" of the extraterrestrial materials, which depends upon the abundance of the terrestrial component (mostly wind-borne dust). On a given ice field, "purity" worsens toward the margin; on the other hand, it also drastically improves with decreasing distance of the margin to the sea shore. Thus, the most favorable ice fields terminate on the sea shore (Jakobshavn and de Quervain Harbour), and not 30 km inland (Sondrestromfjord).

3. Although the relative number of large spherules sharply decreases with increasing sizes (as expected from the mass distri-

bution of the interplanetary flux of IDPs), their concentration in the residual sand markedly increases with increasing size fraction, as a result of a much sharper drop in the amount of coarse-grained terrestrial material. In all sites investigated, with the exception of samples collected on the Port Victort ice field, the <100-μm size fraction can hardly be used ($C_{cs} < 10^{-3}$). In contrast, at all sites, the values of C_{cs} in the >300-μm fraction is much higher (>0.1).

These trends in the "purity" of the cosmic dust component reflect the dominating effect that wind-borne dust (blown from ice-free land) has on the C_{cs} value. This "size fraction" trend is just the opposite on the Antarctic ice sheet (both near the margin and in blue ice fields near Transantarctic mountains). There the major terrestrial contaminant originates from coarse morainic debris; thus the coarser size fraction is heavily contaminated. The Greenland and the Antarctica collections appear remarkably complementary.

Although it is easy to recover a large number of cosmic spherules and IDPs from cryoconite, the two following biases, both related to cryoconite, presently limit the representativity and usefulness of the Greenland collection for <300-μm IDPs.

1. The harsh mechanical cryoconite disaggregation procedure does destroy the most friable chondritic grains, which are the most "unmelted," and possibly the most interesting IDPs. The present collection of Greenland cosmic dust particles is thus biased toward hard particles, including cosmic spherules, scoria-type particles (i.e., partially melted IDPs), and crystalline IDPs.

2. During their metabolism, the cryoconite siderobacteria release colloidal forms of hydrated iron oxides, filling up the structure of porous grains. Such colloids act very efficiently as "ion exchange resin" and adsorb trace elements in melt water, and thus contaminate porous grains. Robin [17] showed that all porous IDPs have a terrestrial REE pattern, while the crystalline IDPs exhibit the typical chondritic pattern.

Despite these two problems related to cryoconite, there are still bright prospects in using Greenland to collect IDPs. First, if we find some cryoconite-free ice fields in north Greenland (see "Curation of Polar IDPs for EUROMET" below), then these fields will probably be the best collector of "giant" IDPs with size >400 μm. The cryoconite is not only a source of large unweathered crystalline IDPs, it can be used to probe the past activity of the IDP flux. Indeed, the ice flow model of Neels Reeh shows that the ≈30 cryoconite samples collected between ≈2 and 50 km from the margin of the Sondrestromfjord ice field could be used to detect changes in the composition of spherules, crystalline grains, and scoria-type particles trapped in cryoconite over the last ≈10,000 years.

Mining of IDPs in Antartica: These biases related to cryoconite led Maurette and Pourchet (Laboratoire de Glaciologie de Grenoble) to sample in the blue ice fields of Cap-Prudhomme (December 1987–January 1988), near the French station of Dumont d'Urville, Antarctica. With ≈$10,000 we got two used steam generators, two used immersion pumps, one water pump, two used electrical generators, the necessary plastic tubing, and the stainless steel sieves (with openings of 50, 100, and 400 μm), and we left for Antarctica with this primitive ice "melter." Pockets of melt water were formed (each with a volume of 2–3 m^3) by injecting a jet of hot water at 70°C (delivered by a steam generator) into a ≈2-m-deep drill hole. IDPs initially trapped in the ice were collected, just pumping the water to the sieves. After one week of unsuccessful attempts, we found an area where the ice was not too contaminated with morainic debris or full of open microcracks, through which water could be lost. In this small ≈2000 m^2 blue ice area we could make two pockets of melt water each day of good weather. We thus melted about ≈100 tons of ice (free of cryoconite) over a six-week period.

The observation of cosmic spherules in the glacial sand recovered in the sieves revealed a sharp decrease in terrestrial contamination with decreasing size fraction, leading to an amazingly high "purity" of the 50–100-μm size fraction (the opposite trend is observed in Greenland). Later laboratory work revealed that the ratio of unmelted to melted IDPs was unexpectedly large (>5) in this size fraction. This is contrary to that predicted by atmospheric entry models, which estimate that >99% of IDPs with sizes ≈100 μm should be completely melted [2]. In this 50–100-μm size fraction, the concentration of IDPs was very high, ≈0.1, and the total number of IDPs recovered from 100 tons of ice exceeds 10,000. Although >400-μm IDPs are still found, they occur in much smaller numbers. Their lower concentrations reflect both an increase in contamination by morainic debris, a decreasing flux of large IDPs in the interplanetary medium, and a stronger frictional heating in the atmosphere.

In December 1990 and January 1991 we returned to the same area with Pourchet to collect IDPs for EUROMET: 260 tons of ice were melted over 25 days of field operation, and an additional sieve size was included to collect IDPs in the 25–50-μm size fraction. We wanted to make a connection between the Antarctic IDPs and the smaller stratospheric IDPs. The three years between the two expeditions allowed the ice sampled in 1987–1988, which has been punctured with ≈40 holes and heavily polluted by our activities, to flow toward the sea and be replaced by fresh, ultraclean ice (the ice in this area moves at about 10 m a year and was formed in preindustrial times ≈50,000 years ago). We improved the EUROMET "melter," by using three new steam generators, and new pumps and fittings. We also hired an expert cartographer (Christian Vincent) to measure the ice flow at and around the collection site. We hope to learn how to identify rare and favorable areas such as this one from aerial photographs.

In 1987, Faure and Koerberl examined samples of neogene tills from the Walcott Névé area and found that they contained abundant cosmic spherules [18]. During the subsequent ANSMET expedition, one of us (R.H.) collected several kilograms of similar samples (surficial eolian and moraine debris) from various locations near local blue ice meteorite stranding surfaces. High concentrations (>20 per g) of large (>250 μm) cosmic spherules were found in all samples. These concentrations have probably formed as extraterrestrial material is exposed by the ablation of the blue ice, allowing strong katabatic winds to move the debris downwind to local eolian traps. Harvey and Maurette [19] searched these sediments for possible IDPs, meeting with little success. In one favorable sample, more than 1000 >100-μm-sized spherules were recovered, while only half a dozen possible IDPs were located. This very small ratio of IDPs to cosmic spherules (at least 100 times smaller than at Cap-Prudhomme) was quite unexpected, and as a result the recovery of IDPs from these sediments becomes very difficult and unlikely. This low ratio might be related to the abundance of coal in the samples, which might camouflage any dark irregular IDPs. In addition, sufficient weathering may have occurred to disaggregate fluffy IDPs, moving their fragments to smaller size fractions (<50 μm). This

fraction has not been fully investigated yet. The value of these sediments lies in their high concentration of >500 μm cosmic spherules and "minimeteorites" (which can be directly obtained from R.H.) and in the relatively unweathered condition of the recovered specimens (as compared to those recovered from deep sea sediments). Similar samples are collected annually by ANSMET expeditions with the hope of finding more unusual samples and perhaps higher concentrations of IDPs.

To identify blue ice fields having the highest concentration of IDPs, and to understand how the concentration of IDPs changes as a function of depth within the ice (being possibly modulated by past climatic conditions), we studied ≈50-kg blocks of blue ice, cut with a wire saw at both Cap-Prudhomme (by D. Barnolla in January 1987) and in the Queen Alexandra range (by the 1990 ANSMET field party). In 1987, using the facilities at Laboratoire de Glaciologie de Grenoble, we just counted the total number [5] of >50-μm-sized chondritic cosmic spherules in the Cap-Prudhomme block to make sure that our future (December 1987) collection at this site would be fruitful. In 1992, with J. Cragin from the Cold Regions Research and Engineering Laboratory (CRREL), we measured the concentration of IDPs and cosmic spherules with sizes >35 μm within the Queen Alexandra block [20], and we are presently determining the depth profiles of the concentration of various trace elements and/or micrometer-sized aerosols in the same block.

So far, the striking result is that the concentration of >50-μm-sized chondritic cosmic spherules (≈100 per ton) is very similar in these two very different ice fields, and about 20 times larger than the background level (≈5 per ton). This background was determined by making a ≈2 m^3 pocket of melt water at a depth of 5 m at the same location where the ice block was taken at Cap-Prudhomme. Thus an efficient concentration mechanism, still to be understood, exists at these two very different ice fields.

Some analyses of polar MMs point out limitations that we hope to overcome during our next expedition. These include (1) the lower S, Ca, and Ni contents of IDPs recovered from the ice, which are probably related to the dissolution of highly soluble carbonates and sulfates in melt water; and (2) the corrosion of the steam generator pipes (made of ordinary steel, as no stainless steel and/or copper pipe was available), which released a large amount of fine-grained rust, which heavily polluted the 25–50-μm fraction. Contaminant trace elements such as Pb and Ur were also detected in some of the grains [13,21].

Curation of "Polar" IDPs for EUROMET: The present curatorial facilities at CSNSM have to be improved in order to properly store the EUROMET collection of polar IDPs, which includes (1) ≈50 distinct samples of Greenland wet cryoconite, collected from July 1987 to July 1988, stored into polyethylene bags, and representing a total mass of ≈200 kg; (2) >40,000 IDPs from Cap-Prudhomme, Antarctica, distributed in four size fractions (25–50, 50–100, 100–400, and >400 μm), but mostly found in the 50–100-μm size fraction. This is by far the purest and the richest sample of IDPs ever extracted from terrestrial sediments. The ≈60 g of Cap-Prudhomme sand extracted from 360 tons of ice have been encapsulated in about 250 vials (made of either glass and/or plastic). There is a very sharp drop of IDPs with increasing size, as we only collected 10 partially melted IDPs and 93 cosmic spherules with size of >400 μm from 260 tons of melt-ice water. We also clearly showed that it is feasible to collect a very pure 25–50-μm IDP size fraction [22] at the condition of eliminating the rust grains.

Currently the EUROMET collection of vials and plastic bags is stored in a freezer. We have to get funding (≈$20,000) to repair and modernize a small dust-free room, which will be used to store, handle, and preserve this collection. We have no SEM equipped with a fast EDS system (the basic instrument for curatorial work on IDPs). Fortunately, since 1989 we have a new instrument available at the Naturhistorisches Museum in Vienna, which we utilize about 20 weeks a year. We still need to improve the rapidity of the SEM analyses, by acquiring a fast system of automated analysis, costing $70,000.

Because of past problems we are reluctant to distribute samples of bulk cryoconite, with just a note explaining how to extract IDPs from these sediments. Instead, we prefer to distribute ≈500 mg aliquots of the >100-μm-sized sand material extracted from ≈100 g of wet cryoconite. These sand aliquots contain about 80 spheres and 20 IDPs of the scoria and crystalline types. A method, based on one already developed by geochemists to remove iron hydroxydes from "rusty" clays, should be developed to remove such hydroxides from porous IDPs.

The major characteristic of the 1991 EUROMET collection of IDPs are outlined elsewhere [23]. To receive a few milligrams of the 50–100-mg sand, containing a few hundred IDPs, or an aliquot of 20 IDPs from the 100–400-μm size fraction, a researcher has only to write an approximately one-page proposal to Michel Maurette (fax: 003-1-69-41-52-68). If one hand-picks the dark, irregular grains, showing no bright color, only about 10% of mostly crystalline and light colored IDPs will be missed.

Both the 25–50-μm fraction and the few "giant" IDPs from the >400-μm size fraction are given only to groups with the best expertise in either the handling of stratospheric IDPs or in the multidisciplinary microanalyses of >400-μm grains. The nine "giant" IDPs recovered from 260 tons of melt-ice water have not been allocated, but any short proposal will be considered by EUROMET. During our forthcoming expedition at Cap-Prudhomme we hope to collect a very pure 25–50-μm size fraction. If so, we plan to lend about one-third of this material to NASA, which has developed better expertise in handling and curating IDPs in this size range.

Future Prospects: From the Hans Tausen Project in Greenland to Melt-Ice Water at the South Pole and Dome C: As part of the international Hans Tausen project in Greenland, C. Hammer is organizing a 1995 glaciological expedition to a high northern ice cap, which is considered to be extremely sensitive to climatic variations. At this northern latitude the Arctic summer is too short for the siderobacteria (that make the bulk of cryoconite) to grow. Melt-ice water, however, is still running right at the shallow margins of the ice fields. One of our major goals is to filter this water and collect a cryoconite-free sand, rich in "minimeteorites," with sizes >1 mm. In one month of operation with ≈10 stacks of sieves, about 100,000 tons of melt water could be filtered. Simultaneously, we will look for meteorites near the margin of the ice field.

In 1992, Maurette received funding from IFRTP (Institut Français de Recherches et de Techniques Polaires) to develop an all-stainless-steel ice melter. Almost all components of this melter in contact with the ice or melt water (pipes of the steam generators, hot water pipes, immersion pumps, ice coring device, etc.) will be made of the same stainless steel used in the water pipes of French nuclear

reactors. This steel is ranked as one of the best with regard to corrosion resistance in water. Thanks to the cooperation of IN2P3, one of us (G.I.) was authorized to work full time on this melter, which has been built and was transported to the French station of Dumont d'Urville in December 1992. It will be used during the next Antarctic summer to obtain a new EUROMET collection of IDPs. These samples should be free of rust particles and of contaminants released during the formation of the rust and the dissolution of the plastifiers used in the plastic tubing. They should yield a very pure 25–50-μm size fraction. We shall also attempt to collect a 10–25-μm size fraction.

Harvey is planning to build a "minimelter" (a smaller version of the EUROMET melter) for the collection of IDPs from remote meteorite stranding surfaces during future ANSMET seasons. This will allow the investigation of the micrometeorite content of ice that is relatively free of terrestrial debris, as well as the collection of IDPs from ice of different ages. In addition, the meteorite and IDP content of a parcel of ice can be compared.

Yiou et al. have shown that >50-μm IDPs and cosmic spherules (about 1 per ≈10 kg of ice) can be extracted from Antarctic ice cores [24]. This difficult work has to be encouraged in the future, as it gives the exciting prospect of detecting possible changes in the composition of the IDP flux over a timescale of ≈200,000 years. Hammer and Maurette are also considering drilling a ≈100-m-deep core in Greenland, specifically dedicated to a search for Tugunska "ashes."

Taylor and Harvey are hoping to obtain funding to retrieve IDPs from the bottom of the new water well at the U.S. South Pole station. Over the lifetime of the well, 5–10 years, a cylinder 15 m in diameter and 100 m deep will be melted in the clean firn and ice and thousands of IDPs, released from the ice, should be on the bottom. As the age of the melted ice is well known, by sampling yearly it might be possible to detect changes in the type and flux of IDPs as a function of time. Harvey and Taylor also hope to exploit the surface snow melter built by Westinghouse to provide water (≈10,000 tons a year) at the South Pole station. A miniaturized version of this system will also be used at the future Italian-French station "Concordia," to be constructed at Dome C.

Acknowledgments: Our two first expeditions in Greenland were made possible by grants from INSU in France, and the Commission for Scientific Research in Greenland. The two expeditions at Cap-Prudhomme have been entirely funded and logistically supported by IFRTP (Institut Français de Recherches et de Techniques Polaires). One of us (M.M.) also acknowledge both the EEC Programme "SCIENCE (Twinning and Operations)" (Contract SC1-CT91-0618 SSMA), the support of IN2P3, the invaluable technical help of M. Pourchet, and the generous scientific cooperations of D. E. Brownlee, M. C. Michel-Levy, C. T. Pillinger, and R. M. Walker. R. Harvey received support from NSF (grant DPP 8314496) for field work and analytical studies. The analytical work of G. Kurat is funded in Austria by contract P8125-GEO of FWF.

References: [1] Zolensky M. E., this volume. [2] Brownlee D. E. (1985) *Annu. Rev. Earth Planet. Sci., 13*, 147. [3] Maurette M. et al. (1989) in *From Mantle to Meteorites* (K. Gopalan et al., eds.) Indian Academy of Sciences, Bangalore. [4] Taylor S. and Brownlee D. E. (1991) *Meteoritics, 26*, 203. [5] Maurette M. et al. (1991) *Nature, 351*, 44. [6] Steele I. M. (1992) *GCA, 56*, 2923. [7] Kurat G. et al., this volume. [8] Michel-Levy M. C. and Bourot-Denise M. (1992) *Meteoritics, 27*, 73. [9] Presper T. et al. (1992) *Meteoritics, 27*, 278. [10] Perreau M. et al. (1993) *LPS XXIV*, 1125. [11] Kurat G. et al. (1992) *Meteoritics, 26*, 246. [12] Presper T. et al. (1993) *LPS XXIV*, 1177. [13] Flynn G. J. et al. (1992) *Proc. NIPR Symp. Antarct. Meteor.*, in press. [14] Jessberger E. K. et al. (1992) *EPSL, 112*, 91. [15] Grün E. et al. (1985) *Icarus, 62*, 244. [16] Callot G. et al. (1987) *Nature, 328*, 147. [17] Robin E. (1988) Ph.D. thesis, Université de Paris-Sud, Centre d'Orsay. [18] Koerberl C. and Hagen E. H. (1989) *GCA, 53*, 937. [19] Harvey R. P. and Maurette M. (1991) *Proc. LPSC, Vol. 21*, 569. [20] Maurette M. et al. (1992) *Meteoritics, 27*, 257. [21] Lindstrom D. J. and Klöck W. (1992) *Meteoritics, 27*, 250. [22] Maurette M. et al. (1992) *LPS XXIII*, 857. [23] Maurette M. et al. (1992) *Meteoritics, 27*, 473. [24] Yiou F. et al. (1991) *Meteoritics, 26*, 311.

SOLAR SYSTEM EXPOSURE HISTORIES OF INTERPLANETARY DUST PARTICLES.

A. O. Nier, School of Physics and Astronomy, University of Minnesota, Minneapolis MN 55455, USA.

For many years it has been recognized that the existence of zodiacal light was strong evidence that dust existed in interplanetary space. It was realized that some of this dust should settle on the Earth, so many attempts were made to collect and classify the particles [1]. Collections were made in the low and in the high atmosphere, on polar ice, in the deep oceans, as well as in less remote places. The results of analyses were not decisive due to the presence of very much larger amounts of dust of terrestrial origin. Small iron spherules have been found, which from isotopic analyses appeared to be of extraterrestrial origin. However, it was never demonstrated that they were not merely ablation products of meteorites.

Stratospheric Collection of Interplanetary Dust Particles (IDPs): An important breakthrough came when Brownlee et al. [2] showed that some of the particles collected on adhesive surfaces placed on the leading edges of wings of planes flying in the stratosphere had unique characteristics that precluded their being of terrestrial origin. Extensive studies of their nature [3–5] showed that, in many respects, their composition was similar to that of CI chondritic meteorites. They are irregular in shape and range from fluffy to solid. In falling through the atmosphere they are heated as they are decelerated, the extent of heating depending upon their size and density. As a result, ones larger than 50–100 μm in "diameter" are generally melted, or may be altered in other ways. Most of the interest has been in small particles, ranging in size from a few to some tens of micrometers and having masses measured in nanograms, since they are less likely to have been altered as a result of atmospheric heating.

Because of the scarcity of particles, research has been devoted almost entirely to the investigation of individual IDPs. The small size of the particles has required the use of highly sophisticated instrumentation and considerable ingenuity by the investigators.

In the case of meteorites, the extraction and isotopic analysis of the noble gases has been a fruitful experience. In the general case, the gases are made up of several components having different origins—a primordial component, one due to spallation reactions caused by cosmic ray bombardment over long periods of time, and in some cases gas resulting from radioactive decay. For IDPs the

situation is somewhat different. If the particles have their origin in comets or asteroids, as is generally believed, they exist as independent particles in interplanetary space for only a relatively short time—of the order of 10,000 years—before they settle to the stratosphere, where they are concentrated. This is not sufficient time to accumulate measurable amounts of cosmic-ray-produced spallation products. Moreover, the spallation products are created with kinetic energy, and have ranges longer than particle diameters, and hence would not be retained. On the other hand, like lunar soil grains, the IDPs are subject to bombardment by the solar wind and solar flares, including the so-called solar energetic particles (SEPs). Noble gas analyses hence are valuable, but in a different way from the corresponding analyses of meteorities.

The first noble gas analyses on IDPs were made by Rajan et al. [6]. In a study of 10 individual particles, having masses in the range of 0.2–24 ng, ^{4}He concentrations comparable to those observed in lunar grains were found. These were attributed to solar wind accumulation. Calculations have shown [7] that in the 10,000-year time span when the particles may have been free in interplanetary space, solar wind bombardment could readily account for all the He observed. In an investigation by Hudson et al. [8], 13 particles were combined and an attempt made to measure the ^{20}Ne/^{22}Ne ratio. The investigators concluded that the ratio fell in the range expected for solar wind Ne, and this provided further evidence that the particles were of extraterrestrial origin.

Additional evidence for an extraterrestrial origin was obtained by Bradley et al. [9] who, in a study of several IDPs collected in the stratosphere, observed solar flare tracks. The densities of the tracks were consistent with the particles being exposed to solar cosmic rays in the interplanetary medium for a period of roughly 10^4 yr. Moreover, the fact that the tracks existed and had not been erased by temperature annealing indicated that the particles had not been heated above 500°–600°C in their deceleration in the atmosphere. More recently, Sandford [10] has considered the general problem of interpreting solar flare track densities in IDPs.

Sources of Interplanetary Dust Particles: The likely source of interplanetary dust has been a subject of interest for many years. Until recently it was generally believed that most of the dust came from comets as they were heated in their approach to the Sun. Several lines of evidence [11,12] now point to asteroids as the likely source for a large proportion of the particles. One of these considerations is based on the release pattern of the He as the particles are heated in laboratory experiments, and the relation of this pattern to the thermal history of the particles [13].

Whipple [14] considered the general problem of deceleration heating of particles that entered the Earth's atmosphere. His computations were extended by a number of investigators [15–17]. The net result of the calculations may be summarized in an approximate form as follows: a particle outside the Earth's atmosphere picks up speed toward the Earth's center as it experiences the Earth's gravitational pull. When it reaches a sufficiently dense part of the atmosphere, below 100 km but above the stratosphere, it is decelerated by the drag force of the atmosphere. The kinetic energy of the particle is converted to heat, warming the particle. The extent of the heating depends primarily on the speed of the particle and its diameter and mass density.

IDPs having their origin in asteroids have little velocity relative to the Earth when they begin to feel the Earth's gravitational pull and hence, in their fall, reach speeds of only approximately 12 kms^{-1}, the same as the escape velocity of objects leaving the Earth's gravitational attraction. On the other hand, IDPs having their origin in comets carry with them the velocity of the comet and hence have a total velocity higher than that of typical asteroids when they begin their deceleration. Consequently they will be heated to higher temperatures during deceleration. In the case of low-periapsis comets, the total velocity may reach 15–20 km s^{-1} and the heating several hundred degrees C above that of the 12 km s^{-1} particles. The actual situation is more complex since particles reach the Earth coming from various directions, so there is actually a distribution of velocities and heating. The orbital dynamics problem has been discussed in some detail by Jackson and Zook [18]. In any event, the deceleration in the atmosphere takes place very rapidly, so the heat pulse experienced by the particles lasts only a few seconds [17], a fact that can be utilized in laboratory simulation experiments [13], which will be discussed later.

Solar Wind and Noble Gas Isotopic Ratios in IDPs: *Gas extraction experiments.* The noble gas studies mentioned earlier have been extended to include measurements on individual particles for ^{3}He/^{4}He, ^{20}Ne/^{22}Ne, and, in a few cases, ^{21}Ne/^{22}Ne isotopic ratio measurements on individual particles. Summary results are given in Table 1. In an initial study [19], summarized in line A, 16 individual IDPs having diameters of approximately 15 μm were heated sufficiently to extract all the gas. As noted, the average ^{4}He content measured in cm^{3}STP g^{-1} was approximately one-sixth that found for typical lunar fines having the same size. The isotopic ratios ^{3}He/^{4}He, ^{20}Ne/^{22}Ne, and ^{4}He/^{20}Ne were all lower, but comparable to those of the lunar fines. This would suggest a similar source for the gas, namely, the solar wind. While no attempt was made to study the extraction of the gas as a function of the temperature by step-heating, there is little question but that the IDPs were heated in their deceleration in the atmosphere, and hence almost certainly lost some gas. The loss would tend to be greater for the lighter species. This would explain, at least qualitatively, the lower ratios than the corresponding lunar ones. It should also be pointed out that the ^{3}He/^{4}He and ^{20}Ne/^{22}Ne ratios fall in the general range attributed to solar energetic particles (SEPs) by Wieler et al. [21] in their lunar grain etching experiments. Moreover, they are not far different from the primordial constituents found in carbonaceous chondrites [22] and gas-rich meteorites [23]. While some, or most, of the He and Ne found in IDPs is due to solar wind and SEP entrapment, one cannot rule out completely the possibility that at least a small fraction may be of primordial origin.

Step-heating gas extraction experiments. The success of the first investigation led to a second one in which the gas in individual IDPs was extracted by step heating [20]. The results are summarized in line B of Table 1. This study was motivated by the possibility of using the results to distinguish between particles of asteroidal and cometary origin. As discussed earlier, many IDPs having a cometary origin would be heated more than average asteroidal particles during their deceleration in the atmosphere. For these one might expect less gas, and this would not be released until higher temperatures are reached in the extraction process.

In an investigation of 20 IDPs it was found that 12 held a reasonable amount of ^{4}He—on the average $(38 \pm 10) \times 10^{-3}$ cm^3 STP g^{-1}—with the greatest release rate occurring at a temperature of 582° ± 22°C, at which point approximately 30% of the He has been extracted. Four of the 20 IDPs held substantially less He, and this was clearly released at a higher temperature. The four remaining

TABLE 1. Results of noble gas extractions from IDPs.

Investigation	Heating	No. of Particles	Avg. Dia. μm	^{4}He cm^{3}STP× 10^{11}	^{4}He cm^{3}STP/g × 10^3	^{3}He/^{4}He ×10^4	^{4}He/^{20}Ne	^{20}Ne/^{22}Ne	Avg. temp.°C
A Ref[19]	total	16	~15	16±6	27±2	2.4±0.3	33±7	12.0±0.5	
B Ref[20]	step	20	~15	4.6±1.3	38±10	2.8±0.2			582±22§
C Ref[13]	pulse	24	~20	4.7±2.0	5.6±2.4	5.3±0.9‡	35±9		798±24¶
D Ref[12]	pulse	22	5–10	10.4±2.0	170±50	5.3±0.7	58±10		629±28**
Solar wind*						4.3±0.2	~600	13.7±0.3	
Lunar fines†					150±20	3.7±0.1	62±5	12.6±0.1	

* Geiss J. et al. (1972) *NASA SP-315*, 14.1–14.10.

† Average of Eberhardt P. et al. (1970) *Proc. Apollo II Lunar Sci. Conf.*, 1037–1070; Eberhardt P. et al. (1972) *PLSC 3rd*, 1821–1856; Hintenberger H. et al. (1971) *PLSC 2nd*, 1607–1625; Pepin R.O. et al. (1974) *PLSC 5th*, 2149–2184; Pepin R.O. et al. (1975) *PLSC 6th*, 2027–2055.

‡ Average for 8 IDPs that appeared "normal"; average for 14 others was (60±13)× 10^{-4}.

§ For 30% of helium extraction.

¶ For 50% of helium extraction.

** For 50% of helium extraction.

particles contained essentially no He.

The analysis in this case is complicated by the fact that the particles used in this study were actually fragments approximately 15 μm in diameter of parent IDPs approximately 50 μm in diameter. Consequently, they were heated more than if they had been 15-μm particles during atmospheric deceleration. The greater general heating, due to size alone, would tend to blur the distinction between asteroidal and cometary particles, so the experiment is not as decisive as it might have been. On the basis of the laboratory results alone one might tentatively conclude that at least half the particles were of asteroidal origin. Final judgment should be deferred until results are obtained from the elemental and mineralogical investigations being conducted on fragments, companion to those employed in the present study.

Pulse-heating extraction experiments. The theoretical analyses of Love and Brownlee [17], as well as earlier calculations, show that the heat pulse felt by IDPs during their deceleration in the atmosphere lasts only about 2 s. This suggests that if a comparison is to be made between this heating and subsequent laboratory step heating it would be more realistic to employ a succession of heat pulses with increasing temperature and of the approximate shape of the deceleration heating pulses. This was done for the data presented in lines C and D of Table 1.

In the line C investigation, 24 particles were employed that had diameters of approximately 20 μm, but were fragments of IDPs that had diameters around 40 μm [13]. As in the step-heating experiments, other fragments of these IDPs are undergoing elemental and mineralogical study in various laboratories.

In the line D investigation [12], 22 IDPs were employed that were relatively small—5–10 μm in diameter—but were not fragments of larger particles as in the line B and C investigations. It was expected that the use of the smaller particles would reduce the deceleration heating inherent in the line B and C studies, and thus provide a sharper distinction between asteroidal and cometary particles, associated with differences in their velocities. The results [12] appear to have justified the choice. Not only did the particles contain more He than the much larger fragments used in the line B and C experiments, but results showed that a large majority of the particles suffered only a modest amount of heating prior to being collected, suggesting that they were very likely of asteroidal origin. In the case of the fragments of line C, which were derived from large IDPs, the greater deceleration heating associated with the size largely masked any heating difference that would be associated with a difference in the incoming velocity.

While the average isotopic ratios given in Table 1 are more or less consistent, the averages hide variations that may be significant and worthy of note. For example, among the particles summarized in line A was one (L2015A5) for which the amount of ^{4}He was near average, as was the ^{20}Ne/^{22}Ne ratio, yet the ^{3}He/^{4}He was six times the average and the ^{3}He/^{20}Ne only about one-tenth the average for the 16 particles. Why?

As noted in the third footnote c of Table 1, the ^{3}He/^{4}He ratios include some peculiarities. Among the 24 particles studied, the average ratio for eight of the particles was $(5.3 \pm 0.7) \times 10^{-4}$, a value about double that found in the earlier investigations, but significantly different. On the other hand, for 14 of the particles the average ratio was $(60 \pm 13) \times 10^{-4}$, a value 11 times higher! For these same particles the average concentration of ^{4}He was $(1.2 \pm 0.2) \times 10^{-3}$ cm^{3}STP g^{-1} compared with 14.5×10^{-3} cm^{3}STP g^{-1} for the more "normal" particles. Likewise, the average ^{4}He/^{20}Ne ratio for the abnormal particles was 13.6 ± 3.3, whereas it was 79 ± 15 for the more normal particles. In spite of these large differences, the average temperature for 50% extraction of the ^{4}He was almost the same, 800°C, for the two groups.

Summary and Conclusions: For all but a few of the 82 individual particles analyzed, ^{3}He/^{4}He ratios could be determined. They generally fell in the range $2–6 \times 10^{-4}$, a value in the general range found for lunar soil grains and the solar wind. However, there are particles for which the ratio is considerably higher—enough so as to raise the possibility of other sources of He. In the case of the

smallest particles, which are not heated extensively in passing through the atmosphere, the He concentrations are comparable to those found for lunar surface grains.

The pulse-heating procedure appears to have the power to provide evidence on the thermal history of IDPs. In the case of small particles it should help distinguish between particles of asteroidal and those of cometary origin.

References: [1] Hodge P. W. (1981) *Interplanetary Dust*, Gordon and Breach, New York. [2] Brownlee D. E. et al. (1977) *Proc. LSC 8th*, 149–160. [3] Fraundorf P. et al. (1982) in *Comets* (L. I. Wilkening, ed.), 383–409, Univ. of Arizona, Tucson. [4] Bradley J. P. et al. (1988) in *Meteorites and the Early Solar System* (J. F. Kerridge and M. S. Mathews, eds.), 861–895, Univ. of Arizona, Tucson. [5] Brownlee D. E. (1985) *Annu. Rev. Earth Planet. Sci., 13*, 147–173. [6] Rajan R. S. et al. (1977) *Nature, 267*, 133–134. [7] Pillinger C. T. (1979) *Rep. Prog. Phys., 42*, 897–961. [8] Hudson B. et al. (1981) *Science, 211*, 383–386. [9] Bradley J. P. et al. (1984) *Science, 226*, 1432–1434. [10] Sandford S. A. (1986) *Icarus, 68*, 377–394. [11] Zook H. A. and McKay D. S. (1986) *LPSC XVII*, 977–978. [12] Brownlee D. E. et al. (1993) *LPSC XXIV*, 205–206. [13] Nier A. O. and Schlutter D. J. (1993) *LPSC XXIV*, 1075–1076. [14] Whipple F. L. (1950) *Proc. Natl. Acad. Sci. U.S.A., 36*, 687–695; (1951) *Proc. Natl. Acad. Sci. U.S.A., 37*, 19–30. [15] Fraundorf P. (1980) *GRL, 10*, 765–768. [16] Flynn G. J. (1989) *Icarus, 77*, 287–310. [17] Love S. G. and Brownlee D. E. (1991) *Icarus, 89*, 26–43. [18] Jackson A. A. and Zook H. A. (1992) *Icarus, 97*, 70–84. [19] Nier A. O. and Schlutter D. J. (1990) *Meteoritics, 25*, 263–267. [20] Nier A. O. and Schlutter D. J. (1992) *Meteoritics, 27*, 166–173. [21] Wieler R. et al. (1986) *GCA, 50*, 1997–2017. [22] Anders E. et al. (1970) *GCA, 34*, 127–131. [23] Black D. C. (1970) *GCA, 34*, 132–140. [24] Eberhardt P. et al. (1970) *Proc. Apollo 11 Lunar Sci. Conf.*, 1037–1070. [25] Eberhardt P. et al. (1972) *Proc LSC 3rd*, 1821–1856. [26] Hintenberger H. et al. (1971) *Proc. LSC 2nd*, 1607–1625. [27] Pepin R. O. et al. (1974) *Proc. LSC 5th*, 2149–2184. [28] Pepin R. O. et al. (1975) *Proc. LSC 6th*, 2027–2055.

STATUS REPORT—SMALL PARTICLES INTACT CAPTURE EXPERIMENT (SPICE).

K. Nishioka[1], G. C. Carle[2], T. E. Bunch[2], D. J. Mendez[3], and J. T. Ryder[3], [1]SETI Institute, Mt. View CA 94043, USA, [2]NASA Ames Research Center, Moffett Field CA 94035, USA, [3]LMSC, Palo Alto CA 94304, USA.

Introduction: The Small Particles Intact Capture Experiment (SPICE) will develop technologies and engineering techniques necessary to capture nearly intact, uncontaminated cosmic and interplanetary dust particles (IDPs). Successful capture of such particles will benefit the Exobiology and Planetary Science communities by providing particulate samples that may have survived unaltered since the formation of the solar system. Characterization of these particles may contribute fundamental data to our knowledge of how these particles could have formed into our planet Earth and, perhaps, contributed to the beginnings of life. The term "uncontaminated" means that captured cosmic and IDP particles are free of organic contamination from the capture process and the term "nearly intact capture" means that their chemical and elemental components are not materially altered during capture.

The key to capturing cosmic and IDP particles that are organic-contamination free and nearly intact is the capture medium. Initial

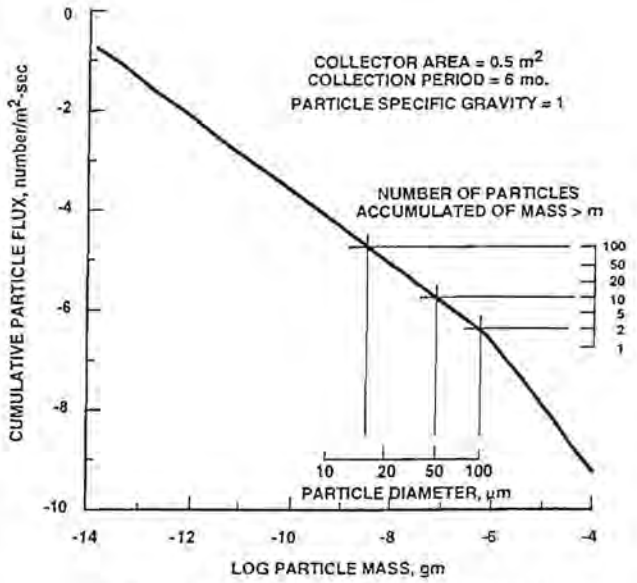

Fig. 1. Cumulative micrometeroid flux model [1].

screening of capture media included organic foams, multiple thin foil layers, and aerogel (a silica gel), but, with the exception of aerogel, the requirements of no contamination or nearly intact capture were not met. To ensure no contamination of particles in the capture process, high-purity aerogel was chosen. High-purity aerogel results in high clarity (visual clearness), a useful quality in detection and recovery of embedded captured particles from the aerogel. P. Tsou at the Jet Propulsion Laboratory (JPL) originally described the use of aerogel for this purpose and reported laboratory test results [1]. He has flown aerogel as a "GAS-can Lid" payload on STS-47 and is evaluating the results [2]. The Timeband Capture Cell Experiment (TICCE), a Eureca 1 experiment, is also flying aerogel and is scheduled for recovery in late April. The issue of residual organics in the aerogel as a contamination source during the capture process was not addressed in these experiments.

SPICE Project Instrument Description: SPICE is a passive instrument; the only moving part is the protective cover shielding the aerogel surface during integration onto the spacecraft, launch, on-orbit episodes, and recovery of the instrument. Primary instrument subsystems are structures, electronics, simple diagnostic sensors, and aerogel. No structural issues are foreseen, with the possible exception of mass and shape/size constraints imposed by the flight platform. The required diagnostics are time-tagging and locating of impacts on the aerogel surface. Microphonics is one method for time-tagging impacts while coordinates for each impact could be obtained by embedding layers of wire grids in the aerogel to sense electric or magnetic field changes caused by the impacts.

SPICE Development Phases: SPICE experiment development follows a standard three-phase approach starting with technical feasibility validation (completed), conceptual design, and final design and fabrication. As stated earlier, aerogel is the key to SPICE's performance, so clear systematic understanding is required of the interactions between chemical components, densities, purity, clarity, and residual organics in the manufacture of aerogel for consistent batch-to-batch performance qualities.

Phase 1. Phase 1 has resolved the critical issues of orbital flight

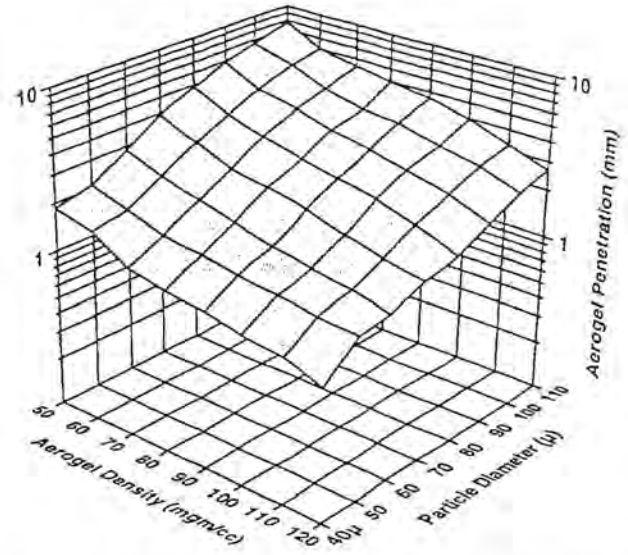

Fig. 2. Simulant penetration for Allende, V = 6.0 km/s [4].

platforms availability, abundance of cosmic and IDP particles in low-Earth orbit, and the feasibility of manufacturing high-purity aerogel. Science Applications International Corporation (SAIC) [3] addressed the first two issues and identified WESTAR and Eureca as desirable flight platforms and found that a six-month mission using a half square meter of capture area results in encountering about a hundred 10-μm or larger and several 100-μm or larger particles. This is illustrated in Fig. 1.

The Lockheed Missiles and Space Corporation's (LMSC) study [4] addressed the third issue, the manufacturing feasibility of high-purity aerogel with necessary capture performance. Results from their previous study [5] for the Johnson Space Center surveying the technology status for aerogel were useful to the task of manufacturing high-purity aerogel. Purity of the manufactured aerogel was evaluated at the LMSC, Palo Alto Materials Laboratory, and capture performance tested at Ames Research Center's Hypervelocity Gun Range (HVGR). Both results were encouraging, showing that for the levels of aerogel densities (50–120 mg cc^{-1}) and attainable test velocities (4–6 km s^{-1}), the aerogel's capture performance was satisfactory and the clarity of the aerogel aided in recovering captured particles. Simulant particles included Allende, Murchison, and diamonds in these tests. Figure 2 shows a typical performance summary chart for Allende particles for four parameters (velocity 6 km s^{-1} vs. size range approximately 70–110 μm vs. aerogel densities 50–120 mg cc^{-1} vs. aerogel penetration depths 1–8 mm). Similar performance charts for velocities at 4 and 5 km s^{-1} were obtained. The aerogel organics purity issue and the survivability of organics in the test particles could not be determined conclusively because of funding limitations, but appeared adequate. These issues will be resolved in Phase 2.

Phase 2. This phase started in September 1992, and is scheduled for completion in November 1993. LMSC is conducting a rigorously controlled manufacturing process development for aerogel to validate high-purity aerogel production using a specially designed and instrumented autoclave, and verified purity base chemicals. This is to identify and understand critical parameters such as purity of base chemicals and environmental parameters that affect chemical processes and reaction times and their effect on the manufactured aerogel's quality. Documentation of these parametric values, including detailed characterization of the manufactured aerogel, will become the basis for future aerogel manufacturing specifications.

The cosmic particle simulants for HVGR testing will be deliberately contaminated with known concentrations of organics (PAHs and amino acids) into the aerogel before launch. Analyses of both pristine and deliberately contaminated particles before and after testing will verify organics survival rates to the capture process.

Handling procedures for aerogel prior to and after HVGR testing will be developed and documented. Similarly, analytical procedures and processes for finding particle entry points, entry tracks, analysis of aerogel material surrounding entry tracks, and impact particle recovery and characterization analysis will be developed and documented for HVGR tests. These procedures and processes, with appropriate modifications following these tests, will be used in Phase 3. Also, the brassboard aerogel containment cell developed during this phase for use in HVGR tests provides a strawman design for Phase 3 flight instrument aerogel containment cells.

Phase 3. This phase is expected to take 24–30 months and the detailed tasks will be developed during FY'93 as part of Phase 2. The primary tasks will be the design and fabrication of an integrated flight instrument based on Phase 1 and 2 results that fulfill the science and technical requirements for SPICE.

Flight testing is necessary because ground test facilities have two major shortcomings: their inability to impart velocities greater than around 6–7 km s^{-1} to particles in the micrometer to tens of micrometer sizes, and the tendency of the hypervelocity gun's shock wave to disintegrate aerogels of densities less than about 50 mg cc^{-1}.

References: [1] Tsou P. et al. (1988) *Proc. LPSC 19th.* [2] Tsou P. (1992, 1993), personal communication. [3] Swenson B. L. (1992) *SAIC Report No. 92/1008.* [4] Mendez D. (1993) *LMSC Report No. P006695.* [5] Mendez D. (1991) *LMSC Report No. F369369.*

A PROPOSITION FOR THE CLASSIFICATION OF CARBONACEOUS CHONDRITIC MICROMETEORITES.

F. J. M. Rietmeijer, Department of Earth and Planetary Sciences, University of New Mexico, Albuquerque NM 87131, USA.

Classification of interplanetary dust particles (IDPs) should be unambiguous and, if possible, provide an opportunity to interrelate these ultrafine IDPs with the matrices of undifferentiated meteorites. I prefer a scheme of chemical groupings and petrologic classes that is based on primary IDP properties that can be determined without prejudice by individual investigators. For IDPs of 2–50 μm these properties are bulk elemental chemistry, morphology, shape, and optical properties [1–4]. The two major chemical groups are readily determined by energy dispersive spectroscopic analysis using the scanning or analytical electron microscope [1,3,5,6]. Refinement of chondritic IDP classification is possible using the dominant mineral species, e.g. olivine, pyroxene, and layer silicates, and is readily inferred from FTIR [7], and automated chemical analysis [8]. Petrographic analyses of phyllosilicate-rich IDPs will identify smectite-rich and serpentine-rich particles (Table 1). Chondritic IDPs are also classified according to morphology, viz., CP and CF IDPs are aggregate particles that differ significantly in porosity,

while the dense CS IDPs have a smooth surface (Table 2). The CP IDPs are characterized by an anhydrous silicate mineralogy, but small amounts of layer silicates may be present. Distinction between the CP and CF IDPs is somewhat ambiguous, but the unique CP IDPs are fluffy, or porous, ultrafine-grained aggregates. The CP IDPs, which may contain silicate whiskers [9,10], are the most carbon-rich extraterrestrial material presently known. The CF IDPs are much less porous than CP IDPs. Using particle type definitions from Table 2, CP IDPs in the NASA JSC Cosmic Dust Catalogs are ~15% of all IDPs that include nonchondritic spheres. Most aggregate particles are of the CF type.

The common occurrence of amorphous materials in chondritic IDPs has only recently been appreciated. These materials have variable compositions within, and among, individual IDPs [12,13] (Table 3). The presence of amorphous materials interferes with chondritic IDP classification using the automated, point-count, (chemical) analysis technique since the typical distribution pattern of particles dominated by layer silicates [8] will be indistinguishable from that expected for amorphous materials [14].

Some CS IDPs have an affinity to matrixes of type CI [15] and CM [16,17] carbonaceous chondrites. The importance of these observations to the study of IDPs is the fact that the mineralogy and textures of these meteorite-like particles stand out among all other chondritic IDPs. These observations confirm the conclusion by [11] that CP, CF, and most CS IDPs form a unique group of ultrafine-grained materials that differ significantly in form and texture from components of carbonaceous chondrites and contain mineral assemblages that do not occur in any meteorite class. The chondritic IDPs have high bulk C contents, viz., C/Si in CP IDPs is 2.39 μm CI and it is 1.32 μm CI in CS IDPs [18,19]. I designate these C-rich chondritic IDPs as a group of CC (i.e., carbonaceous chondritic) particles. Hence, the existing chondritic IDP types (Table 2) are reclassified as CCP, CCF, and CCS IDP subgroups. Also, from a petrological viewpoint, CC IDPs consist of four major components, viz., granular units (GUs) [9], polyphase units (PUs), single-crystal platelets (~0.5–2.0 μm in size), and single-crystal whiskers and euhedral silicates. The majority of CC IDPs are mostly variable mixtures of GUs and PUs [13], which I designate as principal components (Table 4).

Most GUs are of the GU_2 type. They are conspicuous in the CCP IDPs where they form the loosely packed matrix. They consist of ultrafine platey grains (~1.5 nm thick) and 2–1000 nm in diameter that are embedded in the carbonaceous materials. These grains are mostly Mg,Fe-olivines and Ca-poor pyroxenes, Fe,Ni-sulfides, and oxides [9,10]. The size distributions of ultrafine grains, and their morphology, support continuous thermal annealing (crystallization) of amorphous precursor material [21].

I propose that the interrelationships among the CC IDPs can be described as variations in the GU/PU ratio, viz., CCP IDPs : GU » PU, CCF IDPs: G ≈ PU, and CCS IDPs: GU « PU [13]. The ratio of ultrafine minerals to carbonaceous material, or GU_1/GU_2 ratio, varies among and within individual GUs [8,13]. These principal components provide an opportunity to study dust accretion and protoplanet alteration using silicate and C petrology. The mineralogical evidence supports CC IDP alteration under hydrocryogenic ($T < 0°C$) [22] and low-temperature aqueous($T \gg 300°C$) [5,10–14] conditions, as well as thermal annealing (dry crystallization) [21]. These phases of CC IDP evolution delineate petrologic classes that are defined by the GU and PU mineralogies in the CCP, CCF, and CCS IDPs: class 0: unaltered solar nebula dust; class 1: hydrocryogenic alteration (diagenesis); class 2: aqueous alteration (diagenesis) (cf. Table 3); class 3: thermal annealing (dry crystallization and fractionation); and class 4: dynamic pyrometamorphism [23,24].

The characteristic mineralogy of each class is presented in Table 5. I emphasize the role of amorphous materials and the ultrafine grain size to create high free energy regimes that are conducive to mineralogical activity at (very) low temperatures. Thus, IDP W7029C1 [11] becomes a $CCP_{1,2,3}$ IDP, that is, a C-rich CP IDP with evidence for petrologic classes 1, 2, and 3. Particle L2005L2, which contains

TABLE 1. Chemical groupings of interplanetary dust.

Particles with a Chondritic Bulk Composition
Particles dominated by amorphous materials plus carbons
Particles dominated by neso- and ino-(anhydrous) silicates plus carbons
Olivine-rich particles
Pyroxene-rich particles
Particles dominated by phyllosilicates (i.e., hydrous silicates) plus carbons
Smectite-rich particles
Serpentine-rich particles
Particles containing silicates only
Particles with a Nonchondritic Bulk Composition
Single mineral grains, such as iron-sulfides, olivine
Aggregates of fine-grained hibonite, melilite, and perovskite

TABLE 2. Morphological types of chondritic IDPs.

Chondritic porous [CP] IDPs; CP IDP W7010*A [9] and Figs 11.1.2.a and 11.1.3.a in [10]
Chondritic filled [CF] IDPs,
Chondritic smooth [CS] IDPs; W7017B12 [11] and Figs 11.1.2.b and 11.1.3.b in [10]

TABLE 3. Amorphous materials in chondritic IDPs.

Magnesiosilica
Ferromagnesiosilica, Mg/(Mg+Fe) (wt%) = 0.23 and 0.73-0.95 (Na-rich), ferromagnesio-aluminosilica (both high and low Al_2O_3)
Silica-rich
Chondritic (approximately) (rare)

TABLE 4. Principal components of CC IDPs.

GU_1: carbonaceous GUs (~0.2–2.0 μm in diameter) of (refractory) hydrocarbons and amorphous carbons; carbons >> ultrafine minerals, or mineral-free
GU_2: carbon-rich, chondritic GUs (~0.3–2.0 μm in diameter) of (refractory) hydrocarbons, amorphous carbons and ultrafine minerals [Figs. 2b and 3 in ref. 9]
PU: amorphous and holocrystalline, both coarse and fine-grained [20], with compositions listed in Table 3; PUs are about 1.0 μm in diameter

Sources: [10] and [13].

amorphous material, saponite, forsterite, and pyroxene [14], is a $CCF_{0,2,3}$ IDP. At first glance the subscripts seem chaotic and cumbersome, but I claim they provide information on CC IDP evolution.

Class 0. This classification predicts the existence of fully amorphous CCP, CCF, or CCS IDPs, depending on the GU/PU ratio.

Classes 1 and 2. The CC IDPs contain evidence for the onset of mineralogic activity in the solar system that was probably chaotic and nonequilibrium in nature. The mineral reactions were sensitive to reaction kinetics, to the surface free energy of nanocrystals, to catalytic support by carbonaceous materials, metals or metal oxides, and to subtle (spatial and temporal) variations in the presence of heat sources, the water/rock ratio, fluid transport efficiency, fluid pH, and salinity [12]. When GU/PU ratios determine the particle type it is important to realize that CCS IDPs are only produced via hydration of C-rich CCP and CCF IDPs in the presence of an efficient process to remove solid C, e.g., catalytically supported solid C gasification [25]. The effects of diagenesis and thermal annealing are not necessarily uniform throughout an individual particle.

Layer Silicates: The transition of petrologic classes 1–2 is symbolized by a reaction of poorly ordered (possibly nonstoichiometric) serpentine to well-ordered talc [11]

$$3\,Mg_5Al_2Si_7O_{20}(OH)_4.X_i.n.H_2O + 5\,Si(OH)_4\,(aq.) + 5/2\,O_2 = 5\,Mg_3Si_4O_{10}(OH)_2 + 3\,Al_2Si_2O_5(OH)_4 + \{3X_i.(OH)_{10} + 3n.H_2O\} \quad (1)$$

(X_i denotes monovalent interlayer cations in smectite; the braces symbolize the composition of the coexisting aqueous phase. Participation of carbons or sulfides in the reaction conceivably produces sulfate and cabonate minerals.)

Phase relations in class 2 occur in an aqueous fluid that is buffered in the C-H-O-S system [26]. Individual CC IDPs show a variety of product phases depending on the timing of aqueous alteration relative to dry crystallization and fractionation (class 3). The mineralogy of $CCF_{0,2,3}$ IDP L2005L2 [14], assuming co-precipitation of magnesite, supports the C-producing reaction occurring at 140°–300°C [26]

$$4\,Mg_2SiO_4 + X_i + 4\,SiO_2.(0.25n).H_2O + 0.5\,CH_4 + CO_2 = Mg_6Si_8O_{20}(OH)_4.X_i.n.H_2O + MgSO_4 + MgCO_3 + 3\,C \quad (2)$$

wherein X_i denotes monovalent interlayer cations in smectite. This temperature is similar to those calculated for the formation of layer silicate from feldspars in CCP IDPs at 175°–195°C [12]. These calculations assumed phase equilibrium, but it remains to be shown that the assumption is correct.

Carbons: The various forms of carbonaceous materials and other C species in CC IDPs, which also express the complex petrologic history of these particles, are shown in Table 6.

Sulfides: Sulfur is not locked up in the interstellar dust. Yet sulfides are common in most undifferentiated solar system materials [10,13,28]. Two types of sulfide-producing reactions include

$$MgFeSiO_4 + H_2S = MgSiO_3 + FeS + H_2O \quad (3a)$$

and

$$MgFeSiO_4 + H_2S + 1.5\,C = MgSiO_3 + FeS + 0.5\,CH_4 + CO \quad (3b)$$

with loss of solid C.

Reactions (3a,b) yield enstatite while reactions (4a,b) produce ferrosilite and Mg-enriched olivine

TABLE 5. Petrologic classes of CC IDPs based on GU and PU mineralogy.

	GU_1	GU_2	PU
CLASS 0	hydrocarbons;amorphous carbons	amorphous carbon-rich chondritic material	amorphous chondritic material
CLASS 1	hydrocarbons; amorphous carbons; loss of volatiles	?	poorly ordered layer silicates
CLASS 2	lonsdaleite; pregraphitic carbons, incl. mixed-layered turbostratic carbons	?	well-ordered layer silicates; salts
CLASS 3	amorphous carbons; poorly graphitized carbons; graphite nanocrystals	ultrafine silicates, sulfides, oxides, etc.; graphite nanocrystals	Fe, Mg-silicates, alkali- and plagioclase feldspars; variable ratios amorphous-crystalline 'silicates'
CLASS 4	poorly graphitized carbon domains	poorly graphitized carbon domains	magnetite - maghemite nanocrystals; Mg,Fe-silicate reequilibration

NOTES: question marks, see text; platey single-crystals, or fragments thereof, are not a major component of chondritic IDPs and they could be fragments of type 2 or 3 PUs [13].

TABLE 6. Petrology of CC IDP carbons.

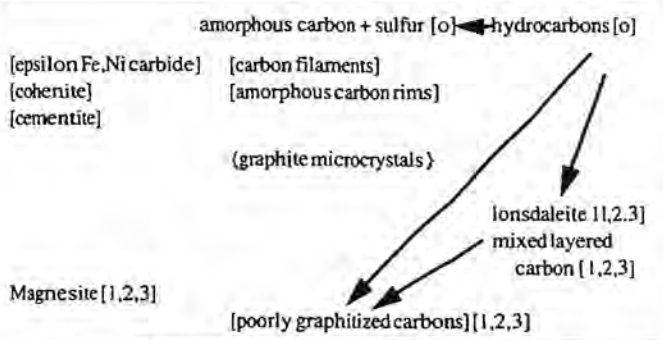

Numbers in brackets denote the possible petrologic classes. Possible class 4 carbons are shown in brackets and braces. Modified after [27]; a review of carbons in CC micrometeorites.

$$1.5\ MgFeSiO_4 + 0.5\ H_2S = Mg_{1.5}Fe_{0.5}SiO_4 + 0.5\ FeSiO_3 + 0.5\ FeS + 0.5\ H_2O \quad (4a)$$

and

$$1.5\ MgFeSiO_4 + 0.5\ H_2S + 0.75\ C = Mg_{1.5}Fe_{0.5}SiO_4 + 0.5\ FeSiO_3 + 0.5\ FeS + 0.5\ CO + 0.25\ CH_4 \quad (4b)$$

again solid C loss from the particle. Reactions (3) and (4) predict a negative correlation between the olivine/pyroxene ratio and increased amounts of FeS. Nonequilibrium orthoferrosilite plus Mg-rich olivine is probably related to the ultrafine grain size of CC IDPs. Whether this type of reaction is limited to class 2 or also defines class 3 is not known. Sulfides in GUs could indicate parent body alteration (class 3) or solid-gas reactions in the nebula but not involving metallic iron. The petrographic textures support *in situ* formation [9]. I note that there is evidence for ferrosilite that might support reaction (4) in olivine-rich GUs [9].

Class 3. The timing of crystallization of GU_2 minerals is uncertain; hence the question marks in Table 5. Studies of layer silicates in CCP and CCF IDPs show that ultrafine-grained GUs co-occur with well-ordered phyllosilicates formed by feldspar alteration [13]. The relative timing of processes of the petrologic classes 2 and 3 is unknown, but it is probably random in both time and space. It is possible that GU_2 crystallization was simultaneous with formation of well-ordered phyllosilicates and salts, viz., CCP IDP W7029C1 with both class 1 and 2 layer silicates is characterized by GU_1 units of class 2 [11]. The data are inconclusive to constrain formation of GU_2 units of class 1, although the hydrocryogenic regime does not appear to be conducive to GU_2 crystallization.

Conclusion: The IDP classification based on chemical group and morphology is an excellent scheme that incorporates the major IDP types. It is readily determined at the bulk level of an individual particle. I submit that particle classification using petrologic class, which is readily determined by TEM and AEM analyses, in combination with chemical subgroupings is a meaningful approach to study the onset of mineralogical activity in the solar system.

Acknowledgments: I am grateful to A. Brearley, R. Jones, and J. Papike for helping me focus the proposed classification scheme. This work was supported by NASA grant NAG 9-160.

References: [1] Fraundorf P. et al. (1982) *Proc. LPSC 13th*, in *JGR*, *87*, A403–A408. [2] Mackinnon I. D. R. and McKay D. S. (1986) *LPS XVII*, 510–511. [3] Mackinnon I. D. R. et al. (1982) *Proc. LPSC 13th*, in *JGR*, *87*, A413–A421. [4] Kordesh K. M. et al. (1983) *LPS XIV*, 389–390. [5] Brownlee D. E. (1985) *Annu. Rev. Earth Planet. Sci.*, *13*, 147–173. [6] Zolensky M. E. (1987) *Science*, *237*, 1466–1468. [7] Sandford S. A. and Walker R. M. (1985) *Astrophys. J.*, *291*, 838–851. [8] Bradley J. P. (1988) *GCA*, *52*, 889–900. [9] Rietmeijer F. J. M. (1989) *Proc. LPSC 19th*, 513–521. [10] Bradley J. P. et al. (1988) in *Meteorites and the Early Solar System* (J. F. Kerridge and M. S. Matthews, eds.), 861–898. [11] Mackinnon I. D. R. and Rietmeijer F. J. M. (1987) *Rev. Geophys.*, *25*, 1527–1553. [12] Rietmeijer F. J. M. (1991) *EPSL*, *102*, 148–157. [13] Rietmeijer F. J. M. (1992) in *Trends in Mineral.*, *1*, 23–41. [14] Zolensky M. E. and Lindstrom D. (1992) *Proc. LPS, Vol. 22*, 161–169. [15] Keller L. P. et al. (1992) *LPS XXIII*, 675–676. [16] Bradley J. P. and Brownlee D. E. (1991) *Science*, *251*, 549–552. [17] Rietmeijer F. J. M. (1992) *LPS XXIII*, 1153–1154. [18] Schramm L. S. et al. (1989) *Meteoritics*, *24*, 99–112. [19] Thomas K. L. et al. (1993) *GCA*, in press. [20] Germani M. S. et al. (1990) *EPSL*, *101*, 162–179. [21] Rietmeijer F. J. M. and McKay D. S. (1985) *Meteoritics*, *20*, 743–744. [22] Rietmeijer F. J. M. (1985) *Nature*, *313*, 293–294. [23] Rietmeijer F. J. M. (1992) *LPS XXIII*, 1151–1152. [24] Rietmeijer F. J. M. (1993) *LPSC XXIV*, in press. [25] Rietmeijer F. J. M. and Mackinnon I. D. R. (1990) *Proc. LPSC 20th*, 323–333. [26] Rietmeijer F. J. M. (1985) *LPSC XVI*, 696–697. [27] Rietmeijer F. J. M. (1992) in *Asteroids, Comets, Meteors, 91* (A. W. Harris and E. Bowell, eds.), 513–516, LPI, Houston. [28] Rietmeijer F. J. M. (1988) *Astrophys. J.*, *331*, L137–L138.

CHEMICAL COMPOSITIONS OF PRIMITIVE SOLAR SYSTEM PARTICLES.

S. R. Sutton and S. Bajt, Department of the Geophysical Sciences and Consortium for Advanced Radiation Sources, The University of Chicago, Chicago IL 60637, USA.

Introduction: Chemical studies of micrometeorites are of fundamental importance primarily because atmospheric entry selection effects (such as destruction of friable objects) are less significant than those for conventional meteorites [1]. As a result, particles that have experienced very little postaccretional processing have a significant chance of surviving the Earth encounter and subsequent collection. Thus, chemical analyses of these relatively unaltered micrometeorites may lead to a better understanding of the compositions of the most primitive materials in the solar system and thereby constrain the conditions (physical and chemical) that existed in the early solar nebula.

Micrometeorites have been collected from the stratosphere, polar ices, and ocean sediments, but the stratospheric collection is the best source for the most unaltered material because they are small and are not heated to their melting points. Despite the fact that the stratospheric micrometeorites have masses in the nanogram range, a variety of microanalytical techniques have been applied to bulk chemical analyses with part-per-million sensitivity. In some cases, multi-disciplinary studies (e.g., chemistry and mineralogy) have been performed on individual particles. The first-order conclusion is that the chondrite-like particles are chemically similar to carbonaceous chondrites but in detail are distinct from members of

the conventional meteorite collection. The purpose of this paper is to provide an overview of the results to date and identify important areas for further study.

Analytical Techniques: Chemical analytical techniques with high sensitivity are required for analysis of IDPs because of their small size (typically in the nanogram range). As a first step in the chemical characterization process, qualitative electron microprobe analysis (EMPA) is obtained on each particle as part of the curatorial process at NASA JSC (see any of the Cosmic Dust Catalogs produced by the Curatorial Facility). These results fingerprint the relative abundances of elements with atomic number typically between Na and Ni. EMPA has also been used to obtain quantitative concentrations of Mg, Al, S, Ca, Cr, Fe, and Ni [2]. Light elements (C and O) have also been analyzed with the electron microprobe [3]. More sensitive techniques have made it possible to obtain trace- element analyses. These methods include synchrotron X-ray fluorescence (SXRF) [4], proton-induced X-ray emission (PIXE)[5], instrumental nuclear activation analysis (INAA)[6], and secondary ion mass spectrometry (SIMS)[7]. The scanning auger microprobe (SAM) has been used for analyses of particle surfaces [8]. The laser microprobe/mass spectrometer (LM/MS) has provided analyses of volatile/hydrocarbon species in stratospheric particles[9].

Results and Discussion: *Major elements (>0.5%).* In the most extensive study of major elements in micrometeorites, Schramm et al. [2] analyzed 200 stratospheric micrometeorites by EMPA for Mg, Al, Si, S, Ca, Cr, Mn, Fe, and Ni. The particles were grouped morphologically into porous and smooth types. The porous particles were found to have compositions close to that of CI meteorites, but the smooth ones were depleted in Ca and Mg analogous to depletions in CI and CM matrix attributed to parent body leaching (most likely on an asteroidal parent body). Schramm et al. concluded that the porous, most chemically primitive particles should be considered a new types of carbonaceous chondrite unrepresented in the meteorite collection. Thomas et al. [10] showed that IDPs tend to be enriched in C relative to C-rich meteorites. INAA results [11] led to the conclusion that Na and K contents are within a factor of 2 of CI abundance.

Trace elements (<0.5%). The value of trace elements in IDPs was first demonstrated by Ganapathy and Brownlee using INAA [12]. Trace elements for which there are quantitative data on IDPs comprise a surprisingly long list, a direct result of the complementary nature of the various analytical techniques. Unfortunately, there are few cases where these trace-element techniques have been applied to the same particle. The multitude of data on elements of different cosmochemical character coupled with the scarcity of analytical intercomparisons on individual particles makes the task of summarizing the state of the art extremely complex. In general, the trace-element results on chondritelike particles agree with those of the major element analyses, i.e., particles that have "chondritic" major-element compositions also have "chondritic" trace-element compositions. The most intriguing deviations from this conclusion concern the volatile elements.

Volatile-element enrichments. Undoubtedly, the deviations from the nominal chondritic abundance pattern that have received the greatest attention are the general enrichments in volatile elements first documented with PIXE by Van der Stap et al. [13]. Subsequently, similar enrichments in many particles have been observed [14 and references therein]. The average compositions of 51 chondritic IDPs determined by SXRF show an abundance pattern enriched from CI in volatiles and complementary to the depletions in the non-CI carbonaceous meteorites [15]. Considerable debate continues about whether these volatile enrichments are indigenous or atmospheric contamination [e.g., 14]. However, if proven to be the former, the implication is that the primitive IDPs are perhaps the most primitive solar system material available for study.

Volatile-element depletions. Trace-element abundance patterns for some IDPs are very similar to the unaltered chondritic particles but have varying degrees of Zn depletion [16,17]. The magnitude of the Zn depletion is well correlated with the thickness of the magnetite rim suggesting an atmospheric heating mechanism. Determination of volatile depletions may prove to be a powerful, nondestructive indicator of atmospheric heating of IDPs. A quantitative method to determine thermal history of the particles would be useful in inferring the proportions of cometary and asteroidal dust based on orbital differences between these two populations [18].

Volatile/hydrocarbon molecules. Individual IDPs show a wide diversity of volatile molecular species including hydrocarbons, sulfur-bearing species, carbonates, and hydroxyl. Bustin et al. [19] found that the composite volatile spectrum of 14 IDPs was similar to that of Murchison, suggesting an association with CM meteorites. An interesting observation was that the hydrated IDPs (those yielding OH) tend to have lower volatile yields than the anhydrous ones. The first definitive observations of complex organic molecules (PAHs) in IDPs have also been made [20].

Conclusions and Future Studies: Primitive stratospheric IDPs have chemical compositions similar to CI carbonaceous meteorites but clearly most of them are not fragments of CI meteorites. Volatile elements in IDPs are generally enriched relative to CI meteorites suggesting that they represent a new (and perhaps more primitive) class of carbonaceous meteorites. Future studies need to be done in the following areas: (1) Consortia studies: Consortia studies are needed to provide complete characterization of individual particles analogous to the consortia currently being organized for interesting meteorites such as SNCs. This research will be particularly fruitful in understanding abundance anomalies and atmospheric heating effects by comparing composition with mineralogy. Desperately needed are trace-element microanalyses with spatial resolutions (submicrometer) comparable to those of the TEM mineralogical studies. (2) Meteorite associations: The use of elemental ratios for determining associations with meteorites appears promising. Lindstrom [6] showed the potential value of Sc/Fe and Co/Fe ratios and additional work is needed to explore the suitability of other elemental ratios. (3) Contamination: Contamination is a major concern in samples of this size. Potential sources include the atmosphere, collection apparatus, and all processing subsequent to analysis. In addition, the analytical techniques themselves may alter compositions by heating, for example. Additional systematic studies need to be done to quantify these effects. (4) Orbital collections: Orbital collections are desperately needed to allow the chemical analyses described here to be performed on particles of known orbital parameters.

References: [1] Love S. G. and Brownlee D. E. (1991) *Icarus, 97*, 70–84. [2] Schramm L. C. et al. (1989) *Meteoritics, 24*, 99–112. [3] Thomas K. L. et al. (1993) *GCA*, in press. [4] Flynn G. J. and Sutton S. R. (1990) *Proc. LPSC 20th*, 335–342. [5] Wallenwein R. et al. (1987) *Anal. Chim. Acta, 195*, 317–322. [6] Lindstrom D. J. (1992) *LPSC XXIII*, 779–780. [7] Stephan T. et al. (1993) *LPSC XXIV*, 1349–1350. [8] Mackinnon I. D. R. and Mogk D. W. (1985)

GRL, 12, 93–96. [9] Gibson E. K. Jr. (1992) *JGR, 97*, 3865–3875. [10] Keller L. P. et al. (1993) *LPSC XXIV*, 785–786. [11] Lindstrom D. J. and Zolensky M. E. (1990) *LPSC XXI*, 700–701. [12] Ganapathy R. and Brownlee D. E. (1979) *Science, 206*, 1075–1077. [13] Van der Stap C. C. A. H. et al. (1986) *LPSC XVII*, 1013. [14] Jessberger E. K. et al. (1992) *EPSL, 112*, 91–99. [15] Flynn G. J. et al. (1993) *LPSC XXIV*, 495–496. [16] Flynn G. J. and Sutton S. R. (1992) *Proc. LPS, Vol. 22*, 171–184. [17] Thomas K. L. et al. (1992) *LPSC XXIII*, 1427–1428. [18] Flynn G. J. (1989) *Icarus, 77*, 287–310. [19] Bustin R. (1993) *LPSC XXIV*, 239–240. [20] Clemett S. J. et al. (1993) *LPSC XXIV*, 309–310.

QUANTITATIVE ANALYSES OF CARBON IN ANHYDROUS AND HYDRATED INTERPLANETARY DUST PARTICLES. K. L. Thomas[1], L. P. Keller[1], G. E. Blanford[2], and D. S. McKay[3], [1]Lockheed Engineering and Sciences Company, NASA Road 1, Houston TX 77058, USA, [2]University of Houston–Clear Lake, Houston TX 77058, USA, [3]Code SN, NASA Johnson Space Center, Houston TX 77058, USA.

Introduction: Carbon is an important and significant component of most anhydrous and hydrated IDPs. We have analyzed ~40 anhydrous and hydrated chondritic IDPs for major and minor elements, including C and O [1–5]. Quantitative analyses of light elements in small particles are difficult and require careful procedures in order to obtain reliable results. In our work, we have completed extensive analytical checks to verify the accuracy and precision of C abundances in IDPs (described in detail in [1]). In our present work, additional methods are used to verify C abundances in IDPs including analysis of IDP thin sections embedded in S, and direct observation of carbonaceous material in thin sections. Our work shows conclusively that C is strongly enriched in IDPs relative to CI abundances.

Carbon Analysis Procedures: Uncoated IDPs supported on Be substrates were analyzed using a thin window energy-dispersive X-ray detector on a scanning electron microscope equipped with a turbomolecular pump. This procedure eliminates C contamination and contributions from C-bearing substrates. Spectra were processed through the PGT bulk particle data reduction (BSAM) program, which performs peak overlap corrections, background subtractions for elements $Z > 6$, and calculates the ratios of X-ray counts from the unknown to counts from a pure, flat element standard (k-ratio). Carbon k-ratios were determined manually for each spectrum. After manual background subtraction for C, we recorded counts in a window between 170 and 340 eV. These counts were divided by the average of measurements of a cleaved diamond standard to obtain carbon k-ratios. All k-ratios were used as input to the CITPIC (Ver. 2.03) matrix and $\phi(\rho\varphi)$ correction procedure developed by [6].

The CITPIC program was designed for analyzing small, irregularly shaped particles. We evaluated our analytical procedure by analyzing particle standards from three sources under the same conditions as those for IDPs: small particles with homogeneously distributed C (calcite), and IDP analog materials including small particles of the Orgueil CI chondrite and the Allende CV3 chondrite. The detailed results of these studies are given in [1], and in general, show that our C abundances are accurate and have relative errors of ~10%. Carbon abundances in 29 Orgueil particles ranged from 0 to 7.4 wt% with a mean value of 3.4 wt%, in excellent agreement with literature values [7].

Since IDPs are contaminated with silicone oil, which contains ~30% C by weight, Orgueil and Allende particles were saturated with silicone oil, washed in hexane, and analyzed for major elements, C, and O (results for Allende are given in [1]). Results from these particles show that there is a real contamination problem from the silicone oil, which causes an ~10% enhancement in Si abundances. Although silicone oil contains C and O, we are not detecting excesses of these elements. The hexane rinse may be effective in removing silicone oil from the particle surfaces, beyond the depth of detection for C and O. The actual contamination of IDPs from silicone oil is based on particle parameters such as porosity and the extent to which the particle was rinsed. We believe IDP C abundances are not significantly affected even though the Si abundances are overestimated.

A frequent criticism of our techniques is that they are essentially a surface analysis and they also assume a homogeneous distribution within the sample volume. To address this criticism, we are now quantitatively analyzing thin sections of IDPs embedded in S for C and are directly observing C distribution in the TEM. IDPs are initially embedded in glassy S, thin sectioned, and placed on Be support films [8]. Analysis of C in S-embedded thin sections of one IDP shows excellent agreement with that determined by our bulk particle method (results given in [8]).

Carbon can also be directly observed in anhydrous IDPs by point counting of individual particle thin sections in the TEM [1]. Our results indicate that the distribution of C in anhydrous IDPs appears to be rather homogeneous; C surrounds the internal grains and is distributed unevenly on the particle surface. The C seems to act as a matrix holding the individual grains together.

Anhydrous IDPs: Our results show that anhydrous IDPs have a chondritic composition within a factor of 2 of CI chondrites for most major and minor elements with the exception of C, which ranges up to ~13× CI. We have identified a relationship between C abundance and silicate mineralogy that, in general, shows that particles dominated by pyroxenes have higher C abundances than those dominated by olivines. Pyroxene-dominated IDPs have C > 3× CI and olivine-dominated IDPs have C < 3× CI. Particles containing equal amounts of pyroxene and olivine can be grouped with either the pyroxene or olivine-dominated IDPs based on C abundances.

Carbon can be directly observed in all our pyroxene-dominated IDPs because of their high C abundances, but it is more difficult to observe C in thin sections when C < 3× CI (e.g., olivine-dominated IDPs). We performed point-count analyses of thin sections of two pyroxene-dominated IDPs: W7027H14 and L2006B23. Results show that W7027H14 contains 40–50 vol% carbonaceous material, which is in good agreement with an estimate of ~40 vol%, assuming a particle diameter of 10 μm, a particle density of 1 g cm^{-3} [9], and ~23 wt% C (bulk). L2006B23 has ~45 wt% C, the highest reported bulk C of any IDP. The volume percent of C is ~90, determined by point counting, and agrees with the theoretical estimate of 90 vol% based on a particle diameter of 15 μm, density of 1 g cm^{-3} [9], 45 wt% C (bulk), and ~50% porosity.

The nature of the carbonaceous material in anhydrous IDPs is poorly known. We have not observed graphitized C (i.e., 0.34 nm spacings) in any particles, nor have we observed C in the form of carbonates. Rather, the carbonaceous material could be poorly graphi-

tized or amorphous. The C-rich phases in L2006B23 have a vesicular texture, indicating the loss of volatiles, probably hydrocarbons. It seems plausible that several C phases could co-exist in anhydrous IDPs.

Hydrated IDPs: Our results show that 12 hydrated IDPs have a chondritic composition within a factor of 2 of CI for analyzed elements, with the exception of C, which ranges from ~2 to 6× CI [3,4,10]. Carbon abundances are <3× CI in six of the hydrated IDPs. The range of C abundances in hydrated IDPs overlaps that of anhydrous IDPs. No relationship has been observed between C abundance and the presence of any particular silicate phase. Carbonaceous material may be distributed in hydrated IDPs in a similar manner to that in anhydrous IDPs, but it is difficult to differentiate carbonaceous material from fine-grained, poorly crystalline phyllosilicate matrix, which dominates hydrated IDPs. Therefore, it has been impossible to directly observe amorphous or poorly graphitized C in IDP thin sections. Fine-grained carbonates have been found in three IDPs with 8, 15, and 20 wt% C. Carbonates can account for some, but not all, of the high C in these IDPs. Two IDPs, L2005P9 and L2006J14, have 20 and 22 wt% C respectively, and lack carbonates. Therefore, poorly graphitized C, amorphous C, or hydrocarbons must be present in these C-rich IDPs.

Most hydrated IDPs show evidence of being heated during atmos-pheric entry [3,10]. It is uncertain if C abundances could be higher in these heated particles. If some C was present as a volatile species (e.g., hydrocarbons), then the actual C abundances of heated IDPs may be higher than we report.

Conclusions: (1) We are able to accurately quantify C abundances in small particles. (2) Point counting and analysis of IDP thin sections embedded in S are two additional techniques used to validate C abundances in IDPs. (3) Most anhydrous and hydrated IDPs have C abundances much higher than those of any known meteorite. Anhydrous IDPs have C abundances up to 13× CI. They can be classified into three groups based on C abundance and mineralogy: pyroxene-rich IDP with C > 30× CI, olivine-rich with C < 3× CI, and mixed mineralogy with C abundances ranging between olivine- and pyroxene-rich IDPs. One anhydrous IDP has the highest reported bulk C (45 wt%) of any IDP. Carbonaceous material acts as a matrix holding individual mineral grains together. (4) Hydrated IDPs have C abundances ranging from 2 to 6× CI. Carbon abundance is not correlated with any silicate phase. Although some IDPs have abundant carbonates, other forms of carbonaceous material must be present to account for high C abundances. The distribution of C in hydrated IDPs is poorly known.

Acknowledgments: This work was supported by NASA RTOPS 15-17-40-23 and 199-2-11-02.

References: [1] Thomas K. L. et al. (1993) *GCA, 57*, in press. [2] Thomas K. L. et al. (1993) *LPS XXIV*, 1425–1426. [3] Keller L. P. et al. (1993) *LPS XXIV*, 785–786. [4] Thomas K. L. et al. (1992) *Meteoritics, 27*, 296–297. [5] Keller L. P. et al., this volume. [6] Armstrong J. T. and Buseck P. R. (1975) *Anal. Chem., 47*, 2178–2192. [7] Anders E. and Grevesse N. (1989) *GCA, 53*, 197–214. [8] Bradley J. P. et al. (1993) *LPS XXIV*, 173–174. [9] Flynn G. J. and Sutton S. R. (1991) *Proc. LPS, Vol. 21*, 541–547. [10] Keller L. P. et al. (1992) *LPS XXIII*, 675–676.

ORIGIN OF THE HYDROCARBON COMPONENT OF INTERPLANETARY DUST PARTICLES.

T.J. Wdowiak and W. Lee, Department of Physics, University of Alabama at Birmingham, Birmingham AL 35294-1170, USA.

Using experiments as a basis, we have developed a scenario for the origin of the hydrocarbon material of carbonaceous chondrites. This scenario can also serve as an explanation for the origin of the hydrocarbon component of interplanetary dust particles (IDPs). The formation of polycyclic aromatic hydrocarbon (PAH) molecules in the atmospheres of C stars undergoing a late stage of stellar evolution is indicated by the observed unidentified infrared (UIR) emission bands. Those molecules are then transported through interstellar space where they become enriched with D through ion molecule reactions when passing through cold, dark clouds. Many of those PAH molecules are subsequently hydrogenated and cracked in a H-dominated plasma such as would have occurred in the solar nebula. The resulting mixture of alkanes and residual D-rich PAH molecules was then incorporated into the mineral fraction of the parent bodies of carbonaceous chondrites and IDPs.

Introduction: It is highly likely there exists a relationship between the hydrocarbon material of chondritic IDPs and that found as a component of carbonaceous chondrites. Earlier research on the origin of such hydrocarbons focused largely on the Fischer-Tropsch process where CO and H_2 were converted at high temperatures with the aid of a catalyst to meteoritic hydrocarbons [1,2]. Some very recent laboratory experiments have suggested a pathway that is different from those previously considered. In this new model polycyclic aromatic hydrocarbons, first formed in the atmospheres of C stars, are transported through the interstellar medium. Such molecules are capable of surviving the harsh interstellar environment where they are subjected to ultraviolet radiation and shocks. While in cold, dark clouds they become enriched in D through ion molecule reactions. Finally, much of the aromatic material is converted to the alkane form found to be the principle hydrocarbon component of carbonaceous chondrites [3]. The last process appears to have probably taken place in the plasma environment of the solar nebula prior to incorporation of the hydrocarbon material into the parent bodies of carbonaceous chondrites and IDPs. The T Tauri stage of the Sun was probably an important factor in the production of the necessary plasma conditions. The hydrogenation will yield an alkane product having a lower D content than the aromatic precursor by virtue of simple dilution. This is consistent with what is observed for meteoritic hydrocarbons.

The presence of a hydrocarbon component in IDPs has been demonstrated by Wopenka [4] where a laser-induced luminescence was observed when 514-nm light was directed on an IDP sample. She found the emission spectrum peaked at about 600 nm for what she called a type-3 particle. Another IDP, known as Viburnum, exhibited a more extreme emission, peaking at about 720 nm. This emission was interpreted as being due to a mixture of large polycyclic aromatic hydrocarbons in the microcrystalline form as had been proposed earlier by Wdowiak [5]. Following that initial report, a more comprehensive paper argued on the basis of Raman and laser-induced luminescence for a connection between interstellar PAH molecules and the carbonaceous component of IDPs [6]. Recently mass spectroscopy of the IDPs Aurelian and Florianus has shown the

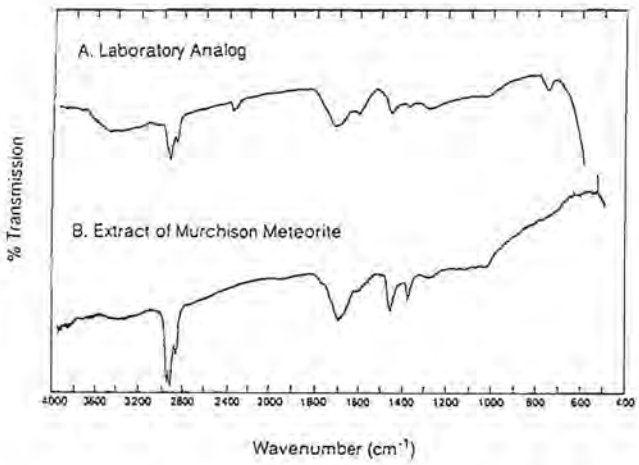

Fig. 1. Comparison of the spectrum of a portion of the laboratory analog (A) and the spectrum obtained by Cronin and Pizzarello [11] of the benzene-methanol (9:1) extract of the Murchison meteorite (B). Spectrum A also shows artifacts due to H_2O (around 3450 cm^{-1}) and incomplete cancellation of atmospheric CO_2 (around 2350 cm^{-1}).

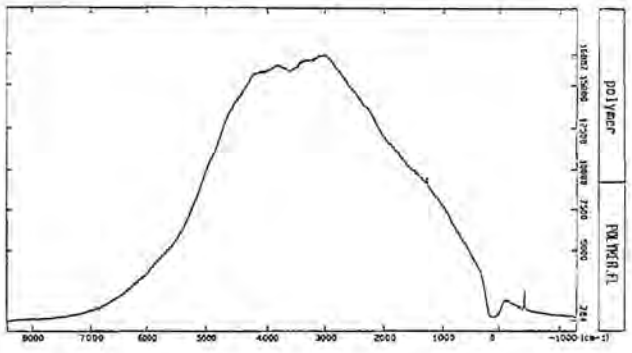

Fig. 2. Laser-induced luminescence spectrum of a piece of film of the laboratory analog. The excitation wavelength is 514 nm.

presence of PAH molecules, with those having a mass around 250 amu being the most abundant. A second group around 370 amu was also found to be fairly abundant. The very low abundance of PAHs in the 78–192-amu range was attributed to their being heated during entry of the IDPs into the terrestrial atmosphere [7]. Calculation of the peak atmospheric entry temperatures of micrometeorites indicates that it is highly probable that many IDPs will be flash-heated to temperatures in excess of 600°C [8,9]. Experiments involving heating milligram amounts of the acid-insoluble residue of the Orgeuil (CI) carbonaceous chondrite to specific temperatures in a vacuum suggest that thermal alteration of the hydrocarbon component will take place during atmosphere entry [9,10]. While not an attempt to simulate IDP entry, these experiments are a good indicator of the chemical change that occurs when chondritic hydrocarbons are heated.

Experimental Techniques: We have carried out experiments [3] with the simple PAH naphthalene ($C_{10}H_8$), which was chosen for the ease with which it can be placed into the gas phase. The $C_{10}H_8$ was converted through hydrogenation in a plasma to a material having a mid-infrared (4000 – 400 cm^{-1}) spectrum that is remarkably similar to that obtained by Cronin and Pizzarello of the hydrocarbon substance extracted with a benzene-methanol mixture (9:1) from the Murchison CM2 carbonaceous chondrite [11]. A high-molecular-weight residue was formed when the gaseous $C_{10}H_8$ and H mixture was subjected to a 9400-VAC electrical discharge in a specially constructed tube. It was deposited at two places on the water-jacket-cooled internal glass surface of the discharge tube that have direct exposure to the electrodes placed in side arms. Approximately 300 mg of $C_{10}H_8$ was placed inside the sapphire tube, which was then inserted into the discharge tube to a position halfway between the two electrodes. Additional deposits were formed on the internal walls of the side arms in close vicinity to the electrodes and on the inner wall of a sapphire tube through which the discharge passed. The H gas was introduced through a small side inlet. A mechanical pump held the pressure at 0.5 torr as measured with a McLeod gauge. Based upon the pumpdown pressure of 0.05 torr prior to the introduction of the H, the composition of the gas mixture is estimated to be 90% H_2, 8% N_2, and 2% O_2. The N and O components are due to backstreaming of atmospheric gases from the pump. The presence of O appeared to play an important role in the character of the deposited material as deduced from its IR spectrum as discussed later. The amount of recovered material is approximately 15 mg and residues are not present in the absence of $C_{10}H_8$. A N-cooled trap is incorporated in the line between the discharge tube and the vacuum pump, and was used in some of the experimental runs.

The samples were prepared for spectroscopy by removing the filmlike material from various positions of the discharge tube, washing it in benzene and methanol, drying it under vacuum, and then mounting the material on a KBr or NaCl disk for IR measurements. The IR spectra were obtained with a Mattson Polaris FT-IR spectrometer capable of a resolution of 4 cm^{-1}. The laser-induced luminscence measurements were performed using a modified EG&G Dilor XY Raman system where both Raman and luminescence spectra can be recorded from the same micrometer-sized area of the sample. The light signal was directed into the entrance slit of the spectrometer, which employed a focal plane CCD detector. The luminescence spectrum of the deposit sandwiched between a cover glass and a glass slide was taken with a 150-grooves/mm grating (resolution 17 cm^{-1}) during a data acquisition time of 5 s. The exciting Ar+ laser was selected to have an output of 10 mW at the excitation wavelength of 514.53 nm.

Results and Discussion: *Infrared spectroscopy.* Spectrum A in Fig. 1 shows the mid-infrared spectrum of the filmlike deposit removed from the water-cooled surface facing one of the electrodes. It was mounted on a NaCl disk. The spectrum was measured against air. Spectrum B, reported by Cronin and Pizzarello [11], is of the hydrocarbon component extracted from the Murchison meteorite and mounted on a KBr substrate. The similarity between the two spectra is remarkable, all the more because the meteorite sample, which is the product of a rigorous attempt to obtain an uncontaminated sample, is the major organic constituent of the meteorite. As such it may be representative of the complex hydrocarbon material present throughout the early solar system. The differences that exist betwen the spectra can be accounted for easily. There are features in the laboratory analog spectrum that are due to a small amount of residual aromatic material that has been minimally altered or has escaped alterations altogether. Those at the aromatic C-H stretch

position of 3000 cm^{-1} are very weak. There is slightly more absorption around 1600 cm^{-1}, which is due to the aromatic C-C deformation mode. Finally, there is a definite band at 750–765 cm^{-1} again probably due to an aromatic vibration. This band most likely arises from the C-H out-of-plane wag for the situation of three or four H atoms attached per external aromatic ring. This last band is normally one of the strongest infrared bands of an aromatic molecule. None of these bands are as strong as the alkane bands discussed in the following paragraph. There is also an artifact due to atmospheric CO_2 at 2350 cm^{-1} due to incomplete cancellation between the sample and the reference spectrum.

Very relevant to the question of our deposit being a good laboratory analog of the meteoritic hydrocarbon component are the relative strengths of the alkane C-H stretching and deformation bands due to $-CH_3$ and $-CH_2-$ in the 2900 cm^{-1} and 1400 cm^{-1} regions. Comparison of those bands due to $-CH_3$ at 2960 cm^{-1} and 2870 cm^{-1} and $-CH_2-$ group at 2925 cm^{-1} and 2860 cm^{-1} in both spectra suggests the laboratory deposit has a slightly lower fraction of $-CH_3$ than exists in the meteorite extract. The $-CH_2-/-CH_3$ ratio deduced from the meteorite material spectrum is about 2, whereas in our residue it is 3–4. The observation that the meteorite extract has a greater fraction of material with $-CH_3$ terminations suggests it may contain a greater fraction of low-molecular-weight material. However, the $-CH_3$ content of our sample, indicated by the absorption bands, can be considered high. Substituting a PAH molecule with more rings than two-ringed $C_{10}H_8$, which was chosen for its volatility, would probably result in a high proportion of $-CH_3$ terminations when the ring system is cracked. Experiments to investigate this are being initiated. Hydrogenation without total cracking can result in cycloalkanes, which have been reported to be present in the Murchison CM2 meteorite [11]. There is also very strong and broad absorption in both spectra at around 1700 cm^{-1}, which is quite probably due to the C=O stretch in the carboxyl group. We consider it likely that this functional group in the laboratory material results from the presence of atmospheric O in the gas mixture as discussed earlier. Apart from these strong agreements, the spectral detail exhibited by our laboratory analog is also very consistent with that of the meteoritic component.

Laboratory-induced luminescence spectroscopy. The laser-induced luminescence of a piece of film of the laboratory analog is displayed in Fig. 2. The 514-nm excited luminescence spectrum has a similar shape to those exhibited by the IDPs Lea and Calrissan [6]. The peak of emission between 3000 and 4000 cm^{-1} relative to the excitation corresponds to 600–650 nm in wavelength. The match of this spectrum of the laboratory analog along its IR spectrum with both the luminescence spectra of two IDPs and the IR spectrum of the hydrocarbon component of a CM2 carbonaceous chondrite indicates it is probably not only an analog for meteoritic material, but IDP hydrocarbons as well.

Conclusions: Our ability to produce a hydrocarbon material exhibiting an IR absorption spectrum matching very closely that of the hycrocarbon extract of the Murchison CM2 carbonaceous chondrite and having a laser-induced luminescence spectrum similar to carbonaceous IDPs strongly suggests that the processes involved in the experiment simulate cosmic conditions. From the standpoint of astrophysics the utilization of a mixture of H and the PAH $C_{10}H_8$ in an energetic experimental environment is a valid combination. This is because PAH molecules remain the best hypothesized source of the cosmic UIR emission bands first observed in 1973 [12], which are ubiquitous in the Milky Way and other galaxies.

In summary, our model is that PAH species are formed in stellar atmospheres and then ejected (R CrB, planetary nebulae, etc.) into the interstellar medium. These molecules probably become deuterated in cold, dark clouds through exchange with interstellar D. Much of the material is then hydrogenated into alkanes in a plasma perhaps at the time of the formation of the Sun prior to incorporation into the parent bodies of carbonaceous chondrites and IDPs. Importantly, this has the effect of diluting the D content of those molecules that have been hydrogenated. Remaining D-rich aromatics can be considered to be unaltered interstellar molecules.

Acknowledgments: We are grateful for the assistance of T. McCauley and Y. Vohra in obtaining the laser-excited luminescence spectrum. This work was supported by NASA grant NAGW-749.

References: [1] Studier M. H. et al. (1965) *Science, 149,* 1455. [2] Anders E. et al. (1973) *Science, 182,* 781. [3] Lee W. and Wdowiak T. J. (1993) *Astrophys. J., 417,* L49. [4] Wopenka B. (1988) *EPSL, 221.* [5] Wdowiak T. J. (1986) in *NASA CP-2403,* A-41–A-44. [6] Allamandola L. et al. (1987) *Science, 237,* 56–59. [7] Clemett S. J. et al. (1993) *Science, 262,* 721. [8] Love S. G. and Brownlee D. E. (1991) *Icarus, 89,* 26. [9] Flynn G. J. (1989) *Icarus, 77,* 287. [10] Wdowiak T. J. et al. (1988) *Astrophys. J., 328,* L75. [11] Cronin J. and Pizzarello S. (1990) *GCA, 54,* 2859–2868. [12] Gillett F. C. et al. (1973) *Astrophys. J., 183,* 87.

$^6Li/^7Li$, $^{10}B/^{11}B$, AND $^7Li/^{11}B/^{28}Si$ INDIVIDUAL IDPs. Y.-L. Xu [1], L.-G. Song[2], Y.-X. Zhang[2], and C.-Y. Fan[3], [1]Purple Mountain Observatory, Nanjing 210008, China, [2]Department of Physics, Fudan University, Shanghai 200432, China, [3]Department of Physics, University of Arizona, Tucson AZ 85721, USA.

Introduction: At the initial stage of the development of our solar system, the solar nebula is presumably composed of ^1H, ^2H, ^3He, ^4He, and ^7Li, which were made during the Big Bang [1], and C, N, O, . . ., which are products of nearby supernova explosions. ^6Li nuclei (together with about equal amounts of ^7Li), ^9Be, ^{10}B, and ^{11}B were produced later by cosmic ray particles bombarding the local interstellar C, N, O, . . ., nuclei before the nebula condensed to become the Sun and the planets [2]. Thus, the ratio $^6Li/^7Li$ is a

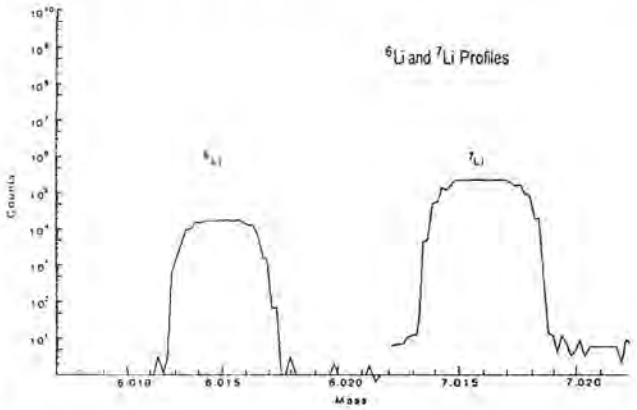

Fig. 1.

measure of the length of the early epoch of the solar system. In this paper we shall report the measurement of $^{7}Li/^{6}Li$, $^{11}B/^{10}B$, and $^{7}Li/^{11}B/^{28}Si$ of four IDPs obtained from Johnson Space Center and discuss the findings.

Experimental Method and Results: The detection of Li, Be, and B isotopes in two IDPs was previously reported by us in 1991 [3]. The equipment used for the measurement was a CAMACA IMS-3F Secondary Ion Microanalyzer at Fudan University. At that time, however, we did not have standards for the calibration, and the apparatus was not properly tuned for the measurement. Therefore, we reported the $^{7}Li/^{6}Li$ and $^{11}B/^{10}B$ values, but could not make a precise estimate of the experimental errors. In 1992, M. Zolensky of Johnson Space Center supplied us with seven more IDPs. By calling numerous laboratories in the country, we found a standard Li isotope source in the form of Li_2CO_3 from G. D. Flesch of Iowa State University [4]. With a B isotope standard purchased from the National Bureau of Standards in the form of H_2BO_3, a mixture of Li, B, and SiO_2 prepared in our own laboratory, and the microanalyzer upgraded for measuring isotopes of small samples, we were ready to refine our measurements.

The microanalyzer was first set to measure the standards. Taking the Li standard as an example, the profile of ^{6}Li and ^{7}Li were obtained first, as shown in Fig. 1. From the profiles, we decided that a resolution of $m/\Delta m = 1000$ was sufficient for the isotopic abundance measurement. The microanalyzer was then set to scan the ^{6}Li and ^{7}Li intensity alternatively at a rate of about 1 s per scan. It took about 183 s to complete 65 cycles. Experimental errors were calculated for every 5 cycles. Finally, the ratio of ^{6}Li to ^{7}Li was calculated. The difference between the measured and the standard value gives us the needed correction factor. A similar procedure was followed for ^{10}B and ^{11}B and $^{7}Li/^{11}B/^{28}Si$, except that, for the latter measurement, $m/\Delta m$ was set at 2200.

The standard sources were then replaced by one of the IDPs. The intensities of ^{6}Li and ^{7}Li were alternatively measured for about 70 cycles, then ^{10}B and ^{11}B, and finally $^{7}Li/^{11}B/^{28}Si$. The experiment was finished in one day and we found that the microanalyzer was extremely stable by rechecking it with the standards. The plots of these scans for IDP W7074C3 are displayed in Figs. 2a,b,c as an illustration. The final results on four IDPs are listed in Table 1.

Conclusion and Discussion: Comparing our $^{6}Li/^{7}Li$ and $^{10}B/^{11}B$ value with that in chondrite meteorites published by Anders and Ebihara [5], we found good agreement, although the meteorites might have gone through physical or chemical fractionation processes. On the other hand, the variation in the abundances of Li, B, and Si in the four IDPs is as large as their differences from the published values in meteorites. Before we can make many more measurements, it is meaningless to draw any conclusion.

^{1}H, ^{2}H, ^{3}He, and ^{7}Li were made in the first 10^3 s of the beginning of the universe, according to the hot Big Bang cosmological model. Their abundances can be calculated for a given nucleon to photon ratio η [1]. For η in the range of $4-8 \times 10^{-10}$, the calculated abundances agree with astronomical observations within observational uncertainties. The elements C, N, O, and heavier were synthesized in stars or supermassive objects. Since ^{6}Li, ^{9}Be, ^{10}B, and ^{11}B can easily be destroyed in the hot interior of stars, it was suggested that they are the spallation products induced by cosmic ray particles bombarding on interstellar gas [2]. This idea led Meneguzzi et al. [6] to study in detail the production of Li, Be, and B by cosmic ray particles. Within a factor of 2, their results agree with experimental abundances. The differences could well be due to the uncertainties in spallation cross sections, cosmic ray spectrum as well as cosmic intensity variation in the past. On this basis, $^{6}Li/^{7}Li$ can be regarded as a clock for measuring the length of the epoch of the solar nebula before the formation of the primitive accretion

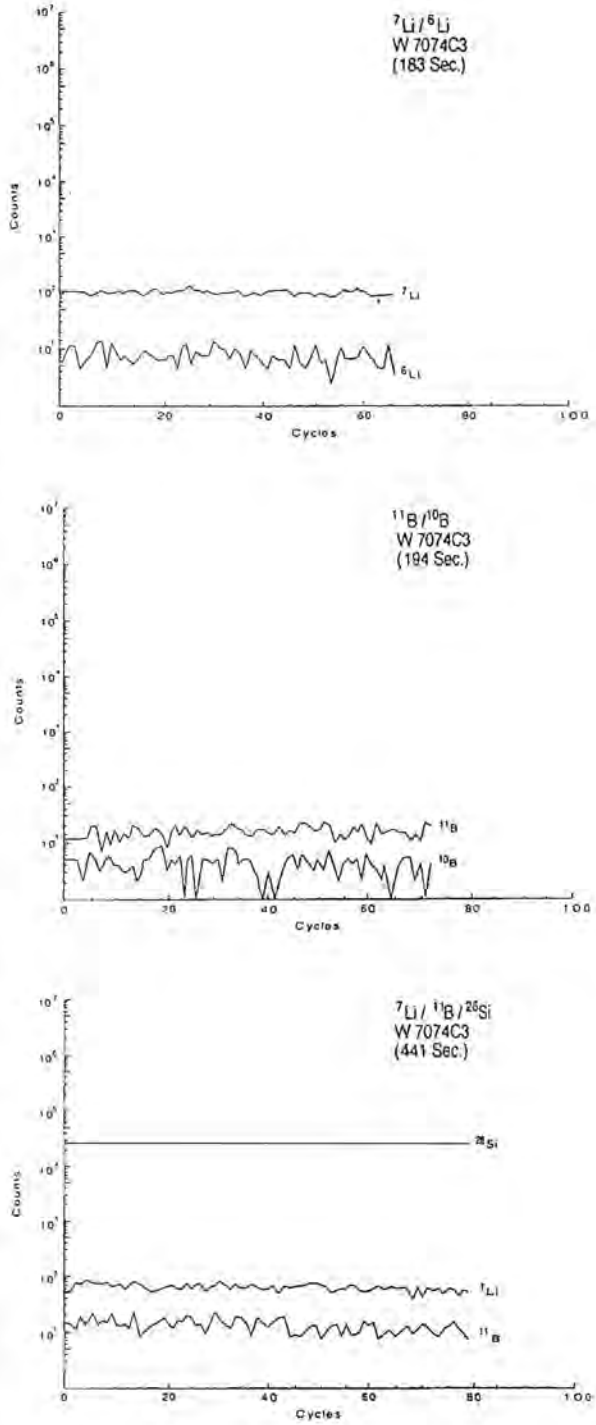

Fig. 2.

TABLE 1.

IDP	$^7Li/^6Li$	$^{11}B/^{10}B$	$^7Li/^{11}B/^{28}Si$
W7074I8	11.72 ± 0.60	4.31 ± 0.49	47.1 ± 1.1/8.31 ± 0.83/10^6
W7074C3	12.24 ± 0.51	4.12 ± 0.26	204.2 ± 1.1/7.06 ± 0.45/10^6
W7074A7	11.78 ± 0.65	4.26 ± 0.21	57.0/8.33/10^6
W7074C15	11.80 ± 0.30	3.96 ± 0.30	57.0/8.33/10^6
Avg.	11.89 ± 0.52	4.16 ± 0.32	

disk.

Let $(^7Li/H)_o$ and $(^7Li/H)_c$ be the abundance of ^7Li relative to H by Big Bang synthesis and from spallation respectively, and $(^6Li/H)_c$, the abundance of ^6Li relative to H due to cosmic ray production (denoted respectively by R_o, R_c, and r_c). R_c/r_c is about 0.9 according to the experimental results of Olson et al. [7]. Then the measured $^6Li/^7Li$, taken to be 11.89, is

$$11.89 = \frac{R_o + R_c}{r_c} = \frac{R_o}{r_c} + 0.9$$

or

$$\frac{r_c}{R_o} = 0.09$$

The calculated value of r_c by Meneguzzi et al. [6] is 2.5×10^{-28} s^{-1} and the theoretical value of R_o is 10^{-9}. These values yield the length of the early epoch of our solar system as 10 b.y.

Acknowledgments: This work is partially supported by NASA under grant NAGW 2249 and by the Chinese Academy of Science. The authors are grateful to M. Zolensky for supplying the IDPs, and to G. D. Flesch for supplying the Li_2CO_3 standard.

References: [1] Yang J. et al. (1984) *Astrophys. J., 281*, 493. [2] Reeves H. (1974) *Annu. Rev. Astron. Astrophys., 12*, 437. [3] Xu Y. L. et al. (1991) *Science in China, 34*, 209. [4] Flesch G. D. et al. (1973) *Int. J. Mass Spectrom. Ion Phys., 12*, 265. [5] Anders A. and Ebihara M. (1982) *GCA, 46*, 2363. [6] Meneguzzi M. et al. (1971) *Astron. Astrophys., 15*, 337. [7] Olson D. L. et al. (1983) *Phys. Rev., C28*, 1602.

COMPOSITIONAL VARIATIONS OF OLIVINES AND PYROXENES IN CHONDRITIC INTERPLANETARY DUST PARTICLES.

M. Zolensky[1] and R. Barrett[2], [1]Code SN2, NASA Johnson Space Center, Houston TX 77058, USA, [2]Lockheed Engineering and Sciences Company, 2400 NASA Road 1, Houston TX 77058, USA.

Introduction: A principal goal of meteoritics is to characterize the mineralogy, mineral chemistry, and microstructures of primitive extraterrestrial materials, and to use this information to identify source bodies and (more importantly) characterize origin and evolution of these bodies [1]. It is a commonly held belief that hydrated interplanetary dust particles (IDPs) experienced aqueous alteration on hydrous asteroids, while the anhydrous IDPs could be derived from the more primitive asteroids and comets. We wish to discover whether the anhydrous IDPs are actually from the same parent body, being related by aqueous alteration of one to produce the other. We report here analyses of olivines and pyroxenes, and petrofabrics of 27 chondritic IDPs, comparing those from anhydrous and hydrous types. Based on mineralogical evidence, we find that hydrous and anhydrous IDPs are, in general, not directly related.

Techniques: All the particles described here were collected in the stratosphere by NASA ER-2 and WB-57 aircraft. All samples were selected on the basis of "chondritic" bulk composition as determined by preliminary energy dispersive X-ray spectrometer (EDX) analyses [2]; chondritic compositions were verified by microparticle instrumental neutron activation analysis (INAA) [3,4]. Following the INAA procedure we embedded all particles in EMBED 812 low-viscosity epoxy, and microtomed them into 90-nm-thick serial sections. Microtoming was halted approximately half

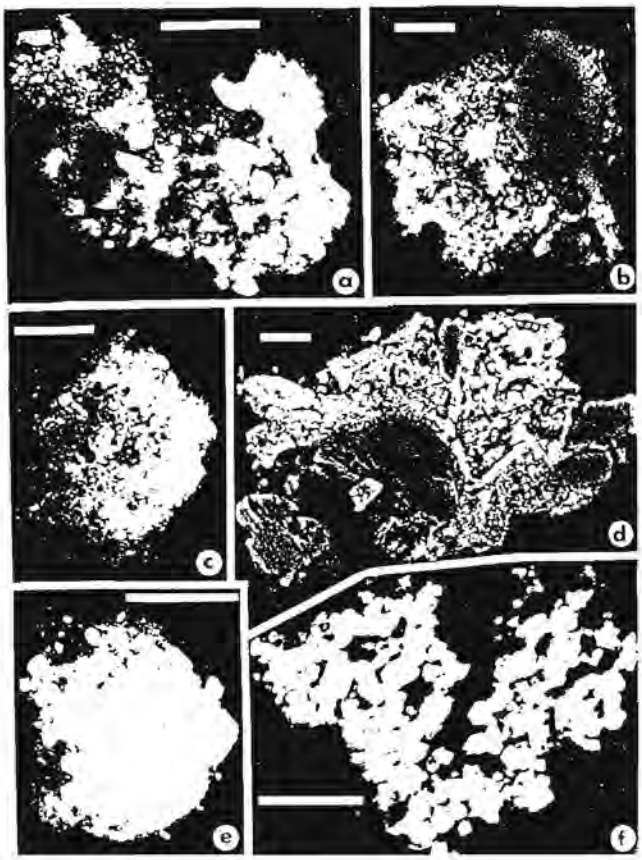

Fig. 1. Backscattered electron images of selected chondritic IDPs; scale bars measure 5 μm. Particles (**a–d**) are anhydrous, while particles (**e**) and (**f**) are hydrous. The majority of white grains are Fe-Ni sulfides; most of the black regions are epoxy-filled voids, although some must represent low-Z material. (**a**) Particle #L2005 F39: an anhydrous IDP with numerous subhedral olivine and orthopyroxene crystals; (**b**) L2005 E36: an anhydrous IDP with a large zoned enstatite crystal, and smaller orthopyroxene and diopside crystals; (**c**) L2005 C37: a uniformly fine-grained anhydrous IDP containing abundant olivine and orthopyroxene; (**d**) L2005 Z17: a compact anhydrous IDP with large anhedral orthopyroxene crystals; (**e**) L2005 Z14: a compact saponite-type IDP containing small orthopyroxene and diopside crystals; (**f**) L2011 R3: a highly porous (~40%), saponite-type IDP, with abundant orthopyroxene.

way through each particle, and the remaining potted butt was then microprobed for major-element composition using a CAMECA CAMEBAX microprobe. These potted butts were also used to make backscattered electron (BSE) images of the interiors of the IDPs using a JEOL 35C SEM operating at 15 kV, which offered optimum values of resolution vs. electron penetration (and excitation) of the samples. We observed the microtomed sections using a JEOL 2000FX STEM equipped with a LINK EDX analysis system. We used natural mineral standards, and in-house determined k factors for reduction of compositional data; a Cliff-Lorimer thin-film correction procedure was employed [5]. In general, mineral identifications were made on the basis of both composition and electron diffraction data.

Results: Chondritic IDPs have been classed according to whether they are anhydrous and dominated by either olivine or pyroxene, or contain the hydrous phases saponite or serpentine. We have previously noted that IDPs belonging to the olivine and pyroxene classes have the same basic mineralogy, and are mineralogically separable only by consideration of the relative proportion of olivine to pyroxene. In this paper we consider anhydrous IDPs as a single group, simply for convenience. We also consider hydrous IDPs to be those that contain any amount of phyllosilicates. An alternate method is to base classification on the dominant crystalline silicate, which would have the effect of moving some hydrous IDPs into the anhydrous group. Unfortunately, the classification of IDPs has not yet been standardized [4]. Examination of the BSE images of chondritic IDPs reveals that some anhydrous IDPs show low porosity, and that some hydrous ones show relatively high porosity, as has been noted previously (Fig. 1).

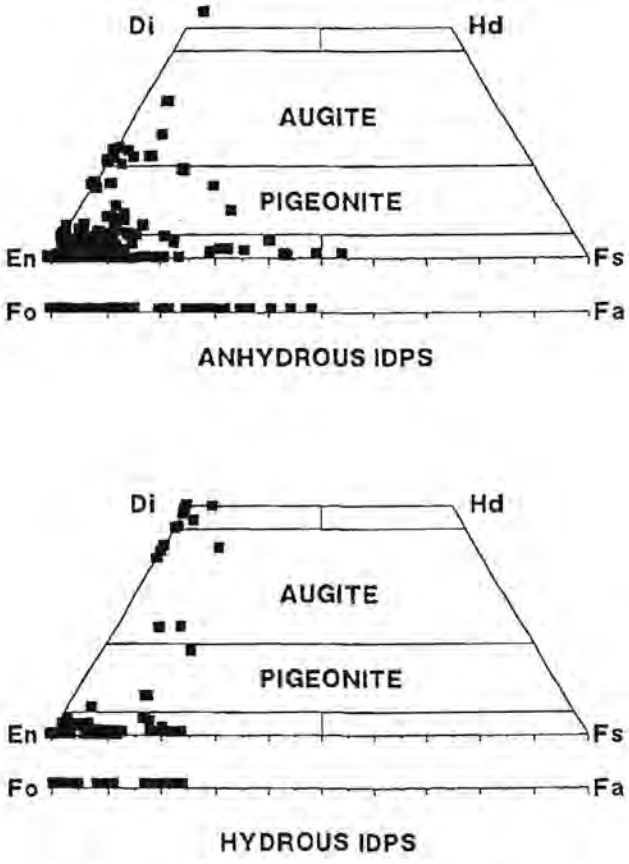

Fig. 2. The compositional ranges exhibited by olivines and pyroxenes in chondritic IDPs, with data plotted separately for 9 phyllosilicate-bearing (hydrous) and 15 anhydrous IDPs. Pyroxene analyses are shown projected onto the enstatite (En) - ferrosilite (Fs) - diopside (Di) - hedenbergite (Hd) quadrilateral. Olivines analyses are plotted along the forsterite (Fo) - fayalite (Fa) binary. Data for three olivine-dominated, anhydrous IDPs are from Christoffersen and Buseck [9]. The compositional ranges of olivines and pyroxenes for the hydrous IDPs are more restricted than those for the anhydrous IDPs, although the former contain practically all of the diopside located.

The vast majority of hydrous chondritic IDPs contain saponite as the dominant phyllosilicate, and are otherwise very similar to the anhydrous IDPs; the only major difference appears to the presence of phyllosilicates. For example, the so called "granular units" [6] are observed both in saponite class and anhydrous chondritic IDPs [4]. These granular units are typically composed of submicrometer-sized aggregates of amorphous phases enclosing many diminutive crystals of olivines, pyroxenes, metals, and sulfides.

Serpentine-dominated IDPs are the rarest type, and appear to be mineralogically distinct from other chondritic IDPs. We have not observed granular units within serpentine-class IDPs, and found that they rarely contain anhydrous silicates. Serpentine-class IDPs have not been found to contain saponite, unlike IDPs of the saponite class, which frequently contain a small amount of serpentine [4]. Several workers have concluded that specific serpentine-class IDPs are derived from the same hydrous asteroids that produced CM2 carbonaceous chondrite meteorites [7]. Only one of the hydrous IDPs that we discuss in this paper is from the serpentine-dominated class.

The compositional ranges of olivines and pyroxenes in IDPs should be useful clues to their histories [8]. To this end we have located and analyzed pyroxenes and olivines in 24 chondritic IDPs (9 hydrous, 15 anhydrous; olivines or pyroxenes were not located in an additional 3 IDPs). Maximum observed grain sizes of olivines and pyroxenes vary from a few hundredths of nanometers (for most particles) to 16 μm in one exceptional particle. To these data we have added olivine analyses from three olivine-class IDPs, as reported by Christoffersen and Buseck [9]. The results of these analyses are presented in Fig. 2.

Augite, pigeonite, and diopside are found in many particles. While it is possible that some of the augites described here are actually diopside and enstatite in an exsolution relationship, we did not observe evidence of this and exsolution laminae would have been obvious. We found that there exists no significant difference in the compositions of olivines from olivine vs. pyroxene-dominated IDPs [10]. The degree of heterogeneity of these minerals from anhydrous IDPs is approximately Fo_{52-100} and En_{46-100}. Only a single grain of diopside was found in the 18 anhydrous IDPs examined.

Olivines in the hydrous IDPs range in composition from Fo_{76-100}, while enstatites range from En_{76-100}. These ranges are significantly narrower than those from the anhydrous IDPs. Four out of the nine hydrous IDPs contain diopsides, in contrast to their obvious rarity in anhydrous IDPs. However, both anhydrous and hydrous IDPs show a considerable clustering at Mg-rich compositions.

Discussion: Are anhydrous and hydrous IDPs genetically related by simple hydrolysis of the former material? The presence of primarily Mg-rich (Fe-poor) olivines and pyroxenes in the hydrous

IDPs could be due to the preferential early dissolution of Fe-rich olivines and pyroxenes during aqueous alteration, meaning that chondritic IDPs represent a mineralogical continuum. The experimentally determined rate of fayalite (Fo_6) dissolution in a reducing atmosphere at a pH of 2–7 at 25°C is six times higher than for forsterite (Fo_{91}) [11]. This relationship probably continues to the pH range 7–12 (the range appropriate to asteroid alteration, according to geochemical modeling) [12], although the absolute rate of olivine dissolution should be adversely affected by this change in pH [13]. While pyroxenes weather at a generally slower rate than olivines under these conditions [14], it is probable that dissolution of Fe-rich pyroxenes is similarly more rapid than Mg-rich varieties. Weathering rates are known to be dependent upon many additional factors, for example, the presence of bidentate organic ligands will increase the dissolution rate of olivine of all compositions by forming metal complexes at the grain surface [11]. Carbon and organic compounds are known to be present in considerable abundance in chondritic IDPs, although their chemistry remains largely uncharacterized [15]. Nevertheless, if these differential weathering-rate relationships hold for alteration on hydrous asteroids, then they provide a mechanism for the relative destruction of Fe-rich anhydrous silicates, and therefore permit a genetic relationship between hydrous and anhydrous IDPs.

However, this simple mechanism does not explain why diopsides should preferentially be found in hydrous IDPs. Diopside (and other clinopyroxenes) weathers at a generally slower rate than ortho-pyroxenes, probably due to the development of transport-limiting surface neoformation products on the former, and rapid development of fractures and alteration embayments on the latter [14,16]. These results suggest that diopside should be a relatively resistant phase during the aqueous alteration of chondritic IDPs, compared to orthopyroxenes and olivines. Accordingly, diopside must never have been present in the vast majority of anhydrous chondritic IDPs, although it is demonstrably present in approximately half of all hydrous IDPs containing remnant olivines and/or pyroxenes. From this we conclude that at least half of the observed hydrous chondritic IDPs have not been derived from bulk of the anhydrous IDPs by aqueous alteration.

Presence or absence of diopside can therefore be used to separate the chondritic hydrous IDPs into at least two separate populations. Population A (22 out of the 27 particles) includes the IDPs without diopside. These materials exhibit a wide range of porosities, from 40% to nearly 0%, and practically the complete range of degree of hydration, although anhydrous particles predominate by a ratio of 14:5. Population A should be further divisible into several groups, one of which being anhydrous cometary grains. Population B particles (5) contain diopside and show the complete range of degree of hydration, but have a significantly lower range of porosities (15–0%). These particles are dominated by hydrous particles, by a ratio of 4:1.

What does the presence of diopside reveal regarding the origin and history of primitive solar system materials? The presence of diopside could indicate a more Ca-rich source, although this is unlikely since all the analyzed particles contain approximately the same (chondritic) amount of Ca. Rather, presence of diopside probably indicates relatively slow cooling, and equilibration with orthopyroxene at a low temperature [17]. This was probably not a nebular process, and instead required the presence of a parent body. The lower relative porosities of the diopside-containing particles and their greater relative degree of hydration are consistent with parent-body postaccretion processing [12]. It is noteworthy that the most porous particle we have encountered in this study was hydrous (though to a low degree). If we can assume that the sources for hydrous IDPs are hydrous asteroids, this result indicates that asteroid regoliths can today contain materials with very low porosities. We conclude that olivine and pyroxene major-element compositions can be used to help discriminate between IDPs that are (1) purely nebular condensates, and lately resided in anhydrous or icy (no liquids), primitive parent bodies, and (2) more geochemically active parent bodies (probably hydrous and anhydrous asteroids).

References: [1] Brownlee D. E. (1985) *Annu. Rev. Earth Planet. Sci., 13*, 34–150; Bradley J. P. (1988) *GCA, 52*, 889–900. [2] Zolensky M. E. et al. (1990) *Cosmic Dust Catalog 11, Planetetary Materials Branch Publ. No. 83*, NASA JSC, 170 pp. [3] Lindstrom D. J. et al. (1990) *LPS XX*, 700–701; Lindstrom D. J. (1991) *Nuclear Insts. Methods Phys. Res., A299*, 84–588. [4] Zolensky M. E. and Lindstrom D. J. (1992) *Proc. LPS, Vol. 22*, 161–169. [5] Goldstein J. I. (1979) in *Introduction to Analytical Electron Microscopy* (J. J. Hren et al., eds.), 813–820, Plenum, New York. [6] Rietmeijer F. J. M. (1989) *Proc. LPSC 19th*, 513–521. [7] Bradley J. P. and Brownlee D. E. (1991) *Science, 251*, 549–552; Keller L. P. et al. (1992) *GCA, 56*, 1409–1412. [8] Klöck W. et al. (1989) *Nature, 339*, 126–128. [9] Christoffersen R. and Buseck P. R. (1986) *EPSL, 78*, 53–66. [10] Zolensky M. and Barrett R. (1993) *Microbeam Analysis, 2*, 191–197. [11] Wogelius R. A. and Walther J. V. (1992) *Chem. Geol., 97*, 101–112; Casey W. H. and Westrich H. R. (1992) *Nature, 355*, 157–159. [12] Zolensky M. E. et al. (1989) *Icarus, 78*, 411–425. [13] Grandstaff D. E. (1977) *GCA, 41*, 1097–1104. [14] Eggleton R. A. (1986) in *Rates of Chemical Weathering of Rocks and Minerals* (S. Colman and D. Dethier, eds.), 21–40, Academic, New York. [15] Clemett S. J. et al. (1993) *LPS XXIV*, 309–310; Keller L. P. et al. (1993) *LPS XXIV*, 785–786; Thomas K. L. et al. (1993) *LPS XXIV*, 1425–1426. [16] Colin F. et al. (1985) *Clay Minerals, 20*, 93–113. [17] Lindsley D. H. (1983) *Am. Mineral, 68*, 477–493.

COLLECTION AND CURATION OF INTERPLANETARY DUST PARTICLES RECOVERED FROM THE STRATOSPHERE.

M. E. Zolensky[1] and J. L. Warren[2], [1]Solar System Exploration Division, NASA Johnson Space Center, Houston TX 77058, USA, [2]Lockheed Engineering and Sciences Company, 2400 NASA Road 1, Houston TX 77058, USA.

Since May 1981, the National Aeronautics and Space Administration (NASA) has used aircraft to collect interplanetary dust particles (IDPs) from Earth's stratosphere. Specially designed dust collectors are prepared for flight and processed after flight in an ultraclean (Class-100) laboratory constructed for this purpose at the Lyndon B. Johnson Space Center (JSC) in Houston, Texas. Particles are individually retrieved from the collectors, examined, and catalogued, and then made available to the scientific community for research. Interplanetary dust thereby joins lunar samples and Antarctic meteorites as a critical extraterrestrial material being curated at JSC.

Collection Surfaces: The collection surfaces used are flat plates of Lexan (a space-age plastic) and come in two sizes, conven-

tional collectors and Large Area Collectors having 30 and 300 cm^2 surface areas respectively. These collector surfaces are coated with silicone oil (dimethyl siloxane) and sealed within special airtight housings, to be opened only in the stratosphere or back in the clean-lab facility. The collectors are carried into the stratosphere under the wings of NASA ER-2, WB-57, and (at one time) U-2 aircraft. These collectors were installed in specially constructed wing pylons that ensure that the necessary level of cleanliness is maintained between periods of active sampling. During successive periods of high altitude (20 km) cruise, the collectors are exposed in the stratosphere by barometric controls and then retracted into sealed storage containers prior to descent. In this manner, a total of 20–80 hr of stratospheric exposure is accumulated for each collector. We note that while the collection of IDPs has been the principal goal of this program, terrestrial (including volcanic ash) and space debris particles are collected in great numbers and are also available for study.

Processing of Particles: Particle mounts designed for the JEOL 100CX scanning transmission electron microscope (STEM) are currently the standard receptacles for dust particles in the JSC laboratory. Each mount consists of a graphite frame (size ~3×6×24 mm) onto which a Nucleopore filter (0.4 μm pore size) is attached. A conductive coat of C is vacuum evaporated onto the mount and then a microscopic reference pattern is "stenciled" onto the C-coated filter by vacuum evaporation of Al through an appropriately sized template. Particles are individually removed from collectors using glass-needle micromanipulators under a binocular stereomicroscope. Each particle is positioned on an Al-free area of a Freon-cleaned (Freon 113), C-coated filter and washed in place with hexane to remove silicone oil. Each mount is normally limited to 16 particles. All processing and storage of each particle is performed in a Class-100 clean room. Over the coming year we will be phasing out the use of Freon in our laboratory.

Preliminary Examination of Particles: Each rinsed particle is examined before leaving the Class-100 clean room processing area with a petrographic research microscope equipped with transmitted, reflected, and oblique light illuminators. At a magnification of 500°, size, shape, transparency, color, and luster are determined and recorded for each particle.

After optical description, each mount (with uncoated particles) is examined by scanning electron microscopy (SEM) and X-ray energy-dispersive spectrometry (EDS). Secondary electron imaging of each particle is performed with a JEOL-35CF SEM at an accelerating voltage of 20 kV. Images are therefore of relatively low contrast and resolution due to deliberate avoidance of conventionally applied conductive coats (C or Au-Pd) that might interfere with later elemental analyses of particles. EDS data are collected with the same JEOL-35CF SEM equipped with a Si(Li) detector and PGT 4000T analyzer. Using an accelerating voltage of 20 kV, each particle is raster scanned and its X-ray spectrum recorded over the 0–10-keV range by counting for 100 s. No system (artifact) peaks of significance appear in the spectra.

Following SEM/EDS examination, each particle mount is stored in a dry N gas atmosphere in a sealed cabinet until allocation to qualified investigators.

Cosmic Dust Catalogs: The preliminary information and images of each particle are then published by the JSC Office of the Curator in the form of the Cosmic Dust Catalogs. Each page in the main body of the catalog is devoted to one particle and consists of an SEM image, an EDS spectrum, and a brief summary of preliminary examination data obtained by optical microscopy.

Each cataloged particle receives a provisional first order identification based on its morphology (from SEM image), elemental composition (from EDS spectrum), and optical properties. Particle types are defined for their descriptive and curatorial utility, not as scientific classifications. These tentative categorizations, which reflect judgements based on a decade of collective experience, should not be construed to be firm identifications and should not dissuade any investigator from requesting any given particle for detailed study and more complete identification. The precise identification of each particle in our inventory is beyond the scope and intent of our collection and curation program. Indeed, the reliable identification and scientific classification of cosmic dust is one of many important research tasks that we hope to stimulate.

Sample Requests: Scientists desiring further information concerning the allocation of interplanetary dust, or the Cosmic Dust Catalogs should contact

Curator for Cosmic Dust
Code SN2
NASA Johnson Space Center
Houston TX 77058 USA
Phone: 713-483-5128

ON DUST EMISSIONS FROM THE JOVIAN SYSTEM.

H. A. Zook[1], E. Grün[2], M. Baguhl[2], A. Balogh[3], S. J. Bame[4], H. Fechtig[2], R. Forsyth[3], M. S. Hanner[5], M. Horanyi[6], J. Kissel[2], B.-A. Lindblad[7], D. Linkert[2], G. Linkert[2], I. Mann[8], J. A. M. McDonnell[9], G. E. Morfill[10], J. L. Phillips[4], C. Polanskey[5], G. Schwehm[11], N. Siddique[2], P. Staubach[2], J. Svestka[12], and A. Taylor[9], [1]NASA Johnson Space Center, Houston TX 77058, USA, [2]Max-Planck-Institut für Kernphysik, Postfach 103980, 69 Heidelberg 1, Germany, [3]Imperial College, London, UK, [4]Los Alamos National Laboratory, University of California, Los Alamos NM 87545, USA, [5]Jet Propulsion Laboratory, Pasadena, CA 91109, USA, [6]Laboratory for Atmospheric and Space Physics, University of Colorado, Boulder, CO, USA, [7]Lund Observatory, 221 Lund, Sweden, [8]Max-Planck- Institut für Aeronomie, 3411 Katlenburg-Lindau, Germany, [9]University of Kent, Canterbury, CT2 7NR, UK, [10]Max-Planck-Institut für Extraterrestrische Physik, 8046 Garching, Germany, [11]ESA ESTEC, 2200 AG Noordwijk, The Netherlands, [12]Prague Observatory, 11846 Prague 1, Czech Republic.

As described by Grün et al. [1,2] the dust impact detector on the Ulysses spacecraft detected a totally unexpected series of dust streams in the outer solar system near the orbit of Jupiter. Five considerations lead us to believe that the dust streams emanate from the jovian system itself: (1) The dust streams only occur within about 1 AU of the jovian system, with the strongest stream being the one closest to Jupiter (about 550 R_J away). (2) The direction from which they arrive is never far from the line-of-sight direction to Jupiter. (3) The time period between streams is about 28 (±3) days. (4) The impact velocities are very high—mostly around 40 km s^{-1}. (5) We can think of no cometary, asteroidal, or interstellar source that could give rise to the above four phenomena; such streams have never before been detected.

The logarithm of the dust grain impact rate, in events per day vs. time in days, for a 400-day period centered on Jupiter closest

approach (CA) on Feb. 8, 1992, is plotted in Fig. 1. Depicted is a continuous four-impact running average of all impacts with dust masses above the detector threshold (4×10^{-15} g at 20 km s^{-1} to 6×10^{-16} g at 40 km s^{-1} impact velocity). Sixteen hours before CA, sensitivity was reduced, partly to protect the instrument, so that grains smaller than about 10^{-13} g could not be detected. Full sensitivity was restored about 16 hr after CA. The Ulysses spacecraft velocity well away from Jupiter, but with respect to Jupiter, is about 14 km s^{-1}.

The eye is immediately struck by the rough periodicity of the six dust streams before and after Jupiter CA (two streams before and four after). The average period between streams is 28 to 29 days. A second feature is that the streams only occur within about 1 AU (~2100 R_J) distance from Jupiter and average about 505 R_J apart; the most intense stream is the one closest to Jupiter. A third feature, again striking, is observed in Fig. 2, where each dust grain impact is represented as a symbol on a plot showing spacecraft rotation angle vs. days from CA. The dust detector points nearly perpendicular (85°) to the spacecraft rotation axis, which, in turn, points continuously to Earth; zero degrees rotation means the dust detector then points, during spacecraft rotation, closest to ecliptic north. It is seen that each stream is made up of small grains that arrive from a single direction (allowing for the 140° sensor field-of-view). It is further seen that the radiant of approach of each stream changes by about 150° in rotation angle from before CA to after CA. The direction from which the streams appear to arrive is, in all cases, close to the line of sight direction to Jupiter; interplanetary magnetic field bending of particle trajectory is believed to cause the observed deviations from the line-of-sight directions.

The three considerations given above, plus two more, make the jovian system the only plausible source for these remarkable dust streams. There are two additional considerations: (1) The stream particle impact velocities—about 40 km s^{-1} as measured by the rise time of the impact ion pulse—appear improbably high to have derived from sources such as asteroids or comets in closed solar system orbits (the escape velocity from the solar system at 5.4 AU is 18 km s^{-1}); it is probable, however, that the rotating jovian magnetic field can accelerate charged dust grains to such velocities [3]. (2)

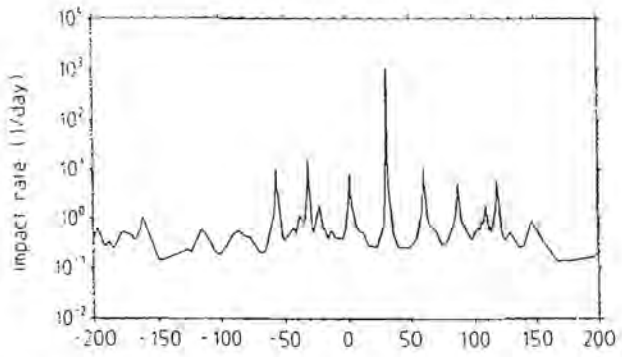

Fig. 1. Logarithm of impact rate, in number of events per day, vs. time in days since Jupiter closest approach (CA). The impact rate increase seen at CA is believed due to particles in jovian orbit and/or to a gravitationally concentrated interplanetary meteoroid flux near Jupiter.

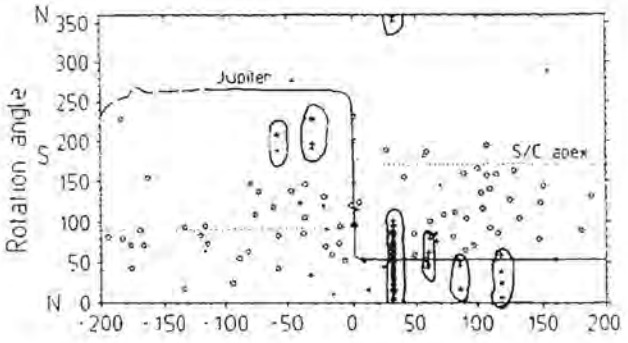

Fig. 2. Spacecraft rotation angle vs. time in days since Jupiter CA. Line-of-sight direction to Jupiter and the spacecraft direction of motion (S/C apex) are also shown.

We can't imagine any source (other than the jovian system), including grains from interstellar space, that would cause the apparent radiant of the particles to change by the 150° shown in Fig. 2.

Because the measured stream velocities are near the upper limits of velocity for the laboratory impact calibrations that have been performed, it is possible that ion and electron current rise times are no longer very sensitive to further increases in impact velocity. This leads to the possibility that particle velocities are much higher, and particle masses much lower, than the values derived from the indicated instrument response. This possibility, among others, is now being explored to clearly understand the rotation angles from which the streams appear to come.

References: [1] Grün E. et al. (1992) *Science, 257*, 1550–1552. [2] Grün E. et al. (1993) *Nature*, submitted. [3] Horanyi M. et al. (1993) *Nature*, submitted.

List of Workshop Participants

Ruth Barrett
Mail Code C23
Lockheed Engineering and Sciences Co.
2400 NASA Road 1
Houston TX 77058
Phone: 713-483-5017
Fax: 713-483-5347

Abhijit Basu
Indiana University
Department of Geological Science
1005 E. 10th Street
Bloomington IN 47405
Phone: 713-486-2082
E-mail: basu@ucs.indiana.edu
Fax: 812-855-7899

Willet I. Beavers
Massachusetts Institute of Technology
Lincoln Laboratory, Group 91
244 Wood Street
Lexington MA 02173-9108
Phone: 617-981-4782
E-mail: beavers@ll.mit.edu
Fax: 617-981-0991

Lucinda Berthoud
Cert-Onera
2, Avenue Edouard Berlin
31055 Toulouse
FRANCE
Phone: 33-61-55-71-17
E-mail: berthoud@reseau.onecert.fr
Fax: 33-61-55-71-69

George Blanford
University of Houston-Clear Lake
2700 Bay Area Boulevard
Houston TX 77058
Phone: 713-283-3773
E-mail: blanford@ch4.cl.uh.edu
Fax: 713-283-3707

Janet Borg
I.A.S.
Batiment 121
91405 Orsay Cedex
FRANCE
Phone: 33 1 6985 8832
Fax: 33-1-6985-8675

John Bradley
MVA, Inc.
5500 Oakbrook Parkway #200
Norcross GA 30093
Phone: 404-662-8509
E-mail: jpb111@delphi.cum
Fax: 404-662-8532

Don Brownlee
Department of Astronomy
Physics Hall
University of Washington
Seattle WA 98195
Phone: 206-543-8575
E-mail: brownlee@astro.washington.edu
Fax: 206-685-0403

Patti Jo Burkett
Mail Code SN2
NASA Johnson Space Center
Houston TX 77058
Phone: 713-483-5022
Fax: 713-483-5347

Bill Cooke
Institute of Space Sciences and Technology
1810 N.W. 6th Street
Gainesville FL 32609
Phone: 904-372-5042

Cassandra Coombs
PGD/SOEST
University of Hawaii
2525 Correa Road
Honolulu HI 96822
Phone: 808-956-3163
E-mail: coombs@kahana.pdg.hawaii.edu
Fax: 808-956-6322

Stanley F. Dermott
Department of Astronomy
211 SSRB
University of Florida
Gainesville FL 32611
Phone: 904-392-5089
E-mail: dermott@astro.ufl.edu
Fax: 904-392-5089

Tammy Dickinson
Code SLC
NASA Headquarters
Washington DC 20546
Phone: 202-358-0284
E-mail: tdickinson@sl.ossa.ms.hq.nasa.gov
Fax: 202-358-3097

Joel Edelman
LDEF Newsletter
14636 Silverstone Dr.
Silver Spring MD 20905
Phone: 301-236-9311

C. Y. Fan
Department of Physics
University of Arizona
Tucson AZ 85721
Phone: 602-621-2778
Fax: 602-621-4721

George J. Flynn
Department of Physics
Hudson Hall -223
State University of New York
Plattsburgh NY 12901
Phone: 518-564-3156
Fax: 518-564-3152

M. N. Fomenkova
Mail Stop 239-4
NASA Ames Research Center
Moffett Field CA 94035
Phone: 415-604-3225
E-mail: marigo@max.arc.nasa.gov
Fax: 415-604-1088

Everett K. Gibson
Mail Code SN2
NASA Johnson Space Center
Houston TX 77058
Phone: 713-483-6224
Fax: 713-483-5276

James Gooding
Mail Code SN2
NASA Johnson Space Center
Houston TX 77058
Phone: 713-483-5126
E-mail: gooding@sn.jsc.nasa.gov
Fax: 713-483-2911

Martha S. Hanner
Mail Stop 183-601
Jet Propulsion Laboratory
4800 Oak Grove Drive
Pasadena CA 91109
Phone: 808-956-8429
E-mail: msh@jplsc8.dnet.nasa.gov
Fax: 818-393-4605

Fred Hörz
Mail Code SN4
NASA Johnson Space Center
Houston TX 77058
Phone: 713-483-5042
Fax: 713-483-5347

Donald Humes
Mail Code 498
NASA Langley Research Center
Hampton VA 23665-5225

A. A. Jackson
Mail Code C23
Lockheed Engineering and Sciences Co.
2400 NASA Road 1
Houston TX 77258
Phone: 713-333-7679
E-mail: jackson@sn.jsc.nasa.gov

James E. Keith
Mail Code SN3
NASA Johnson Space Center
Houston TX 77058
Phone: 713-483-5311
Fax: 713-483-5276

Lindsay P. Keller
MVA, Inc.
5500 Oakbrook Parkway #200
Norcross GA 30093
Phone: 404-662-8509
Fax: 404-662-8532

William Kinard
Mail Code 356
NASA Langley Research Center
Hampton VA 23665-5225
Phone: 804-864-3796

Wolfgang Klöck
Institut für Planetologie
Universät Münster
Wilhelm-Klemm Strasse 10
48149 Münster
GERMANY
Phone: 0251-833673

Kimberly Leago
Lockheed Engineering and Sciences Co.
2400 NASA Road 1
Houston TX 77058

Wei Lee
Physics Department
310 Campbell Hall
University of Alabama at Birmingham
1300 University Boulevard
Birmingham AL 35294-1170
Phone: 205-934-8042
E-mail: leew@phy.uab.edu
Fax: 205-934-8042

David J. Lindstrom
Mail Code SN2
NASA Johnson Space Center
Houston TX 77058
Phone: 713-483-5135
E-mail: dlindstrom@snmail.jsc.nasa.gov
Fax: 713-483-5347

J.-C. Liou
Mail Code SN3
NASA Johnson Space Center
Houston TX 77058
Phone: 713-244-5975
E-mail: liou@snmail.jsc.nasa.gov
Fax: 713-483-5276

Carl R. Maag
T&M Engineering
6831 Sherwood Drive
Laverne CA 91750
Phone: 909-596-3235

Michel Maurette
C.S.N.S.M.
Batiments 104
91405 Campus Orsay
FRANCE
Phone: 33-1-69-41-52-54
Fax: 33-1-69-41-52-68

David S. McKay
Mail Code SN6
NASA Johnson Space Center
Houston TX 77058
Phone: 713-483-5048
E-mail: dmckay@sn.jsc.nasa.gov
Fax: 713-483-5347

David J. Mendez
Lockheed Missiles and Space Co.
3251 Hanover St.
Palo Alto CA 94304
Phone: 408-743-2080

Scott Messenger
McDonnell Center for Space Sciences
Washington University
Campus Box 1105
One Brookings Drive
St. Louis MO 63130
Phone: 314-935-6274
E-mail: dbunny@howdy.wustl.edu
Fax: 314-935-4083

Douglas W. Ming
Mail Code SN4
NASA Johnson Space Center
Houston TX 77058
Phone: 713-483-5839
Fax: 713-483-2696

Alfred O. Nier
School of Physics and Astronomy
University of Minnesota
116 Church Street S.E.
Minneapolis MN 55455
Phone: 612-624-6804
Fax: 612-624-4578

Kenji Nishioka
SETI Institute
Mail Stop 239-12
NASA Ames Research Center
Moffett Field CA 94035-1000
Phone: 415-604-0103
E-mail: kenji_nishioka.sss_mail@qmgate.arc.nasa.
Fax: 415-604-0092

Laurence E. Nyquist
Mail Code SN4
NASA Johnson Space Center
Houston TX 77058
Phone: 713-483-5038
E-mail: nyquist@sn.jsc.nasa.gov
Fax: 713-483-5347

J. Oliver
Institute of Space Sciences and Technology
1810 N.W. 6th Street
Gainesville FL 32609
Phone: 904-372-5042
E-mail: oliver@pine.civea.ufl.edu
Fax: 904-372-5042

Doug Phinney
Lawrence Livermore National Laboratory
L-232
P.O. Box 808
Livermore CA 94551
Phone: 510-423-1984

Frans Rietmeijer
Department of Earth and Planetary Science
University of New Mexico
Albuquerque NM 87131
Phone: 505-277-2039/4204
Fax: 505-277-8843

Thomas H. See
Mail Code C23
Lockheed Engineering and Sciences Co.
2400 NASA Road 1
Houston TX 77058
Phone: 713-483-5027
E-mail: see@sn.jsc.nasa.gov
Fax: 713-483-5347

Charles Simon
Institute of Space Sciences and Technology
1810 N.W. 6th Street
Gainesville FL 32609-8590
Phone: 904-371-4778
E-mail: bjc@ufl.edu
Fax: 904-372-5042

Frank Stadermann
University of Darmstadt
Hilpertstrasse 31
64295 Darmstadt
GERMANY
Phone: 49-6151-813223
E-mail: dfgs@hrzpub.th-darmstadt.de
Fax: 49-6151-813222

Steve Sutton
Department of Geophysical Sciences
Consortium for Advanced Radiation Sources
University of Chicago
5640 S. Ellis Avenue
Chicago IL 60637
Phone: 516-282-2187
E-mail: sutton@bnlx26.nsls.bnl.gov
Fax: 516-282-7905

William G. Tanner
Space Science Laboratory
Department of Physics
Baylor University
P.O. Box 97303
Waco TX 76798-7303
Phone: 817-755-3404
E-mail: tannerw@baylor.edu
Fax: 817-755-3878

Kathie Thomas
Mail Code C23
Lockheed Engineering and Science
NASA Johnson Space Center
Houston TX 77058
Phone: 713-483-5029

Gary Toller
General Sciences Corporation
9364 Dewlit Way
Columbia MD 21045
Phone: 301-513-7770

Anthony J. Tuzzolino
Laboratory for Astrophysics and Space Research
University of Chicago
933 E. 56th Street
Chicago IL 60637
Phone: 312-702-7798

Robert M. Walker
Department of Physics
Washington University
Campus Box 1105
One Brookings Drive
St. Louis MO 63130
Phone: 314-935-6225
E-mail: rmw@howdy.wustl.edu
Fax: 314-935-4083

Jack Warren
Lockheed Engineering and Sciences Co.
2400 NASA Road 1
Houston TX 77058
Phone: 713-483-5122

Thomas Wdowiak
University of Alabama at Birmingham
665 Pamela Street
Birmingham AL 35213
Phone: 205-934-8036
E-mail: wdowiak@phy.uab.edu
Fax: 205-934-8042

Jerry Weinberg
Institute for Space Sciences and Technology
Space Astronomy Lab
1810 N.W. 6th Street
Gainesville FL 32609
Phone: 904-371-4778
E-mail: bjc@ufl.edu
Fax: 904-372-5042

Thomas Wilson
Solar System Exploration Division
Mail Code SN3
NASA Johnson Space Center
Houston TX 77058
Phone: 713-483-2147
Fax: 713-483-5347

Michael Zolensky
Mail Code SN2
NASA Johnson Space Center
Houston TX 77058
Phone: 713-483-5128

Herbert A. Zook
Mail Code SN3
NASA Johnson Space Center
Houston TX 77058
Phone: 713-483-5058
E-mail: zook@sn.jsc.nasa.gov
Fax: 713-483-5276